

3106.6-01



**Department of AERONAUTICS and ASTRONAUTICS
STANFORD UNIVERSITY**

AD647424

**N.M. BHATIA
AND
W. NACHBAR**

**FINITE INDENTATION OF ELASTIC AND ELASTIC-PLASTIC
MEMBRANES BY A SPHERICAL INDENTER**

D D C
RECEIVED
MAR 2 1967
RECEIVED
C

Distribution of this document is unlimited.

The findings in this report are not to be construed as an official Department of the Army position, unless so designated by other authorized documents.

ARCHIVE COPY

**AUGUST
1964**

PREPARED FOR THE U.S. ARMY RESEARCH OFFICE (DURHAM)
UNDER GRANT NO. DA-ARO(D)31-124 G464

**SUDAER
NO. 203**

Department of Aeronautics and Astronautics
Stanford University
Stanford, California

FINITE INDENTATION OF ELASTIC AND ELASTIC-PLASTIC
MEMBRANES BY A SPHERICAL INDENTER

by

N. M. Bhatia

and

W. Nachbar

SUDAER No. 203

August 1964

Distribution of this document is unlimited.

The findings in this report are not to be construed as an official Department of the Army position, unless so designated by other authorized documents.

This work was performed at Stanford University
with the sponsorship of the
U. S. Army Research Office under Grant DA-ARO(D)31-124 G464,
Project Number DA-59901007

ABSTRACT

Part I

Rotationally symmetric stresses and deformations are considered for a prestressed elastic sheet of circular outer boundary loaded transversely by a centered indenter with a hemispherical tip. A nonlinear membrane solution is obtained for the portion of the sheet that is in frictionless contact with the rigid tip of the indenter. This solution and the nonlinear membrane solution previously obtained by Nachbar for a prestressed annular membrane are used to obtain a complete solution for stresses and deflections of the indented membrane. Three limiting cases of the exact solution are investigated: 1) an explicit expression for an upper bound P_L on the indenter load above which stresses under the indenter are inelastic; 2) for small values of indenter load, simple closed-form solutions reducing to those found from linearized membrane theory; 3) for fixed values of indenter load and prestress, the limit of the solution as the tip radius tends towards zero. In case 3, the center deflection approaches the finite limit also found by Jahsman, Field and Holmes; the difference between these results and those obtained from linearized membrane theory is found to be due to improper interchange of limiting processes in the latter.

Comparison of computations from this analysis with experimental data of Jahsman, Field, and Holmes on indentation of stretched mylar membranes shows good agreement except in the immediate neighborhood of the indenter. Since the reported experimental values of indenter loads were all considerably in excess of P_L , the theoretical prediction of yielding and plastic deformation of the membrane in the vicinity of the indenter is confirmed.

Part II

The indenter problem defined in Part I is reconsidered under the assumption that the membrane is composed of an elastic-perfectly plastic material. Tresca's yield condition and associated flow rule are used. It is assumed that the plastic region is separated from the elastic

region by a distinct circular elastic-plastic boundary. This boundary may lie either in the constrained region for sufficiently small indenter loads, or in the free region for sufficiently large loads. Both cases are considered.

Nonlinear membrane solutions are obtained for the constrained region (in contact with the indenter) and for the free plastic region of the membrane. These solutions, together with solutions previously obtained for the prestressed elastic membrane, are used to obtain the complete solution for both the cases mentioned above. An upper bound on the indenter load is found, beyond which a (static) solution to the indenter problem does not exist. For the particular case of small indenter radii, it is shown that $P_L \cong P_\ell$, where P_ℓ is defined as the indenter load for incipient plastic flow under the indenter.

The computed results from this analysis are compared with the experimental data of Jahsman, Field and Holmes for stretched mylar membranes. Very good agreement is found. In these calculations, the elastic-plastic boundary radius is shown to be a monotone increasing function of the indenter load for fixed values of prestress. Loads at which rupture of the membrane occurred in the experiments are found to be close to the theoretical upper bound on the indenter load.

TABLE OF CONTENTS

	Page
GENERAL INTRODUCTION	1
1. General Area of Investigation	1
2. Historical Background	3
3. Principal Results of this Dissertation	7
REFERENCES	10
<u>PART I:</u> FINITE INDENTATION OF AN ELASTIC MEMBRANE BY A SPHERICAL INDENTER	
NOTATION	12
SECT. 1. INTRODUCTION	14
2. SHEET IN FRICTIONLESS CONTACT WITH INDENTER .	20
3. SOLUTION OF THE INDENTER PROBLEM	25
4. APPROXIMATE SOLUTIONS FOR LIMITING CASES . .	34
5. NUMERICAL RESULTS AND COMPARISON WITH EXPERIMENTS	48
APPENDIX A	54
REFERENCES	57
<u>PART II:</u> FINITE INDENTATION OF AN ELASTIC-PLASTIC MEMBRANE BY A SPHERICAL INDENTER	
NOTATION	59
SECT. 1. INTRODUCTION	61
2. PLASTIC DEFORMATION OF MEMBRANE IN FRICTIONLESS CONTACT WITH INDENTER	65
3. ELASTIC-PLASTIC BOUNDARY UNDER THE INDENTER .	71
4. ELASTIC-PLASTIC BOUNDARY IN THE FREE REGION OF MEMBRANE	81
5. NUMERICAL RESULTS AND COMPARISON WITH EXPERIMENTS	89
APPENDIX A - PROOF OF CONSISTENCY AND EXISTENCE OF SOLUTIONS FOR PROBLEM OF FIG. 1	100
APPENDIX B	105
REFERENCES	107

LIST OF FIGURES

Part I

Figure	Page
1. Deformation of the Elastic Sheet - Deformed Equilibrium Configuration	15
2. Deformation of the Elastic Sheet - For the Constrained Region	16
3. Deflection w and Stresses σ_r and σ_θ vs. (r/a) for the Membrane	50
4. Deflection w and Stresses σ_r and σ_θ vs. (r/a) for the Membrane in the Neighborhood of the Indenter	51
5. Central Deflection vs. Indenter Load P for Fixed H_0	52
6. Graph of Q as a Function of x [from Eq. (5A)] and of x_L	55

Part II

Figure	Page
1. Deformed Elastic-Plastic Membrane: Elastic-Plastic Boundary under Indenter	63
2. Deformed Elastic-Plastic Membrane: Elastic-Plastic Boundary in Free Region of Membrane	64
3a. Deflection w and Stresses σ_r and σ_θ vs. (r/a) for Complete Membrane, with Prestress $\sigma_{r0} = 2510$ psi	93
3b. Deflection w and Stresses σ_r and σ_θ vs. (r/a) for Membrane in Neighborhood of Indenter, with Prestress $\sigma_{r0} = 2510$ psi	94
4a. Deflection w and Stresses σ_r and σ_θ vs. (r/a) for Complete Membrane, with Prestress $\sigma_{r0} = 1310$ psi	95
4b. Deflection w and Stresses σ_r and σ_θ vs. (r/a) for Membrane in Neighborhood of Indenter, with Prestress $\sigma_{r0} = 1310$ psi	96

LIST OF FIGURES (cont'd)

Part II

Figure		Page
5.	Central Deflection vs. Indenter Load P for Fixed H_0 : Comparison of Theory and Experiments of Ref. 3	97
6.	$\epsilon \equiv (b/a)$ and $\bar{\epsilon} \equiv (d/a)$ vs. Indenter Load P for Fixed H_0	98
7.	β_b and β_d vs. Indenter Load P for Fixed H_0	99

GENERAL INTRODUCTION

1. General Area of Investigation

Very thin-walled shell structures are of considerable interest for aerospace applications especially where large volume or area coupled with low weight are primary design considerations. In particular, due to recent developments of high-strength polymer materials which can be formed into very thin sheets, increasing use is being made of inflatable "membrane" structures. The principal inherent advantage of these structures is that they can be transported to their destination in a compact lightweight package and inflated only just before they are used.

A "membrane" shell is defined as one having zero bending rigidity, which means physically that bending stresses and the resultant bending moments are absent despite flexural deformations of the shell. In practice, this idealized membrane is approached in the limit as the wall-thickness approaches zero. The justification for the idealization is that, in a shell of thickness h , the extensional or membrane stiffness is proportional to h , while the flexural or bending rigidity is proportional to h^3 . Therefore, in the limit of vanishing wall-thickness, bending rigidity of the shell tends to zero faster than the extensional stiffness. Thus, in a membrane shell, resistance to external loading is accomplished by membrane stresses alone.

Certain problems for thin shells, and in particular for membrane shells, involve finite displacements and finite displacement gradients of the shell elements. The governing differential equations for these problems are formulated by considering equilibrium in the deformed state of the shell. The differential equations become nonlinear, and the theory which incorporates this consideration is called a geometrically nonlinear theory. In this dissertation, such a geometrically nonlinear membrane theory is used for a rotationally symmetric problem.

This nonlinear membrane theory, which is developed by neglecting bending stresses, may seem to be useful only for very thin shells. However, it turns out that even for shells that are not very thin but

are loaded in such a manner that membrane stresses are predominant, the membrane theory is adequate and gives good results.

Insofar as the magnitude of the maximum elastic strain in the membrane element is concerned, it may be either small compared to one or finite of order one, depending upon the type of material used. For example, a very thin mylar membrane may have a maximum elastic strain before yielding of order 10^{-2} , whereas, in highly elastic, rubber-like materials, the maximum elastic strain may become of order unity. For the problems considered in this dissertation, it will be assumed that the magnitude of the maximum elastic strain is negligible compared to unity.

In this dissertation, attention is restricted to the analysis of a particular problem of very thin membrane structures. This is the rotationally symmetric, finite deformations and stresses in a "prestressed" circular flat sheet or membrane due to transverse loading by a rigid indenter with a lubricated hemispherical tip. This problem is henceforth referred to as the "indenter problem". The word "prestress" in this dissertation indicates that a prescribed uniform traction, in the plane of the undeformed sheet, is applied along the outer edge or boundary. This prestress does not necessarily imply an "initial stress" in the membrane. In fact, the analysis is valid if both prestress and indenter load are varied arbitrarily and independently. Furthermore, the radial displacement component u along the outer edge is not restricted to be zero.

In Part I of this dissertation, a finite deformation, small strain, elastic solution for the indenter problem is obtained. The membrane material is assumed to be homogeneous and isotropic, and the constitutive relations are assumed to be linear. In Part II, a solution is obtained for the indenter problem under the assumption that the membrane is composed of an elastic-perfectly plastic material. Tresca's yield condition and associated flow rule are used in this analysis.

2. Historical Background

The earliest work on finite deformations in circular elastic membranes under uniform axisymmetric loading is given in the classic papers of Hencky [Ref. 1] in 1915, and Schwerin [Ref. 2] in 1929. Hencky considered the problem of stresses and deformations in an initially unstressed, flat circular membrane which is fixed along its boundary and loaded by uniform lateral pressure. This problem is known as the problem of Föppl-Hencky^{*}. Hencky used Föppl's equations to apply to the Föppl-Hencky problem. These equations contain inherently the assumption that the angle β , which measures rotation of the tangent to the midsurface, obeys the inequality $\beta^2 \ll 1$. This assumption is called the "moderate β " assumption. Hencky obtained a solution by expressing the stresses and the transverse displacement w in terms of an infinite power series in even powers of the radius r .

Campbell [Ref. 5] in 1956, generalized and extended Hencky's power series technique to include the effect of initial stress. Campbell's solution was restricted to the problem of additional stresses due to lateral pressure in a membrane which was initially stressed and then fixed along its edge. In other words, boundary displacements were taken to be zero during the application of lateral pressure.

The problem considered by Schwerin was to some extent different from the Föppl-Hencky problem. He considered rotationally symmetric stresses and deformations of an annular, initially unstressed membrane, fixed along its outer edge; the inner edge was considered to be attached to a rigid circular disk. The membrane was loaded both by uniform lateral pressure on the membrane surface and by a lateral force operating on the rigid disk. The disk was assumed to be held in equilibrium by uniform stress in the membrane along the inner edge. Schwerin also used Föppl's equations. Schwerin showed, by suitable transformation of variables, that the governing differential equations reduced to a simple-

^{*}
See, for instance, the discussion in the paper by Bromberg and Stoker [Ref.3] on nonlinear membrane theory.

The governing differential equations for finite deformations of initially flat and unstressed membranes were first obtained by Föppl [Ref.4] in 1907. Föppl also deduced the equations for the rotationally symmetric case.

looking nonlinear second-order differential equation for a stress function. He obtained a power series solution for this differential equation, following Hencky's technique.

In Schwerin's paper [Ref. 2], results were also obtained for the case when the membrane was loaded only by the lateral force on the disk, and the pressure on the membrane was absent. Schwerin showed that, in this case, the governing differential equations for the rotationally symmetric state reduced to an especially simple nonlinear second-order differential equation. This equation is integrable by quadratures. The solution to this equation involved two constants of integration. With the use of the boundary conditions of zero radial displacement components along the inner and outer edges, the evaluation of the two constants of integration reduced to finding the roots of two transcendental equations which, in Schwerin's paper, were solved graphically.

Schwerin arrived at the interesting conclusion that ". . . . real solutions for the desired stress state exist only⁽¹⁾ for $\nu \leq \frac{1}{3}$, and thus we can conclude that for values of $\nu > \frac{1}{3}$, the assumed axial symmetry of the stress state with bilateral attachment is no longer possible and a wave-like buckling of the membrane occurs".

In 1962, Jahsman, Field and Holmes [Ref. 6] studied analytically and experimentally the problem of a prestressed, centrally loaded membrane. In the analytical portion of Jahsman's paper, the problem considered was that of a circular membrane under fixed distributed tension along its outer edge and a central point load applied laterally. Jahsman started by considering the exact membrane equations of Reissner [Ref. 7]. However, he subsequently assumed that ". . . . rotations while finite, remain small so that $\beta^2 \ll 1$. In addition, by assuming that $u' \ll 1$ ("small strain" assumption), it is possible to eliminate u ". With these assumptions, the exact equations reduced to the membrane equations of Föppl. In Jahsman's paper, u' denotes the derivative of radial displacement component u with respect to the radial coordinate r . The validity of the moderate rotation assumption

(1) ν is Poisson's ratio

was not demonstrated. Jahsman indicated that $u' \ll 1$ was due to the small strain assumption. Actually, the assumption $u' \ll 1$ is valid if both the small strain and moderate rotation assumption are satisfied.

Jahsman followed substantially the steps in the Schwerin analysis to reduce the governing differential equations to a simple nonlinear differential equation, equivalent to that obtained by Schwerin, which was integrable by quadratures. Jahsman observed that the integration constants need not be real in order to generate real solutions; Schwerin had assumed that they were real. Jahsman made the important observation that Schwerin's solution could be extended to all physically meaningful values of Poisson's ratio by allowing one of the integration constants to take on purely imaginary values. The solution itself would still be real-valued.

In the experimental part of Ref. 6, central load-transverse deflection characteristics and the deflection profile were obtained for the indenter problem. The experimental setup consisted of a mylar sheet, 6×10^{-4} in. thick, which was supported in the transverse direction by a rigid circular ring of inner radius 5 inches. The mylar sheet was stretched in its plane by dead-weight loading, which was assumed to have developed uniform stress at the edge of the sheet. A transverse load was applied at the center of the sheet by a rigid indenter having a hemispherical tip of 1/16 inch radius. The magnitude of the load was increased in steps of 0.11 lbs, while the prestress was held constant. The central deflection under the indenter and the deflection profiles were measured.

In order to compare theoretical results with the experimental values, two methods were used in Ref. 6. In the first method, central deflection under the indenter and the indenter load were reduced to the nondimensional parameters \bar{P}_s and \bar{w}_s , respectively, and the experimentally determined relation between these two parameters was compared with the relation determined by the theory described above. Good agreement was shown to exist. In the second method, comparison was made of the deflection profile normalized by the central deflection. This comparison showed discrepancies in considerable excess of estimated experimental errors. Thus, only the first of the two methods showed a good comparison between theory and experiments.

Nachbar [Ref. 8] pointed out several shortcomings of the previous analytical work of Schwerin and Jahsman cited above. He indicated that both papers deal with formal solutions to boundary value problems and do not investigate the question of existence of the solution for the complete, meaningful range of the various physical parameters. In addition, the general consistency of their solutions with the "moderate β " assumption is not investigated. Furthermore, in obtaining the analytical solution for the case of concentrated load at center, Jahsman assumed, without proof, the existence of the solution for stresses and displacements in the limit as the indenter radius tends to zero.

The previous work was extended in several ways by Nachbar. The problem he considered is similar to Jahsman's problem and consists of a prestressed annular membrane, loaded transversely by a rigid plug of finite radius inserted at the center. The finite deformation, small strain equations for thin shells of revolution, as developed by Reissner [Ref. 7], were used to obtain appropriate equations for the case of an initially flat membrane. These equations were valid for arbitrary magnitudes of β . By making the moderate β assumption, and using suitable transformation of dependent and independent variables, the equations simplified to a nonlinear second-order differential equation for a stress function F . This equation is equivalent to that obtained previously by Schwerin, and was integrated by quadratures in closed form. The stress and displacement components were expressed as functions of the stress function. The existence and uniqueness of the solution thus obtained was also investigated for a range of physical parameters involving prestress and indenter load.

The problem of wrinkling of the membrane was also investigated. For this purpose, a wrinkling stability criterion was given by restricting the circumferential stress σ_{θ} to be nonnegative.

3. Principal Results of this Dissertation

The actual indenter problem for which experimental results were obtained by Jahsman [Ref. 6] has not been considered in any of the papers described above. Jahsman's analytical solution was for point loading at the center of the membrane, whereas, in the experiments, an indenter of finite radius was used. In this dissertation, the indenter problem for a finite tip radius is studied in detail, and comparison is made with the experimental results of Ref. 6.

The results of the elastic analysis, Part I, are indicated first. The existence and uniqueness of the elastic solution to the indenter problem is investigated; this was motivated by the following considerations. First, Schwerin and Jahsman encountered difficulties in proving the existence of solutions to their problems for the complete range of Poisson's ratio. Second, we are dealing here with solutions to boundary value problems involving nonlinear differential equations. There are no general proofs of existence and uniqueness of solutions which we found applicable to our problems.

It is shown that an upper bound P_L on the indenter load P can be chosen such that, for prestress exceeding a certain lower bound [see Eq. (4.8), Part I], and for $P \leq P_L$, a unique elastic solution to the indenter problem exists, and the membrane is stable against wrinkles. With the definition of P_L as a certain function of an elastic limit or yield stress [see Eq. (4.6), Part I], it is found that, in general, the stress under the center of the indenter exceeds the limit stress for $P = P_L$. Since, in the experiments reported in Ref. 6, radial wrinkles appeared along the outer edge of the membrane for large indenter loads, a wrinkle stability criterion must be imposed to determine the validity of the rotational symmetry assumption. The wrinkle stability criterion mentioned above is used [Ref. 8].

It is shown that, with further restrictions on prestress and for small indenter radii, yielding of the membrane begins under the indenter

at $P \cong P_L$. The numerically calculated value of this yield load, for Jahsman's experimental problem, turns out to be less than all of the indenter load values for which experimental results were reported. Thus, the theory predicts that, for Jahsman's experiments, yielding of the membrane under the indenter must have occurred for all indenter load values used in the experiments.

A limiting case of the exact solution is investigated for sufficiently small values of indenter load P and for fixed prestress σ_{r0} . It is shown that if P is small enough so that the order relation (4.17d) of Part I is satisfied, then the exact solution reduces to a simple closed-form solution for stresses and displacements which is identical to that found from linearized membrane theory.

Another limiting case of the exact solution is investigated in which the radius of the indenter tends to zero for fixed values of indenter load P and prestress σ_{r0} . The solution is shown to exist in the limit. The numerical calculation of central deflection from this limiting solution and from Jahsman's theory are in agreement for various indenter loads.

The exact limit solution for central deflection w and radial stress σ_r cannot be obtained by allowing the indenter radius to approach zero in the linearized membrane solution. This disagreement is found to be due to an improper interchange of the limiting processes. This result may have some significance with regard to the validity of singular solutions obtained in the linearized membrane theory of shells.

Numerical values of central deflection and the deflection profile computed from the elastic theory for the actual indenter radius are compared with experimental results of Jahsman. Comparison of deflection profiles showed good agreement except in the neighborhood of the indenter. Comparison of central deflections showed discrepancy especially for large indenter loads. This discrepancy is shown in Part II to be due to plastic deformation of the membrane in the neighborhood of the indenter.

To obtain a complete solution for the elastic-plastic problem, it is assumed that the plastic region is separated from the elastic region by a distinct circular elastic-plastic boundary. This boundary may lie

either in the constrained region or in the free region. Both cases are considered.

It is shown in Part II that for both cases mentioned above, a unique elastic-plastic solution exists for values of indenter load P greater than P_ℓ , where P_ℓ is defined as the indenter load for incipient plastic flow under the indenter. For the particular case of small indenter radii, it is further shown that $P_\ell \cong P_L$, which is consistent with the previous result, and that, at $P \cong 2P_\ell$, the entire constrained region is plastic.

Numerical calculations corresponding to the experiments of Ref. 6 are presented for stresses and vertical deflections. In these calculations, the elastic-plastic boundary radius is shown to be a monotone increasing function of the indenter load for fixed values of prestress. Numerical values of central deflection and the deflection profile are compared with the experimental data, and very good agreement is found for all indenter loads up to the wrinkling limits.

An upper bound on the indenter load is found such that for loads greater than this upper bound there exists no (static) solution to the indenter problem. However, at this upper bound load, the moderate β assumption is violated in the vicinity of the indenter. Therefore the derivation of the upper bound may be questionable. However, in two of the experiments, indenter loads at which the membrane ruptured or punctured were reported. These loads are found to be quite close to values calculated from the theoretical upper bound.

REFERENCES

1. H. Hencky, "Über den Spannungszustand in Kreisrunden Platten mit verschwindender Biegesteifigkeit", Z. Math. Phys., Vol.63, 1915, pp. 311-317.
2. E. Schwerin, "Über Spannungen und Formänderungen Kreisringförmiger Membranen", Z. Tech. Phys., No.12, 1929, pp. 651-659.
3. E. Bromberg and J. J. Stoker, "Non-Linear Theory of Curved Elastic Sheets", Q. Appl. Math., Vol.III, No.3, 1945, pp. 246-265.
4. A. Föppl, Vorlesungen über Technische Mechanik, Vol.V, B. G. Teuber, Leipzig, 1907, pp. 132-144.
5. J. D. Campbell, "On the Theory of Initially Tensioned Circular Membranes Subjected to Uniform Pressure", Quart. J. Mech. Appl. Math., Vol.9, Part 1, 1956, pp. 84-93.
6. W. E. Jahsman, F. A. Field and A. M. C. Holmes, "Finite Deformations in a Prestressed, Centrally Loaded, Circular Elastic Membrane", Proc. 4th U.S. Natl. Cong. Appl. Mech., A.S.M.E., 1962, pp.585-594.
7. E. Reissner, "Rotationally Symmetric Problems of Thin Shells of Revolution", Proc. 3rd U.S. Natl. Cong. Appl. Mech., A.S.M.E., 1958, pp. 51-69.
8. W. Nachbar, "Finite Deformation of a Prestressed Elastic Membrane", SUDAER No. 141, November 1962.

PART I

FINITE INDENTATION OF AN ELASTIC MEMBRANE
BY A SPHERICAL INDENTER

NOTATION

a	Outer radius of membrane.
b	Radius at the point of tangency.
c	Radius of the hemispherical head of the indenter.
C_o	Integration constant, Eqs. (1.7a,c).
$C_o(F_o)$	Function determined by Eq. (3.12).
E	Young's modulus.
F	$\equiv 2^{2/3} (\epsilon \rho)^{1/3} y^{1/2} \text{ctn } \beta$.
F_o	$\equiv \left(\frac{H_o}{Eh} \right) \left(\frac{4\pi Eha}{P} \right)^{2/3}$, combined loading parameter.
F_o^*	Value of F_o at which $C_o(F_o) = 0$.
F_{oL}	Value of F_o for $P = P_L$.
F_ϵ	$= F(\epsilon^2) = \left(\frac{2P}{\pi Eha} \right)^{1/3} \frac{c}{a}$.
$F_{\epsilon L}$	Value of F_ϵ for $P = P_L$.
h	Thickness of elastic sheet.
H_o	$\equiv h\sigma_{r0}$, Horizontal component of stress resultant at $r = a$.
P	Central indenter load.
P_L	$\equiv 4\pi Ehc s_L^2$, upper bound on P at elastic limit.
p	Transverse pressure on the elastic sheet under the indenter.
r	Radial coordinate.
$s(\beta)$	$\equiv s_r + s_\theta$.
s_r, s_θ, s, s_L	$\equiv (\sigma_r/E), (\sigma_\theta/E), [(\sigma_r + \sigma_\theta)/E], (\sigma_L/E)$.
u	Horizontal displacement component.
w	Transverse (vertical) displacement component.
w_o	$= -w(0)$, Central deflection.
y	$\equiv (r/a)^2$.

Notation (Continued)

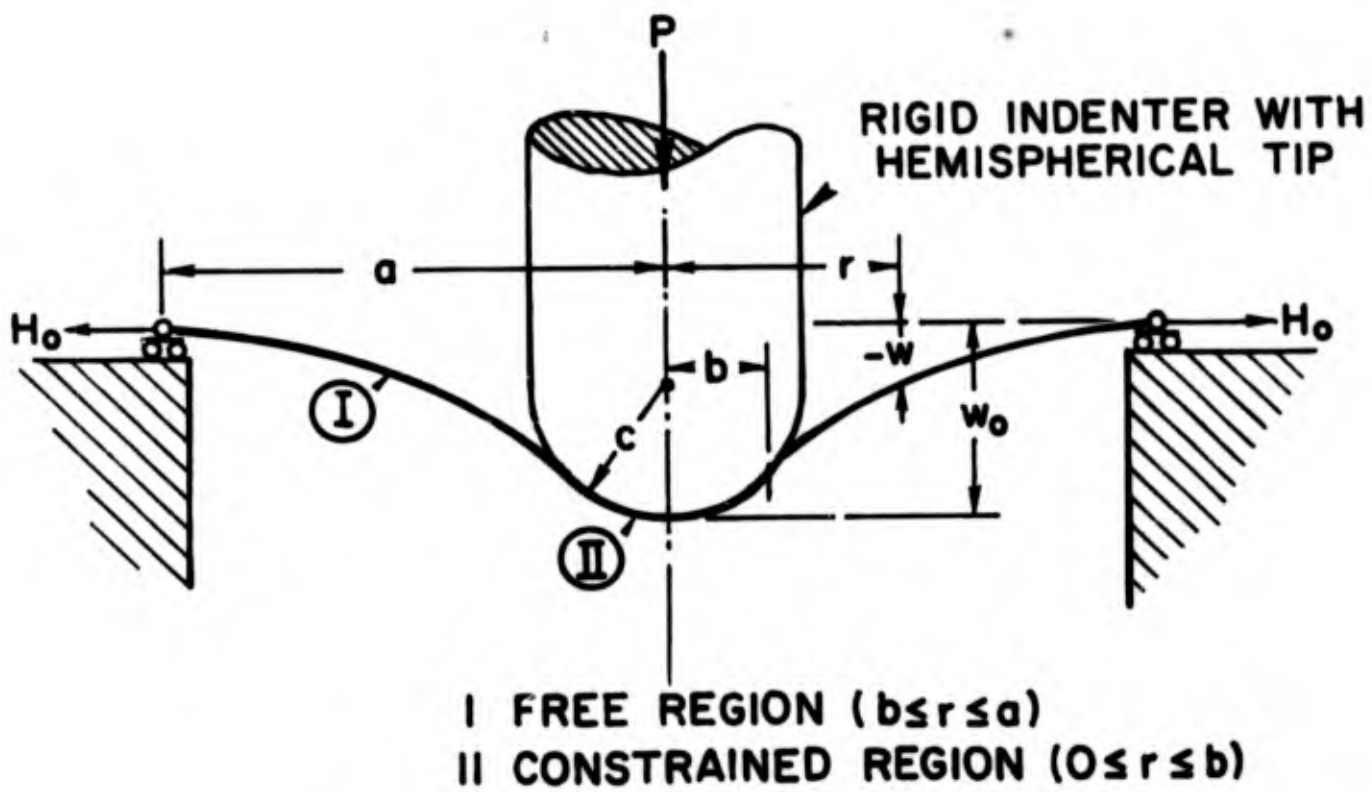
β	Angle of tangent rotation.
β_b	Value of β at point of tangency.
ϵ	$\equiv (b/a)$.
$\epsilon_r, \epsilon_\theta$	Radial and circumferential strain components.
ν	Poisson's ratio.
ρ	$\equiv \frac{P}{2\pi Ehb}$.
σ_r, σ_θ	Radial and circumferential stress components.
σ_{r0}	Applied prestress.
σ_L	Elastic proportional limit stress.
κ	$\equiv \left(\frac{H_0}{Eh}\right)^{1/3} \left(\frac{2c}{a}\right)^{2/3}$.
η	$\equiv \frac{c}{a}$.

SECTION 1. INTRODUCTION

A theoretical analysis has been given by Nachbar [Ref. 1] for the finite, rotationally symmetric deformations and stresses of a prestressed, annular elastic membrane, or sheet, subjected to applied transverse loading only along the inner edge. The sheet is initially flat and is supported at the outer edge where stretching is also applied. An explicit solution was obtained for the case of transverse loading introduced through a rigid plug or disk which is attached centrally to the annular membrane. Experimental results for a similar problem have also been given by Jahsman, Field and Holmes [Ref. 2]. However, the experiments used a complete membrane and a rigid indenter with a hemispherical tip in order to apply transverse load. Thus, stresses and deformations of the membrane in the immediate neighborhood of the indenter tip are to be expected to be different from those predicted by the plug analysis.

In the present paper is considered the problem of finite, rotationally symmetric deformations and stresses in a prestressed circular flat sheet, of outer radius a , due to transverse loading at the center by a rigid indenter with a hemispherical tip of radius c . This problem will henceforth be referred to as the indenter problem. A small strain, elastic solution for the indenter problem is obtained. Figure 1 shows the indenter problem geometry and the nomenclature. The radial distance to the membrane is r , and $r = b$ denotes the point of tangency of the sheet with the indenter; b is a function both of load P and of H_0 . A solution for the portion of the sheet ($0 \leq r \leq b$) in frictionless contact with the indenter is obtained in Section 2. This portion will be called the constrained region. This solution and the results for the free region (annular portion of the membrane which is not in contact with the indenter) are used in Section 3 to obtain the complete solution to the indenter problem.

The results for the free annular region [Ref. 1] which are essential for the present paper are summarized below. These are valid for small strain and moderate rotation restrictions. The inner radius is b and the outer radius is a . Displacements normal and parallel to the initial



DEFORMED EQUILIBRIUM CONFIGURATION

Fig. 1. Deformation of the Elastic Sheet - Deformed Equilibrium Configuration.

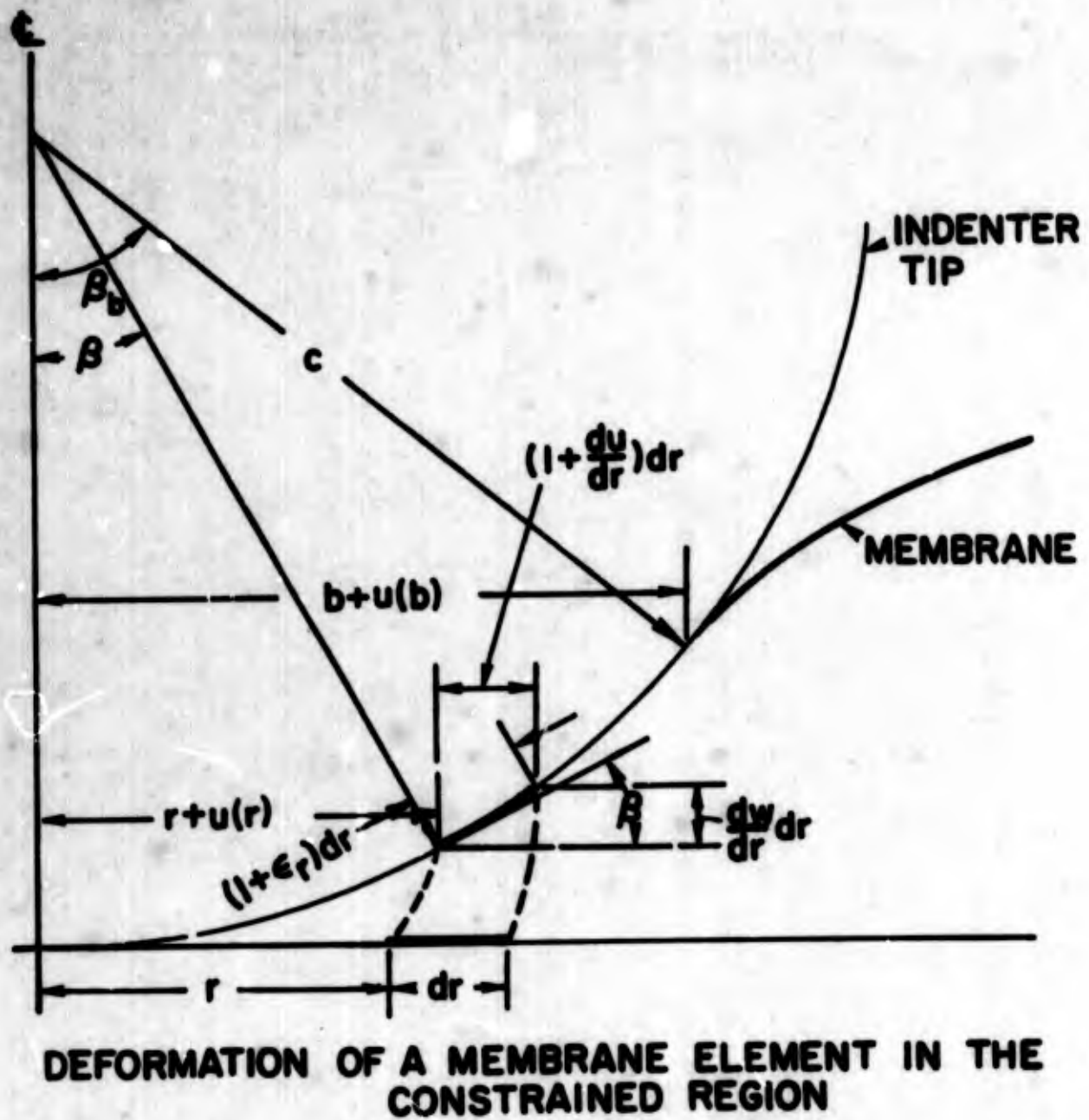


Fig. 2. Deformation of the Elastic Sheet - For the Constrained Region.

plane are w and u , respectively. The angle of rotation of the tangent to the midsurface from the initial plane is β . The sheet has uniform thickness h and elastic coefficients E, ν . Nondimensional stress variables s_r and s_θ are defined as

$$s_r \equiv \frac{\sigma_r}{E} \quad \text{and} \quad s_\theta \equiv \frac{\sigma_\theta}{E} \quad (1.1a)$$

and the independent variable is chosen as

$$y \equiv \left(\frac{r}{a} \right)^2 \quad (1.1b)$$

With use of the nondimensional shape parameter ϵ and the load parameter ρ ,

$$\epsilon \equiv \frac{b}{a}, \quad \rho \equiv \frac{P}{2\pi Ehb}, \quad (1.1c)$$

a nondimensional stress function F is defined as

$$F \equiv (4\epsilon\rho)^{1/3} y^{1/2} \quad \text{ctn } \beta \cong (4\epsilon\rho)^{1/3} y^{1/2} \beta^{-1} \quad (1.1d)$$

Stresses and displacements are given in terms of $F(y)$ by Eqs. (3.7), (3.8), (3.9), (3.11), (3.13) and (3.23) of Ref. 1 as follows:

$$\frac{u}{a} = \left(\frac{1}{2} \epsilon\rho \right)^{2/3} y^{1/2} \left[2 \frac{dF}{dy} - (1 + \nu) \frac{F}{y} \right] \quad (1.2)$$

$$s_\theta = \left(\frac{1}{2} \epsilon\rho \right)^{2/3} \left(2 \frac{dF}{dy} - \frac{F}{y} \right) \quad (1.3)$$

$$s_r = \left(\frac{1}{2} \epsilon\rho \right)^{2/3} \frac{F}{y} \quad (1.4)$$

$$\frac{w}{a} = - \left(\frac{1}{2} \epsilon\rho \right)^{1/3} \int_y^1 \frac{dy}{F} \quad (1.5)$$

$$\beta = (4\epsilon\rho)^{1/3} y^{1/2} F^{-1} \quad (1.6)$$

Equations (1.3) and (1.4) are seen to satisfy identically the differential equations of equilibrium [Eqs.(2.1a,b) below with $p = 0$], and the equation of compatibility [Eq.(2.5b)] becomes, with the use of Eq.(1.6), a differential equation for $F(y)$:

$$\frac{d^2 F}{dy^2} + \frac{1}{2F^2} = 0, \quad \epsilon^2 < y < 1 \quad (1.7a)$$

The integral of this equation corresponding to $s_\theta > 0$ everywhere has the form

$$\frac{dF}{dy} = (F^{-1} + C_0)^{1/2}, \quad \epsilon^2 < y < 1 \quad (1.7b)$$

where C_0 is a real-valued constant. An additional integration gives

$$1 - y = \int_{F(y)}^{F(1)} \left(\frac{1}{v} + C_0 \right)^{-1/2} dv, \quad \epsilon^2 < y < 1 \quad (1.7c)$$

The boundary condition at $y = 1$ is $Ehs_r \equiv h\sigma_{r0} = H_0$. Thus H_0 determines the prestress σ_{r0} . The parameter F_0 expresses the combined loading condition, through use of Eq.(1.4), as

$$F(1) = F_0 \equiv \frac{H_0}{Eh} \left(\frac{4\pi Eha}{P} \right)^{2/3} \quad (1.8a)$$

The boundary condition at $y = \epsilon^2$ is expressed as

$$F(\epsilon^2) = F_\epsilon \quad (1.8b)$$

where F_ϵ is to be determined from conditions of continuity with the constrained region. When $\epsilon, F_0, F_\epsilon$ are given so that $F_0 > F_\epsilon > 0$, C_0 is uniquely determined from Eq.(1.7c) expressed at $y = \epsilon^2$ as follows:

$$1 - \epsilon^2 = \int_{F_\epsilon}^{F_0} \left(\frac{1}{v} + C_0 \right)^{-1/2} dv \quad (1.9)$$

Upon determination of C_0 , the function $F(y)$ which satisfies Eq.(1.7a) and boundary conditions (1.8a,b) is given by Eq.(1.7c). The normal displacement component w is then determined explicitly through use of

Eq.(1.7a) in Eq.(1.5) [see Ref. 1, Eqs.(3.23) and (5.7)]:

$$\frac{w(y)}{a} = - 2 \left(\frac{H_0/Eh}{F_0} \right)^{\frac{1}{2}} \left\{ F_0 \left(\frac{1}{F_0} + C_0 \right)^{\frac{1}{2}} - F(y) \left[\frac{1}{F(y)} + C_0 \right]^{\frac{1}{2}} - C_0(1-y) \right\} \quad (1.10)$$

SECTION 2. SHEET IN FRICTIONLESS CONTACT WITH INDENTER

Finite deformation, small strain equations for the constrained region ($0 \leq r \leq b$) of the sheet are [Ref. 3] those of equilibrium,

$$\frac{d}{dr} (rs_r \cos \beta) - s_\theta + \frac{rp}{Eh} \sin \beta = 0 \quad (2.1a)$$

$$\frac{d}{dr} (rs_r \sin \beta) - \frac{rp}{Eh} \cos \beta = 0 \quad (2.1b)$$

elasticity [$0 \leq \nu \leq (1/2)$],

$$\epsilon_r = s_r - \nu s_\theta \quad (2.2a)$$

$$\epsilon_\theta = s_\theta - \nu s_r \quad (2.2b)$$

and strain-displacement,

$$(1 + \epsilon_r) \sin \beta = \frac{dw}{dr} \quad (2.3a)$$

$$(1 + \epsilon_r) \cos \beta = 1 + \frac{du}{dr} \quad (2.3b)$$

$$\epsilon_\theta = \frac{u}{r} \quad (2.3c)$$

When p is eliminated between Eqs. (2.1a,b), there obtains

$$\frac{d}{dr} (rs_r) = s_\theta \cos \beta \quad (2.4)$$

The compatibility relation obtained by combining Eqs. (2.3b,c),

$$\frac{d}{dr} (r\epsilon_\theta) + 1 - (1 + \epsilon_r) \cos \beta = 0 \quad (2.5a)$$

can be written in a more convenient form, with the use of Eqs. (2.2) and (2.4), as

$$r \frac{d}{dr} (s_\theta + s_r) + (1 + s_\theta + s_r)(1 - \cos \beta) = 0 \quad (2.5b)$$

Since the membrane is assumed to deform smoothly onto the indenter, the geometric relation for the constrained region

$$\sin \beta = \frac{r + u(r)}{c} = \frac{r}{c} (1 + \epsilon_{\theta}) \quad (2.6)$$

is apparent from Fig. 2.

It is next shown that $|\beta|$ must necessarily be of the order of the square root of the maximum elastic strain or smaller. From Eq. (2.3b) and the derivative of both sides of Eq. (2.6) there is obtained

$$\frac{d\beta}{dr} = c^{-1} (1 + \epsilon_r) \quad (2.7)$$

The differential operator transforms as [Eqs.(2.6) and (2.7)]

$$r \frac{d(\quad)}{dr} = \frac{r}{c} \frac{d\beta}{d(r/c)} \cdot \frac{d(\quad)}{d\beta} = \left(\frac{1 + \epsilon_r}{1 + \epsilon_{\theta}} \right) \sin \beta \frac{d(\quad)}{d\beta}$$

Equation (2.5b) can then be written as

$$\frac{d}{d\beta} (s_{\theta} + s_r) + \left[\frac{(1+s_{\theta}+s_r)(1+\epsilon_{\theta})}{(1+\epsilon_r)} \right] \frac{(1 - \cos \beta)}{\sin \beta} = 0$$

Because of the assumption of small strains, $|s_r| \ll 1$ and $|s_{\theta}| \ll 1$, the square bracketed terms in the above equation can be approximated by unity, and the equation becomes

$$\frac{d}{d\beta} (s_r + s_{\theta}) + \tan \frac{\beta}{2} = 0 \quad (2.8)$$

Let $s(\beta) \equiv s_r + s_{\theta}$; then the integral of Eq. (2.8) can be written as

$$s(\beta) = s(0) + 2 \ln \cos \frac{\beta}{2} \quad (2.9)$$

or also as

$$\cos \frac{\beta}{2} = \exp \left\{ -\frac{1}{2} [s(0) - s(\beta)] \right\} \quad (2.10)$$

Equation (2.10) shows that $s(\beta) \leq s(0)$ for all $\beta \geq 0$. Furthermore, since $|s|$ is bounded by some linear elastic limit value denoted by

($2s_L$), where $s_L \ll 1$, then Eq. (2.10) implies

$$[1 - \cos(\beta/2)] \leq 1 - \exp(-s_L) \approx s_L$$

so that $\beta^2 \approx 8s_L$. Therefore, if s_L is sufficiently small, it is necessary to assume as consistent with the small strain approximation that the rotation is finite but "moderate", viz.

$$\beta^2 \ll 1 \tag{2.11}$$

Hence Eqs. (2.6) and (2.9) are approximated as

$$\sin \beta \approx \beta \approx \frac{r}{c} \tag{2.12a}$$

$$s(\beta) \approx s(0) - \frac{1}{4} \beta^2 \tag{2.12b}$$

If Eq. (2.4) is written in the form

$$r \frac{ds_r}{dr} + 2s_r = s - s_\theta (1 - \cos \beta)$$

then with the use of Eqs. (2.12a,b) and the small strain assumption, this becomes

$$\beta \frac{ds_r}{d\beta} + 2s_r = s(0) - \frac{1}{4} \beta^2 \tag{2.13}$$

The solution is

$$s_r = \frac{C_2}{\beta^2} + \frac{s(0)}{2} - \frac{1}{16} \beta^2 \tag{2.14a}$$

and from Eq. (2.12b),

$$s_\theta = -\frac{C_2}{\beta^2} + \frac{s(0)}{2} - \frac{3}{16} \beta^2 \tag{2.14b}$$

With use of these relations in Eqs. (2.2b) and (2.3c), u is determined to be

$$\frac{u}{c} = -(1 + \nu) \frac{C_2}{\beta^2} + \frac{1}{2} (1 - \nu) \beta s(0) - \frac{1}{16} (3 - \nu) \beta^3 \tag{2.15}$$

The contact pressure p between the membrane and the indenter is determined by using Eqs. (2.1b), (2.12a) and (2.14a):

$$p = \frac{Eh}{c} \left[s(0) - \frac{1}{4} \beta^2 \right] \quad (2.16)$$

An expression can be given for $s(0)$ in terms of $s_r(\beta_b)$, where $\beta_b \equiv (b/c)$, by using Eq. (2.14a):

$$s(0) = 2 s_r(\beta_b) - 2 \frac{C_2}{\beta_b^2} + \frac{1}{8} \beta_b^2 \quad (2.17)$$

Equations (2.14) to (2.17) are valid for $C_2 \neq 0$, but if the membrane is to be elastic for all $\beta \geq 0$, then $C_2 = 0$. For the case $C_2 = 0$, Eqs. (2.14) to (2.16) become with use of Eq. (2.17):

$$s_r(\beta) = s_r(\beta_b) + \frac{1}{16} (\beta_b^2 - \beta^2) \quad (2.18a)$$

$$s_\theta(\beta) = s_r(\beta_b) + \frac{1}{16} \beta_b^2 - \frac{3}{16} \beta^2 \quad (2.18b)$$

$$\frac{u(\beta)}{c} = \beta \left[(1 - \nu) s_r(\beta_b) + \frac{(1 - \nu)}{16} \beta_b^2 - \frac{(3 - \nu)}{16} \beta^2 \right] \quad (2.18c)$$

$$p(\beta) = \frac{Eh}{c} \left[2 s_r(\beta_b) + \frac{1}{8} \beta_b^2 - \frac{1}{4} \beta^2 \right] \quad (2.18d)$$

The displacement $w(\beta)$ is found by integration of Eq. (2.3a):

$$w(\beta) = w(\beta_b) - \frac{c}{2} (\beta_b^2 - \beta^2) \quad (2.18e)$$

A necessary condition to be satisfied for contact between indenter and membrane in $0 \leq \beta \leq \beta_b$, is that $p(\beta) \geq 0$. This condition is seen to be fulfilled if

$$s_\theta(\beta_b) > 0 \quad (2.19)$$

This latter condition is necessary, however, for the stability of the free membrane against wrinkling [Ref. 1, Eq. (3.16)] and must be imposed for a rotationally symmetric solution to the indenter problem. It will be shown in the following section [see Eq. (3.35)] that (2.19) is satisfied.

The equilibrium of the indenter at the point of tangency, $\beta = \beta_b$, requires

$$P = 2\pi E h b \beta_b s_r(\beta_b)$$

which is written as

$$\frac{P}{2\pi E h a} = \beta_b^2 \frac{c}{a} s_r(\beta_b) \quad (2.20)$$

SECTION 3. SOLUTION OF THE INDENTER PROBLEM

Solutions from Section 1 for the free region and from Section 2 for the constrained region are now used. Solutions for these two regions are distinguished by the use of y as independent variable in the free region and of β as independent variable in the constrained region. At the point of tangency $r = b$ ($y = \epsilon^2$ for the free region and $\beta = \beta_b$ for the constrained region), conditions of continuity of displacements and normal stress are imposed. From Eq. (1.4),

$$s_r(\epsilon^2) = \left(\frac{1}{2} \epsilon \rho \right)^{2/3} \frac{F(\epsilon^2)}{\epsilon^2} \quad (3.1)$$

where, from Eq. (1.1c),

$$\epsilon \rho \equiv \frac{P}{2\pi Eha} \quad (3.2)$$

Continuity of s_r requires

$$s_r(\epsilon^2) = s_r(\beta_b) \quad (3.3)$$

This equation, after substitution from Eqs. (1.8b), (2.20), (3.1) and (3.2), can be written as

$$F_\epsilon = \left(\frac{2P}{\pi Eha} \right)^{1/3} \frac{c}{a} \quad (3.4)$$

Note that F_ϵ does not depend upon ϵ .

Continuity of the displacement u is invoked to determine b , or what is equivalent, the nondimensional parameter ϵ :

$$u(\epsilon^2) = u(\beta_b) \quad (3.5)$$

Equations (1.2), (1.7b), (1.8b) and (3.2) give

$$\frac{u(\epsilon^2)}{b} = \left(\frac{P}{4\pi Eha} \right)^{2/3} \left[2 \left(\frac{1}{F_\epsilon} + c_0 \right)^{1/2} - (1 + \nu) \frac{F_\epsilon}{\epsilon^2} \right] \quad (3.6)$$

Equation (2.18c) gives

$$\frac{u(\beta_b)}{b} = (1 - \nu) s_r(\beta_b) - \frac{1}{8} \beta_b^2 \quad (3.7a)$$

which can be written in the convenient form, using Eqs. (3.1) to (3.4),

$$\frac{u(\beta_b)}{b} = \left(\frac{P}{4\pi Eha} \right)^{2/3} \left[(1 - \nu) \frac{F_\epsilon}{\epsilon^2} - \frac{\epsilon^2}{2F_\epsilon^2} \right] \quad (3.7b)$$

Substitution from Eqs. (3.7b) and (3.6) into Eq. (3.5) leads to the following equation quadratic in ϵ^2 ,

$$\epsilon^4 + 4F_\epsilon^2 \left(\frac{1}{F_\epsilon} + C_0 \right)^{1/2} \epsilon^2 - 4F_\epsilon^3 = 0 \quad (3.8)$$

The only positive root is

$$\epsilon^2 = -2 F_\epsilon^2 \left(\frac{1}{F_\epsilon} + C_0 \right)^{1/2} + \left[4F_\epsilon^4 \left(\frac{1}{F_\epsilon} + C_0 \right) + 4F_\epsilon^3 \right]^{1/2}$$

which can be written simply as

$$\epsilon^2 = 2F_\epsilon^2 \left[\left(\frac{2}{F_\epsilon} + C_0 \right)^{1/2} - \left(\frac{1}{F_\epsilon} + C_0 \right)^{1/2} \right] \quad (3.9)$$

Equations (1.9) and (3.9) are used to determine ϵ and C_0 with F_0 and F_ϵ , or equivalently, with P and H_0 , through the use of Eqs. (1.8a) and (3.4), considered as independent variables.

Certain characteristics of the solutions ϵ and C_0 to Eqs. (1.9) and (3.9) for fixed $H_0 > 0$ are now studied. Restrictions of these developments to small indenter radii will be made subsequently as sufficient for applied purposes and in the interest of brevity.

First, it is observed that F_ϵ is expressible as a function of F_0 and H_0 by means of Eqs. (1.8a) and (3.9)

$$F_\epsilon = 2 \left(\frac{H_0}{Eh} \right)^{1/2} \frac{c}{a} F_0^{-(1/2)} \quad (3.10)$$

Therefore, for fixed H_0 , F_ϵ may be regarded as a function of F_0 only, viz. $F_\epsilon(F_0)$. Substitution of $F_\epsilon(F_0)$ into Eq. (3.9) yields

the function $\epsilon = \epsilon(F_0, C_0)$. Then the right-hand side of Eq. (1.9) can be defined by the function $I(F_0, C_0)$ as

$$I(F_0, C_0) = \int_{F_\epsilon(F_0)}^{F_0} \left(\frac{1}{v} + C_0 \right)^{-(1/2)} dv \quad (3.11)$$

and then Eq. (1.9) can be written as

$$\epsilon^2(F_0, C_0) + I(F_0, C_0) - 1 = 0 \quad (3.12)$$

Equation (3.12) will be shown to determine implicitly a function $C_0(F_0)$, which can be regarded as the solution to the problem. Since $0 \leq \epsilon < 1$ is a geometrical constraint, then by Eq. (3.12) $0 < I(F_0, C_0(F_0)) \leq 1$. It is necessary to consider the left-hand side of Eq. (3.12) in the F_0, C_0 plane within the allowable domain^{*} which is determined by the two inequalities

$$\frac{1}{F_0} + C_0 > 0 \quad (3.13a)$$

$$0 < F_\epsilon < \left(\frac{H_0}{Eh} \right)^{1/3} \left(\frac{2c}{a} \right)^{2/3} < F_0 \quad (3.13b)$$

Inequality (3.13b) follows from Eq. (3.10) and the inequality $I > 0$, which implies $F_0 > F_\epsilon > 0$.

It is evident from Eqs. (3.9), (3.10) and (3.11) that $\epsilon(F_0, C_0)$ and $I(F_0, C_0)$ are continuous functions of F_0 and C_0 in the allowable domain. The partial derivative with respect to C_0 of the left-hand side of Eq. (3.12) is

^{*}) It is shown in Ref. 1 that if wrinkling is to be avoided, $C_0(F_0)$ must be confined to a smaller domain which lies wholly within the allowable domain.

$$\begin{aligned} \frac{\partial}{\partial C_0} (\epsilon^2 + I - 1) = & -\frac{1}{2} \epsilon^2 \left(\frac{2}{F_\epsilon} + C_0\right)^{-(1/2)} \left(\frac{1}{F_\epsilon} + C_0\right)^{-(1/2)} \\ & - \frac{1}{2} \int_{F_\epsilon}^{F_0} \left(\frac{1}{v} + C_0\right)^{-3/2} dv \end{aligned} \quad (3.14a)$$

Therefore, in the allowable domain, the right-hand side above is negative, and so

$$\frac{\partial}{\partial C_0} (\epsilon^2 + I - 1) < 0 \quad (3.14b)$$

This partial derivative is a continuous function of F_0 and C_0 . The partial derivative with respect to F_0 of the left-hand side of Eq.(3.12) is

$$\begin{aligned} \frac{\partial}{\partial F_0} (\epsilon^2 + I - 1) = & \left(\frac{1}{F_0} + C_0\right)^{-(1/2)} \\ & + \frac{\partial F_\epsilon}{\partial F_0} \left[\frac{2\epsilon^2}{F_\epsilon} - 2\left(\frac{2}{F_\epsilon} + C_0\right)^{-(1/2)} \right] \end{aligned} \quad (3.15a)$$

where with the use of Eq.(3.10),

$$\frac{\partial F_\epsilon}{\partial F_0} = -\frac{1}{2} F_\epsilon F_0^{-1} \quad (3.15b)$$

Then Eq.(3.15a) becomes

$$\frac{\partial}{\partial F_0} (\epsilon^2 + I - 1) = \left(\frac{1}{F_0} + C_0\right)^{-(1/2)} - \frac{\epsilon^2}{F_0} + \frac{F_\epsilon}{F_0} \left(\frac{2}{F_\epsilon} + C_0\right)^{-(1/2)} \quad (3.15c)$$

When $C_0 = 0$, let $F_0 = F_0^*$ be a root of Eq.(3.12). From Eqs.(3.9), (3.11) and (3.12), an equation for F_0^* is easily derived:

$$F_0^{*3/2} = \frac{3}{2} \left[1 - 2\left(\sqrt{2} - \frac{4}{3}\right) F_\epsilon^{*3/2} \right] \quad (3.16)$$

where $F_c^* = F_\epsilon(F_0^*)$.

For convenience, a new parameter κ is now defined as

$$\kappa \equiv \left(\frac{H_0}{Eh} \right)^{1/3} \left(\frac{2c}{a} \right)^{2/3} \quad (3.17)$$

By the right-hand inequality of (3.13b), κ is a lower bound on F_0^* in the allowable domain. In general, κ may have any positive value depending on the prestress and the radius of the indenter. It is shown in Appendix A that there exists a unique value of F_0^* which satisfies Eq.(3.16) and inequalities (3.13a,b) if and only if κ satisfies inequality (10A), which is

$$0 < \kappa < \left(\frac{\sqrt{2}+1}{2} \right)^{2/3} \quad (3.18)$$

For larger values of κ , F_0^* does not exist. But for most practical cases, κ does satisfy inequality (3.18) and, in fact, if the indenter is comparatively small, satisfies the stronger inequality

$$\kappa \ll 1 \quad (3.19a)$$

To show this, we observe that since $\sigma_{r0} < \sigma_L$ and $s_L \equiv (\sigma_L/E) \ll 1$, then $(H_0/Eh) = \sigma_{r0}/E \ll 1$. Therefore, unless the indenter radius is of the order of the membrane radius ($c/a \gtrsim 1$), (3.19a) is surely valid, and, further, with the use of the results of Appendix A, Eq.(3.16) can be written in this case as

$$F_0^* = \left(\frac{3}{2} \right)^{2/3} [1 - O(\kappa^{9/4})] \cong \left(\frac{3}{2} \right)^{2/3} \quad (3.19b)$$

With κ satisfying the weaker inequality (3.18), the existence of C_0 as a continuous function of F_0 is now shown in the subdomain

$$C_0 \geq 0 \quad (3.20a)$$

of the allowable domain (3.13a,b), where (3.13b) can be written equivalently as

$$F_0 > \kappa > F_c \quad (3.20b)$$

For $C_0 = 0$ Eq.(3.15c) is written with the use of Eq.(3.9) as

$$\left. \frac{\partial}{\partial F_0} (\epsilon^2 + I - 1) \right|_{C_0=0} = F_0^{1/2} \left[1 - \left(\frac{3 - 2\sqrt{2}}{\sqrt{2}} \right) \left(\frac{F_\epsilon}{F_0} \right)^{3/2} \right]$$

The right-hand side above is positive by inequality (3.20b). Furthermore, since $C_0 = 0$, $F_0 = F_0^*$ is the root of Eq.(3.12)

$$\left. (\epsilon^2 + I - 1) \right|_{\substack{C_0=0 \\ F_0=F_0^*}} = 0$$

Therefore,

$$\left. (\epsilon^2 + I - 1) \right|_{\substack{C_0=0 \\ F_0 < F_0^*}} < 0 \quad \text{and} \quad \left. (\epsilon^2 + I - 1) \right|_{\substack{C_0=0 \\ F_0 > F_0^*}} > 0 \quad (3.21a)$$

It can be shown, with the use of Eqs.(3.9), (3.10) and (3.11), that

$$\lim_{\substack{C_0 \rightarrow \infty \\ F_0 \text{ fixed}}} \epsilon^2 = 0 \quad \text{and} \quad \lim_{\substack{C_0 \rightarrow \infty \\ F_0 \text{ fixed}}} I = 0,$$

from which it follows that

$$\lim_{\substack{C_0 \rightarrow \infty \\ F_0 \text{ fixed}}} (\epsilon^2 + I - 1) = -1 \quad (3.21b)$$

Inequality (3.14b) implies that $(\epsilon^2 + I - 1)$ is a monotone, strictly decreasing function of C_0 for a fixed F_0 . Therefore, it follows from (3.21a,b) that for each $F_0 \geq F_0^*$, there exists a unique positive value of C_0 such that Eq.(3.12) is satisfied. The continuity of $C_0(F_0)$ follows from a theorem on implicit functions [Ref. 4].

In view of the above results, we will now show that $C_0(F_0)$ is a monotone increasing function of F_0 for $F_0 \geq F_0^*$. However, proof of this will depend upon the additional assumption that κ is small, i.e., that (3.19a) holds. Then the right-hand inequality of (3.20b) shows that

$$F_\epsilon \ll 1 \quad (3.22)$$

For any fixed F_ϵ , let Eq.(3.9) be regarded as expressing the function $\epsilon^2(C_0)$ for $C_0 \geq 0$. It is easily shown that $\epsilon^2(C_0)$ is a monotone decreasing function and hence that

$$\epsilon^2(C_0) \leq 2(\sqrt{2} - 1)F_\epsilon^{3/2} \quad (3.23)$$

where the equality holds only for $C_0 = 0$. Then from (3.22) it follows

$$\epsilon^2 \ll 1 \quad (3.24)$$

for all $C_0 \geq 0$.

For $F_0 \geq F_\epsilon^*$, upper and lower bounds for $C_0(F_0)$ are obtained when Eq.(3.11) is rewritten as

$$I(F_0, C_0) = \int_{F_\epsilon}^{F_0} C_0^{-(1/2)} dv - C_0^{-(1/2)} \left\{ \int_{F_\epsilon}^{F_0} \left[1 - \left(1 + \frac{1}{vC_0} \right)^{-(1/2)} \right] dv \right\}$$

This becomes

$$I(F_0, C_0) = \frac{F_0 - F_\epsilon}{C_0^{1/2}} - C_0^{-(1/2)} R \quad (3.25)$$

where

$$R \equiv \int_{F_\epsilon}^{F_0} \left[1 - \left(1 + \frac{1}{vC_0} \right)^{-(1/2)} \right] dv \quad (3.26)$$

It is easily shown that

$$0 < R < C_0^{-1} \ln \left(\frac{1 + C_0 F_0}{1 + C_0 F_\epsilon} \right) \quad (3.27)$$

Then Eqs.(3.12) and (3.25) are used to obtain

$$(1 - \epsilon^2) C_0^{1/2} = F_0 - F_\epsilon - R < F_0,$$

which yields

$$F_o^2 \left[1 - \frac{F_\epsilon}{F_o} - \frac{1}{F_o C_o} \ln \left(\frac{1 + F_o C_o}{1 + F_\epsilon C_o} \right) \right]^2 < C_o < F_o^2 [1 + O(\epsilon^2)] \quad (3.28)$$

With the right inequality and Eq.(3.10), an upper bound for $F_\epsilon C_o$ is obtained

$$F_\epsilon C_o < 2 \left(\frac{H_o}{Eh} \right)^{1/2} \frac{c}{a} F_o^{3/2} [1 + O(\epsilon^2)] \quad (3.29)$$

Equation (3.15c) with the use of the right-hand inequality of (3.28) yields

$$\frac{\partial}{\partial F_o} (\epsilon^2 + I - 1) > \frac{1}{F_o} \left\{ \left[1 + O(\epsilon^2) + \frac{1}{F_o} \right]^{-(1/2)} - \epsilon^2 + F_\epsilon \left(\frac{2}{F_\epsilon} + C_o \right)^{-(1/2)} \right\} \quad (3.30)$$

From this inequality it is evident that

$$\frac{\partial}{\partial F_o} (\epsilon^2 + I - 1) > 0 \quad (3.31)$$

in the subdomain (3.20a,b).

The differential of Eq.(3.12) yields an expression for the derivative of $C_o(F_o)$:

$$\frac{dC_o}{dF_o} = - \left[\frac{\partial}{\partial F_o} (\epsilon^2 + I - 1) / \frac{\partial}{\partial C_o} (\epsilon^2 + I - 1) \right] \quad (3.32)$$

In view of inequalities (3.14b) and (3.31), this derivative is positive for all $F_o \geq F_o^*$. This implies that the solution to Eq.(3.12) expressed by $C_o(F_o)$ is a continuous, monotone strictly increasing function.

The final topic considered in this section is the stability of the free membrane against wrinkling. It has been shown in Ref. 1 (see Appendix: II, p.43), that the wrinkling stability condition is satisfied if

$$s_\theta(1) \geq 0 \quad (3.33a)$$

and

$$s_{\theta}(\epsilon^2) \geq 0 \quad (3.33b)$$

It can easily be shown that (3.33a) is satisfied if

$$C_0 \geq \frac{F_0^2}{4} - \frac{1}{F_0} \quad (3.34)$$

This inequality is satisfied both for $F_0 = F_0^*$ and for $F_0 \gg 1$. Furthermore, the numerical solutions for $C_0(F_0)$ show that inequality (3.34) is satisfied for all $F_0 \geq F_0^*$.

An expression for $s_{\theta}(\epsilon^2)$ is obtained with the use of Eqs. (2.18b) and (2.20) as

$$s_{\theta}(\epsilon^2) = \frac{1}{8\left(\frac{c}{a}\right)^2 \epsilon^2} \left[\frac{4P}{\pi Ehc} \left(\frac{c}{a}\right)^4 - \epsilon^4 \right] \quad (3.35)$$

Inequality (3.23), with the use of Eq. (3.4), implies that

$$\epsilon^2 < \left(\frac{4P}{\pi Ehc}\right)^{1/2} \left(\frac{c}{a}\right)^2 \quad (3.36)$$

Therefore, with the use of (3.36) and (3.35), it is concluded that inequality (3.33b) is satisfied for all $F_0 \geq F_0^*$. Hence, in particular, the membrane is stable against wrinkles for $P \leq P_L$, where P_L is defined below by (4.6), and when the prestress satisfies inequality (4.8).

SECTION 4. APPROXIMATE SOLUTIONS FOR LIMITING CASES

In Section 3, the exact solution for the indenter problem was shown to exist with κ in the range (3.18), and for $F_o \geq F_o^*$. This solution is now used to obtain approximate solutions for certain limiting cases.

In the first case, we will determine a load P_L which is an upper bound on P , meaning that if $P > P_L$ and $F_o \geq F_o^*$, then the maximum value of the normal stress components will certainly exceed the elastic limit stress σ_L . It will be initially assumed that $P = P_L$ determines a value $F_o = F_{oL}$ such that

$$F_{oL} > F_o^* \quad (4.1a)$$

This restriction on F_{oL} will be shown to imply that the prestress must be chosen to be greater than a lower bound [Eq.(4.8)] for these present results to hold. Furthermore, inequality (4.1a) assures the existence and uniqueness of a positive-valued $C_{oL} \equiv C_o(F_{oL})$ in the exact solution.

Consider any value of $P \leq P_L$. Then $F_o \geq F_{oL}$, and there is a unique value of $C_o > 0$ for this value of P . The corresponding value of ϵ^2 is given uniquely by Eq.(3.9). An upper bound on this value of ϵ^2 is given by inequality (3.23) which, through use of Eq.(3.4), can be written in terms of P :

$$\epsilon^2 < 4(\sqrt{2}-1)\left(\frac{c}{a}\right)^{3/2} \left(\frac{P}{2\pi Eha}\right)^{1/2} \quad (4.1b)$$

It follows from Eqs.(2.18a,b) that the maximum value of normal stress components in the constrained region occurs directly underneath the indenter (i.e., at $\beta = 0$ or $r = 0$); it is, furthermore, a consequence of these equations and Theorem (5.3) of Ref. 1 that this is also the location of the maximum value for the entire membrane. From Eqs.(2.18a) and (2.20), therefore,

$$s_r(0) = \frac{P}{2\pi Ehc} \beta_b^{-2} + \frac{1}{16} \beta_b^2 \quad (4.2a)$$

where, from Eqs.(1.1c) and (2.12a),

$$\beta_b^2 = \left(\frac{b}{c}\right)^2 = \left(\frac{a}{c}\right)^2 \epsilon^2 \quad (4.2b)$$

From Eq.(4.2b) and inequality (4.1b), it can be concluded at once that, if $P \leq P_L$ and (4.1a) holds, then the actual value of β_b^2 must be bounded as

$$0 < \beta_b^2 < \beta_b'^2 \quad (4.3a)$$

where

$$\beta_b'^2 \equiv 4(\sqrt{2}-1) \left(\frac{P}{2\pi Ehc}\right)^{1/2} \quad (4.3b)$$

Now, if the right-hand side of Eq.(4.2a) is considered as a function of β_b^2 for a fixed value of P , then it is readily shown that this function is monotonically increasing as β_b^2 decreases for β_b^2 in the interval

$$0 < \beta_b^2 < 4 \left(\frac{P}{2\pi Ehc}\right)^{1/2} \quad (4.4)$$

The interval (4.3a) for β_b is contained in the interval (4.4), and so the actual value of $s_r(0)$ has a lower bound:

$$s_r(0) \Big|_{\beta_b^2} > s_r(0) \Big|_{\beta_b'^2} \quad (4.5a)$$

Substitution from Eq.(4.3b) into the right-hand side of Eq.(4.2a) then leads to the following condition for the actual value of $s_r(0)$:

$$s_r(0) > \left(\frac{P}{4\pi Ehc}\right)^{1/2} \quad (4.5b)$$

The value $P = P_L$ is taken, by definition, as that which makes the right-hand side of (4.5b) equal to s_L ; thus

$$P_L \equiv 4\pi Ehc s_L^2 \quad (4.6)$$

and

$$F_{oL} \equiv \left(\frac{H_o}{Eh} \right) \left(\frac{4\pi Eha}{P_L} \right)^{2/3} \equiv \left(\frac{H_o}{Eh} \right) \left(\frac{a}{c} \right)^{2/3} s_L^{-4/3} \quad (4.7)$$

From Eq.(4.7) it is seen that condition (4.1a) is satisfied if the pre-stress is large enough and satisfies

$$\frac{H_o}{Eh} > \left(\frac{c}{a} \right)^{2/3} s_L^{4/3} F_o^* \quad (4.8)$$

Since $F_o^* \sim O(1)$, from Eq.(9A), and since (4.8) can be written as

$$\frac{\sigma_{ro}}{\sigma_L} > \left[\left(\frac{c}{a} \right)^2 s_L \right]^{1/3} F_o^*, \quad (4.9a)$$

then this lower bound on σ_{ro}/σ_L can be quite small for sufficiently small indenter radii. If $(c/a) < 1$, then

$$\left[\left(\frac{c}{a} \right)^2 s_L \right]^{1/3} \ll 1 \quad (4.9b)$$

Under certain further restrictions, it can now be shown that $s_r(0) \approx s_L$ for $P = P_L$ and expressions for β_b , $s_r(\beta_b)$ and $s_r(0)$ for P near P_L can be derived. The first restriction is that κ is again assumed to be small and (3.19a) holds. Therefore, (3.22), (3.24), and (3.29) also hold. Upon substitution from Eq.(4.7) of $F_o = F_{oL}$ into the right-hand side of inequality (3.29), there is obtained for $F_\epsilon = F_{\epsilon L}$ and $C_o = C_{oL}$,

$$F_{\epsilon L} C_{oL} < 2 \left(\frac{\sigma_{ro}}{\sigma_L} \right)^2 [1 + O(c^2)] \quad (4.10a)$$

As a second restriction, ratio (σ_{ro}/σ_L) is assumed to satisfy

$$2 \left(\frac{\sigma_{ro}}{\sigma_L} \right)^2 \ll 1 \quad (4.10b)$$

This order relation evidently cannot be satisfied by any σ_{ro} unless

the square of the right-hand side of inequality (4.9a) is also small compared to one; this latter condition is independent of inequalities (3.19a) and (4.10b). However, a third restriction, sufficient but not necessary to insure the existence of a range for σ_{r_0} , is that (c/a) be small (see inequality (4.9b)). It can be seen that these three restrictions will not unduly limit the consideration of practical problems.

It follows then from (4.10a,b) that for $F_0 = F_{0L}$

$$F_{\epsilon} C_0 = F_{\epsilon L} C_{0L} \ll 1 \quad (4.11a)$$

Hence the following order relation will hold, by continuity, for F_0 in some neighborhood of F_{0L} and for P in some neighborhood of P_L :

$$0 < F_{\epsilon} C_0 \ll 1 \quad (4.11b)$$

Let Eq.(3.9) be approximated for small $F_{\epsilon} C_0$ as

$$\epsilon = [2(\sqrt{2}-1)]^{1/2} F_{\epsilon}^{3/4} [1 - O(F_{\epsilon} C_0)] \quad (4.12a)$$

$$\cong 2(\sqrt{2}-1)^{1/2} \left(\frac{c}{a}\right)^{3/4} \left(\frac{P}{2\pi E h a}\right)^{1/4} \quad (4.12b)$$

Hence this can be written as

$$b \cong 2(\sqrt{2}-1)^{1/2} \left(\frac{P c^3}{2\pi E h}\right)^{1/4} \quad (4.12c)$$

Expressions for β_b , $s_r(\beta_b)$ and $s_r(0)$ are now developed for P near P_L . By this is meant that these expressions are approximately valid at $P = P_L$ and also for other values of P such that (4.11b) is satisfied. From Eqs.(4.2b), (2.18a) and (2.20) with the use of the approximation (4.12c), one obtains:

$$\beta_b \cong 2(\sqrt{2}-1)^{1/2} \left(\frac{P}{2\pi E h c}\right)^{1/4} \quad (4.13a)$$

$$s_r(\beta_b) \cong \frac{1}{4(\sqrt{2}-1)} \left(\frac{P}{2\pi E h c}\right)^{1/2} = \frac{1}{16(\sqrt{2}-1)^2} \beta_b^2 \quad (4.13b)$$

$$s_r(0) \approx \frac{\sqrt{2}}{8(\sqrt{2}-1)} \beta_0^2 = \left(\frac{P}{4\pi E h c} \right)^{1/2} \quad (4.13c)$$

It is noted that these relations are independent of the prestress and membrane radius a . Also, the maximum stress in the membrane, which occurs at $\beta = 0$ (i.e., $r = 0$), increases with P . Then for $P = P_L$, the maximum stress in the membrane, evaluated with the use of Eqs. (4.13a,c) and (4.6), is

$$s_r(0) \Big|_{P=P_L} \approx s_L \quad (4.13d)$$

Before considering the second limiting case, we will derive an exact expression for $w(\epsilon^2)$ with the use of Eq.(1.10). We substitute $y = \epsilon^2$ into the right-hand side of Eq.(1.10) and write it as

$$\frac{w(\epsilon^2)}{a} = -2 \left(\frac{H_0/Eh}{F_0 C_0} \right)^{1/2} \left[F_0 C_0 \left(1 + \frac{1}{F_0 C_0} \right)^{1/2} - F_\epsilon C_0 \left(1 + \frac{1}{F_\epsilon C_0} \right)^{1/2} - C_0^{3/2} (1 - \epsilon^2) \right] \quad (4.14)$$

For positive C_0 , the definite integral in Eq.(3.11) can be evaluated in closed form [Ref. 1, Eq.(4.17)], and $I(F_0, C_0)$ can be written as

$$I(F_0, C_0) = C_0^{-3/2} \left\{ F_0 C_0 \left(1 + \frac{1}{F_0 C_0} \right)^{1/2} - F_\epsilon C_0 \left(1 + \frac{1}{F_\epsilon C_0} \right)^{1/2} - \ln \left[\left(\frac{F_0}{F_\epsilon} \right)^{1/2} \frac{1 + \left(1 + \frac{1}{F_0 C_0} \right)^{1/2}}{1 + \left(1 + \frac{1}{F_\epsilon C_0} \right)^{1/2}} \right] \right\} \quad (4.15)$$

In view of Eq.(3.12), $(1 - \epsilon^2)$ in Eq.(4.14) can be replaced by the right-hand side of Eq.(4.15). With this substitution, Eq.(4.14) simplifies to

$$\frac{w(\epsilon^2)}{a} = -2 \left(\frac{H_o/Eh}{F_o C_o} \right)^{1/2} \ln \left[\left(\frac{F_o}{F_\epsilon} \right)^{1/2} \frac{1 + \left(1 + \frac{1}{F_o C_o} \right)^{1/2}}{1 + \left(1 + \frac{1}{F_\epsilon C_o} \right)^{1/2}} \right] \quad (4.16)$$

In the second limiting case, the exact solution of Section 3 is approximated for small values of P and for fixed prestress σ_{ro} . If P is sufficiently small, so that

$$F_o \gg 1, \quad (4.17a)$$

then it can be shown with the use of inequality (3.28) that

$$C_o \approx F_o^2 \quad (4.17b)$$

In view of Eqs.(3.10) and (4.17b), sufficiently large values of F_o are considered such that the order relation

$$F_\epsilon C_o \gg 1 \quad \text{or, equivalently} \quad F_\epsilon F_o^2 \gg 1 \quad (4.17c)$$

holds in addition to (4.17a). This latter inequality, with the use of Eqs.(1.8a) and (3.4), implies that

$$\left(\frac{Eh}{H_o} \right)^2 \frac{P}{8\pi Ehc} \ll 1 \quad (4.17d)$$

The above inequality then gives the restriction on the values of P for the approximate solution derived below to be valid.

In view of the first inequality of (4.17c), the right-hand side of Eq.(3.9) can be written as

$$\epsilon^2 = \frac{F_\epsilon}{C_o^{1/2}} \left[1 - \frac{3}{4F_\epsilon C_o} + O\left(F_\epsilon^{-2} C_o^{-2} \right) \right] \approx \frac{F_\epsilon}{C_o^{1/2}} \quad (4.18a)$$

This approximation for ϵ^2 , with the use of Eqs.(4.17b), (1.8a) and (3.4) reduces to

$$\epsilon^2 \approx \frac{F_\epsilon}{F_0} = \frac{c}{a} \left(\frac{P}{2\pi a H_0} \right) \quad (4.18b)$$

Again, in view of (4.17c), the right-hand side of Eq.(4.16) is written as

$$\begin{aligned} \frac{w(\epsilon^2)}{a} &= -2 \left(\frac{H_0/Eh}{F_0 C_0} \right)^{1/2} \left[\ln \left(\frac{F_0}{F_\epsilon} \right)^{1/2} + \frac{1}{4F_0 C_0} - \frac{1}{4F_\epsilon C_0} + o(F_0^{-2} C_0^{-2}) + o(F_0^{-2} C_0^{-2}) \right] \\ &\approx - \left(\frac{H_0/Eh}{F_0 C_0} \right)^{1/2} \ln \left(\frac{F_0}{F_\epsilon} \right) \end{aligned} \quad (4.19a)$$

This approximate expression for $w(\epsilon^2)$ is then written in terms of the indenter load and the prestress by using Eqs.(4.17b), (1.8a) and (3.4).

$$w(\epsilon^2) \approx - \frac{P}{4\pi H_0} \ln \left[\frac{a}{c} \left(\frac{2\pi a H_0}{P} \right) \right] \quad (4.19b)$$

The central deflection $w(\beta=0)$ is obtained from Eq.(2.18e) as

$$w(0) = - \frac{c}{2} \beta_b^2 + w(\epsilon^2) \quad (4.20a)$$

This is approximated, with the use of Eqs.(4.19b), (4.18b) and (4.2b) as

$$w(0) \approx - \frac{P}{4\pi H_0} \left[1 + \ln \left(\frac{a}{c} \frac{2\pi a H_0}{P} \right) \right] \quad (4.20b)$$

Finally, approximate expressions for $s_r(\beta_b)$ and $s_r(0)$ are obtained for small P by using Eqs.(4.18b), (4.2b), (2.20) and (2.18a):

$$s_r(\beta_b) = \frac{H_0}{Eh} \quad (4.21a)$$

$$s_r(0) = \frac{H_0}{Eh} + \frac{P}{32\pi c H_0} \quad (4.21b)$$

Equations (4.19b) and (4.21a) can also be obtained from the familiar linearized membrane theory in which it is assumed that $s_r(r) = \text{constant} = (Eh)^{-1}H_0$ for the free portion of the membrane $b \leq r \leq a$. Hence, the order relation (4.17d) is necessary and sufficient for linearized membrane theory to be a valid approximation to nonlinear membrane theory. As is also well-known from linearized membrane theory, the deflection of the membrane under a point load has a logarithmic singularity under the load: this behavior is demonstrated in the right-hand side of Eq.(4.19b) when c/a tends to zero for fixed P and H_0 . However, it will be shown in the development to follow that nonlinear membrane theory predicts a markedly different behavior in this limiting case, and the logarithmic singularity is not correct.

In all of the results obtained in this paper up to this point, it has been assumed that the radius c of the indenter is greater than zero. The dependence of the solution upon the parameter c/a has not been investigated. In particular, although existence of a solution has been proven for all $(c/a) > 0$, the existence of a limit solution for c/a going to zero has not been shown.

In the third limiting case, expressions for the stresses and the displacement component w are now obtained from the exact solution in the limit when radius of the indenter c tends to zero for fixed values of indenter load P and prestress H_0 (and, consequently, for fixed F_0). Equation (3.4) shows that

$$\lim_{\substack{(c/a) \rightarrow 0 \\ P \text{ fixed}}} F_\epsilon = 0 \quad (4.22a)$$

Furthermore, since $\epsilon \leq c/a$, it is clear that

$$\lim_{(c/a) \rightarrow 0} \epsilon = 0 \quad (4.22b)$$

It will be shown that for all F_0 obeying

$$F_0 > \left(\frac{3}{2}\right)^{2/3}, \quad (4.23a)$$

$C_0(F_0)$ approaches a finite and positive limit \bar{C}_0 with the bounds

$$0 < \lim_{\substack{(c/a) \rightarrow 0 \\ F_0 \text{ fixed}}} C_0 \equiv \bar{C}_0(F_0) < F_0^2 \quad (4.23b)$$

Let us first review some previously obtained results which apply for c/a positive but arbitrarily small. In Appendix A it is shown that when κ satisfies (3.18) there exists a unique $F_0 = F_0^* < (3/2)^{2/3}$ for which $C_0 = 0$. Furthermore, for small values of κ which satisfy (3.19a), $C_0(F_0)$ is a monotone increasing function of F_0 for all $F_0 \geq F_0^*$, as was shown in Section 3. Hence, if F_0 satisfies (4.23a) and κ satisfies (3.19a), then $C_0(F_0)$ is positive. Furthermore, in view of the right-hand inequality of (3.28), $C_0(F_0)$ has an upper bound value for small (c/a) .

Therefore, it is clear that C_0 remains bounded as $(c/a) \rightarrow 0$ for a fixed F_0 which satisfies (4.23a). Hence, in view of (4.22a), there is obtained

$$\lim_{\substack{(c/a) \rightarrow 0 \\ F_0 \text{ fixed}}} (F_0 C_0) = 0 \quad (4.24)$$

It is now shown that the limiting value of C_0 as $(c/a) \rightarrow 0$ exists. For a fixed H_0 , we write $C_0(F_0, \eta)$ as an implicit function of F_0 and η for F_0 in (4.23a) and $\eta > 0$, where

$$\eta \equiv \frac{c}{a} \quad (4.25)$$

The partial derivative of C_0 with respect to η for fixed F_0 is determined by taking the partial derivative with respect to η of both sides of each of the Eqs. (3.9), (3.10), (3.11) and (3.12) and evaluating as follows:

$$\begin{aligned}
\frac{\partial \epsilon^2}{\partial \eta} &= \frac{\partial \epsilon^2}{\partial F_\epsilon} \frac{\partial F_\epsilon}{\partial \eta} + \frac{\partial \epsilon^2}{\partial C_0} \frac{\partial C_0}{\partial \eta} \\
&= \left[\frac{2\epsilon^2}{F_\epsilon} + \left(\frac{1}{F_\epsilon} + C_0 \right)^{-1/2} - 2 \left(\frac{2}{F_\epsilon} + C_0 \right)^{-1/2} \right] \frac{\partial F_\epsilon}{\partial \eta} \\
&+ F_\epsilon^2 \left[\left(\frac{2}{F_\epsilon} + C_0 \right)^{-1/2} - \left(\frac{1}{F_\epsilon} + C_0 \right)^{-1/2} \right] \frac{\partial C_0}{\partial \eta} \quad (4.26)
\end{aligned}$$

$$\frac{\partial F_\epsilon}{\partial \eta} = 2 \left(\frac{H_0/Eh}{F_0} \right)^{-1/2} \quad (4.27)$$

$$\frac{\partial I}{\partial \eta} = - \frac{\partial F_\epsilon}{\partial \eta} \left(\frac{1}{F_\epsilon} + C_0 \right)^{-1/2} - \frac{1}{2} \frac{\partial C_0}{\partial \eta} \int_{F_\epsilon}^{F_0} \left(\frac{1}{v} + C_0 \right)^{-3/2} dv \quad (4.28)$$

and

$$\frac{\partial \epsilon^2}{\partial \eta} + \frac{\partial I}{\partial \eta} = 0 \quad (4.29)$$

Upon substitution of the right-hand sides of Eqs.(4.26) and (4.28) into Eq.(4.29), there is obtained

$$\begin{aligned}
\frac{\partial C_0}{\partial \eta} &= 4 \frac{\partial F_\epsilon}{\partial \eta} \left[\frac{\epsilon^2}{F_\epsilon} - \left(\frac{2}{F_\epsilon} + C_0 \right)^{-1/2} \right] \left\{ \int_{F_\epsilon}^{F_0} \left(\frac{1}{v} + C_0 \right)^{-3/2} dv - 2F_\epsilon^2 \cdot \right. \\
&\quad \left. \left[\left(\frac{2}{F_\epsilon} + C_0 \right)^{-1/2} - \left(\frac{1}{F_\epsilon} + C_0 \right)^{-1/2} \right] \right\}^{-1} \quad (4.30a)
\end{aligned}$$

In view of (4.24), Eq.(4.30a) is approximated for small $(F_\epsilon C_0)$, with use of Eq.(3.9):

$$\begin{aligned}
\frac{\partial C_0}{\partial \eta} &= 4 \frac{\partial F_\epsilon}{\partial \eta} \left(\frac{3-2\sqrt{2}}{\sqrt{2}} \right) F_\epsilon^{1/2} \left[1 - \frac{(4\sqrt{2}-5)}{4(3-2\sqrt{2})} (F_\epsilon C_0) + o(F_\epsilon^2 C_0^2) \right] \left\{ \int_{F_\epsilon}^{F_0} \left(\frac{1}{v} + C_0 \right)^{-3/2} \right. \\
&\quad \left. + \sqrt{2}(\sqrt{2}-1) F_\epsilon^{5/2} \left[1 - \frac{(2\sqrt{2}-1)}{4(\sqrt{2}-1)} (F_\epsilon C_0) + o(F_\epsilon^2 C_0^2) \right] \right\}^{-1} \\
&\cong 2\sqrt{2}(3-2\sqrt{2}) F_\epsilon^{1/2} \frac{\partial F_\epsilon}{\partial \eta} \left[\int_{F_\epsilon}^{F_0} \left(\frac{1}{v} + C_0 \right)^{-3/2} dv + \sqrt{2}(\sqrt{2}-1) F_\epsilon^{5/2} \right]^{-1} \quad (4.30b)
\end{aligned}$$

The right-hand side above being always positive,

$$\frac{\partial C_0}{\partial \eta} > 0 \quad \text{for } \eta > 0, \quad (4.30c)$$

C_0 decreases monotonically with decreasing η for fixed F_0 . Furthermore, since the integral term on the right-hand side of Eq.(4.30b) is intrinsically positive, then from (4.22a) and Eqs.(4.27) and (4.30b) there is obtained

$$\lim_{\substack{\left(\frac{c}{a}\right) \rightarrow 0 \\ F_0 \text{ fixed}}} \frac{\partial C_0}{\partial \eta} = 0 \quad (4.30d)$$

Since, for each F_0 in (4.23a), $C_0(F_0, \eta)$ is bounded and monotone, then $\bar{C}_0(F_0)$ exists [Ref. 5] and is continuous [Ref. 6]. With the use of Eqs.(3.11) and (3.12), $\bar{C}_0(F_0)$ as an implicit function of F_0 is given by

$$\int_0^{F_0} \left(\frac{1}{v} + \bar{C}_0 \right)^{-1/2} dv - 1 = 0 \quad (4.31)$$

From this, we get

$$\frac{d\bar{c}_o}{dF_o} = \left[\frac{1}{2} \left(\frac{1}{F_o} + \bar{c}_o \right)^{1/2} \int_0^{F_o} \left(\frac{1}{v} + \bar{c}_o \right)^{-3/2} dv \right]^{-1}$$

The right-hand side above is positive, which shows that \bar{c}_o is positive (cf. (4.23b)), and the same expression is also obtained from Eq.(3.32) in the limit.

A limiting finite value for the displacement component $w(\epsilon^2)$ is now obtained from Eq.(4.14):

$$\lim_{\substack{(c/a) \rightarrow 0 \\ F_o \text{ fixed}}} \frac{w(\epsilon^2)}{a} = -2 \left(\frac{H_o/Eh}{F_o \bar{c}_o} \right)^{1/2} \left[F_o \bar{c}_o \left(1 + \frac{1}{F_o \bar{c}_o} \right)^{1/2} - \bar{c}_o^{3/2} \right] \quad (4.32)$$

It is important to note that the right-hand side of Eq.(4.32) is finite, and so the deflection of the membrane at the point of tangency remains finite as c/a tends to zero.

From geometrical considerations, it could be expected that $w(0)$ would approach $w(\epsilon^2)$ as c/a tended to zero for fixed F_o , and that the right-hand side of Eq.(4.32) would also represent the limiting value of $w(0)$. However, this limit cannot be taken even with the exact solution obtained in Section 3. To understand why this is, we look first at Eq.(2.20) and replace β_b^2 there by the complete expression $\sin^2 \beta_b$. It is apparent then that as c/a tends toward zero, with the value for P fixed, $\sigma_r(\beta_b)$ becomes infinite. Thus, the small strain assumption will be violated underneath the indenter for sufficiently small c/a , and this in turn would invalidate our analysis in Section 2. In this case we could not show (2.11), and, indeed, it is easily shown that the limiting value of β_b from the exact solution is infinite.

With use of (4.24), the right-hand side of Eq.(3.9) can be expanded as

$$\epsilon^2 = 2(\sqrt{2}-1)F_\epsilon^{3/2} \left[1 - \frac{F_\epsilon C_0}{2\sqrt{2}} + o\left(\frac{F_\epsilon^2 C_0^2}{F_\epsilon C_0}\right) \right]$$

With neglect of higher-order terms, this expression can be used in Eq.(4.2b) to obtain

$$\begin{aligned} \beta_b^2 &\cong 2(\sqrt{2}-1) F_\epsilon^{3/2} \left(\frac{a}{c}\right)^2 \\ &= 4\sqrt{2}(\sqrt{2}-1) \left(\frac{H_0/Eh}{F_0}\right)^{3/4} \left(\frac{a}{c}\right)^{1/2} \end{aligned} \quad (4.33)$$

Although Eq.(4.33) does lead to the unacceptable conclusion that $\beta_b \rightarrow \infty$ as $c/a \rightarrow 0$, this expression is correct so long as $s_r(0) \ll 1$. Furthermore, with use of Eq.(4.33) we have

$$\lim_{\substack{\left(\frac{c}{a}\right) \rightarrow 0 \\ F_0 \text{ fixed}}} \left[-\frac{c}{2} \beta_b^2 \right] = 0$$

so that Eq.(4.20a) does show $w(0) = w(\epsilon^2)$ in the limit.

In conclusion, we remark that it is evidently not correct to take the limit, as $(c/a) \rightarrow 0$, of the linearized membrane theory expressions for stress and displacement which were obtained in the second limiting case above [Eqs.(4.19b), (4.20b) and (4.21a,b)]. The reason is that these linearized expressions were obtained by assuming that $(F_\epsilon C_0) \gg 1$, whereas the limit of $(F_\epsilon C_0)$ as $(c/a) \rightarrow 0$ is zero (4.24). The results of passing to the limit as $(c/a) \rightarrow 0$ in the linearized and nonlinear membrane theory are compared as follows:

<u>Linearized</u>	<u>Nonlinear</u>
$\lim w(\epsilon^2) = \infty$	$\lim w(\epsilon^2)$ is finite
$\lim w(0) = \infty$	$\lim w(0) = w(\epsilon^2)$
$\lim s_r(\beta_b) = H_0/Eh$	$\lim s_r(\beta_b) = \infty$
$\lim s_r(0) = \infty$	$\lim s_r(0) = \infty$

It is remarkable that the limiting values for $w(\epsilon^2)$ and $s_r(\beta_b)$ obtained with the use of the linearized theory are exactly opposite of the limiting values obtained from the nonlinear theory.

SECTION 5. NUMERICAL RESULTS AND COMPARISON WITH EXPERIMENTS

Experimental results have been reported [Ref. 2] for the central load-transverse deflection characteristics and the deflection profile of a mylar sheet^{*)} stretched in its plane by dead-weight loading. This load is referred to as the platen load. The sheet was supported by a ring of inner radius $a = 5$ inches. The transverse load P was applied at the center of the sheet by a load probe, or indenter, having a hemispherical tip of radius $c = 1/16$ inch. The membrane deflections were measured both by a dial gage and, in the immediate vicinity of the indenter, by measurements from photographic enlargements. Stresses were not measured directly, but σ_r was calculated from an equilibrium equation [the present Eq.(2.1b) with $p = 0$], and values of β were obtained by numerical differentiation of the deflections.

A comparison is now made between predictions of the present theory with the experimental data of Ref. 2. To determine the displacement w and stresses σ_r, σ_θ from the theory, it is first necessary to compute C_0 for each value of F_0 . Since for these experiments $c/a = 0.0125 \ll 1$, inequalities (3.19a), (3.22) and (3.24) are satisfied, and hence there exists a unique positive value of C_0 for each $F_0 > F_0^*$, as was shown in Section 3. The value of F_0^* is very nearly equal to $(3/2)^{2/3} = 1.310371$, as is shown by the right-hand side of Eq.(3.19b). If σ_{11} is taken as the uniaxial yield stress σ_y , then for these experiments $P_L = 0.0704$ lbs as computed from Eq.(4.6). The prestress used in the experiments was sufficiently large so that the condition $F_0 > F_0^*$ is satisfied not only for $P \leq P_L$ but also for a significant range of values for $P > P_L$. Hence, C_0 remains positive in this range, and the definite integral in Eq.(3.11) is given explicitly by Eq.(4.15).

We note that for $F_0 < F_0^*$ in the allowable domain (3.13), values of $C_0 < 0$ are possible and can be computed for the indenter problem

^{*)}Properties of mylar sheet: Thickness $h = 6.0 \times 10^{-4}$ in., $E = 6.7 \times 10^5$ psi, Poisson's ratio $\nu = 0.3$. Yield stress in uniaxial tension $\sigma_y \cong 10^4$ psi.

of these experiments. However, the existence and uniqueness of $C_0(F_0)$ for $F_0 < F_0^*$ has not been shown.

The procedure used to compute the numerical results is now described. For given values of P and σ_{r0} , and hence for a given $F_0 > F_0^*$, the root C_0 of Eq.(3.12) is computed with the use of Eqs.(3.9), (3.10) and (4.15). Since $(\epsilon^2 + I - 1)$ is monotone decreasing with C_0 , and further, since C_0 is bounded as $0 < C_0 < F_0^2$, then the root C_0 is easily computed by the method of bisection. With C_0 known, $\epsilon = \epsilon(F_0, C_0)$ follows immediately.

With the use of these values of ϵ and C_0 , and with application of Eqs.(1.7c), (1.4), (1.3), (1.2) and (1.10), stresses σ_r , σ_θ and deflections w , u in the free region of the membrane are calculated. Stresses and deflections in the constrained region of the membrane are then determined with the use of Eqs.(3.3), (2.18) and (2.20); note that $\beta_b = (a/c)\epsilon$, and that $w(\epsilon^2)$ from Eq.(1.10) is equal to $w(\beta_b)$ in Eq.(2.18e).

The values of σ_{r0} could not be obtained experimentally to within less than 15% error (see Ref. 2, Table A1), probably because of friction between the sheet and the outer supports. Even for constant platen loads in the experiment, σ_{r0} is a weak function of P . To compare predictions of the present theory with the experiments, the numerical value of σ_{r0} for each value of P is determined by adjusting σ_{r0} in the theory so that the predicted deflections near the outer edge $r = a$ are in agreement with the experimental deflections. The values of σ_{r0} thus found agree roughly with the experimental estimates.

In Figs. 3 and 4 are shown curves for the principal stresses and the transverse deflection w as predicted by theory for $P = 0.66$ lbs (300 grams) and a calculated value of $\sigma_{r0} = 850$ psi; for these values, $F_0 = 1.44$ and $F_{0L} = 6.4$. Also $(\sigma_{r0}/\sigma_L)^2 = 7.2 \times 10^{-3}$, so that, in view of inequality (4.10b) and Eq.(4.13d), the membrane is below yield if and only if $P < P_L$. However, $P = 0.66$ was the smallest value of P for which experimental data on deflection profiles were reported, although central deflection data were given for P as low as 0.11 lbs

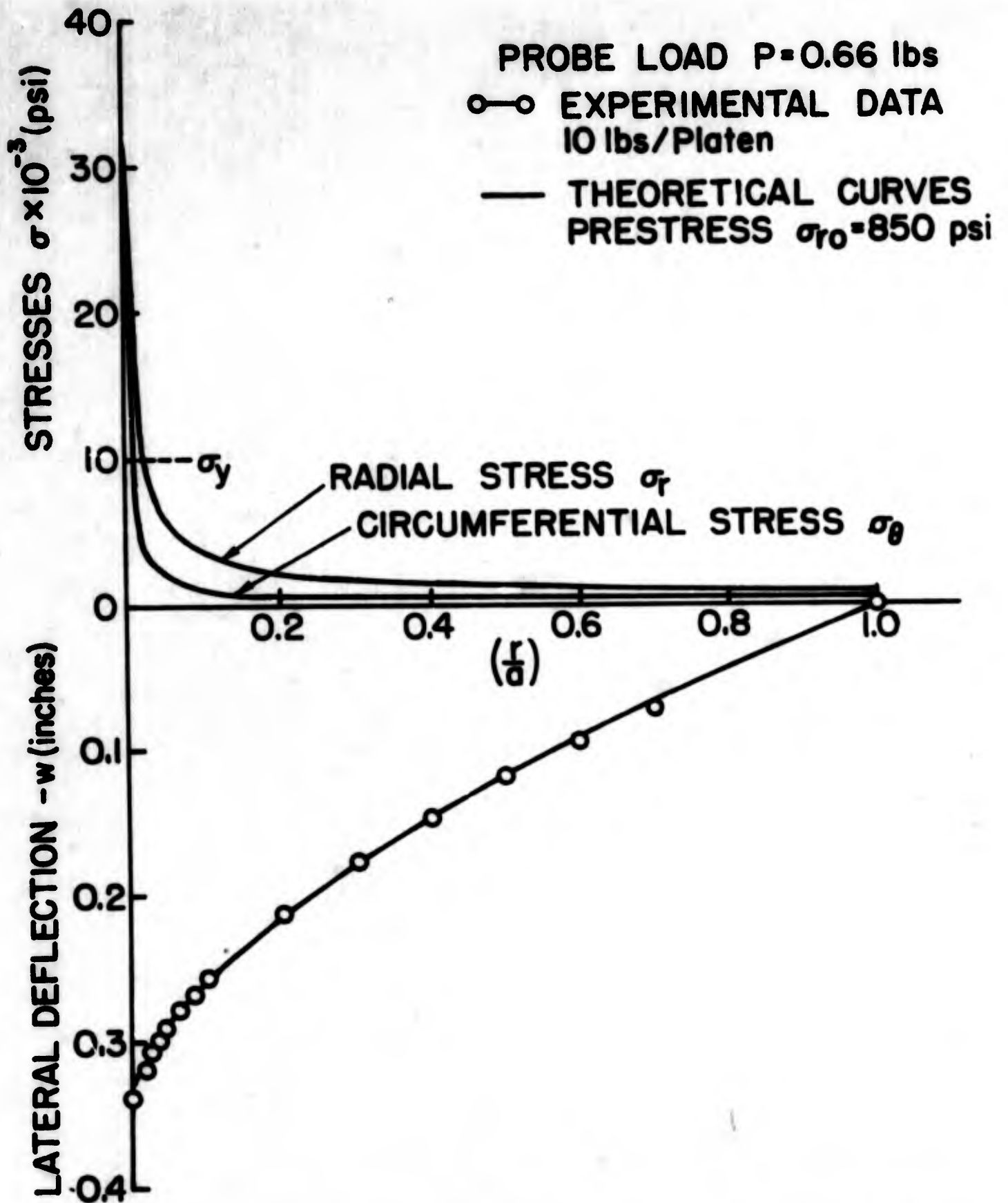


Fig. 3. Deflection w and Stresses σ_r and σ_θ vs. (r/a) for the Membrane.

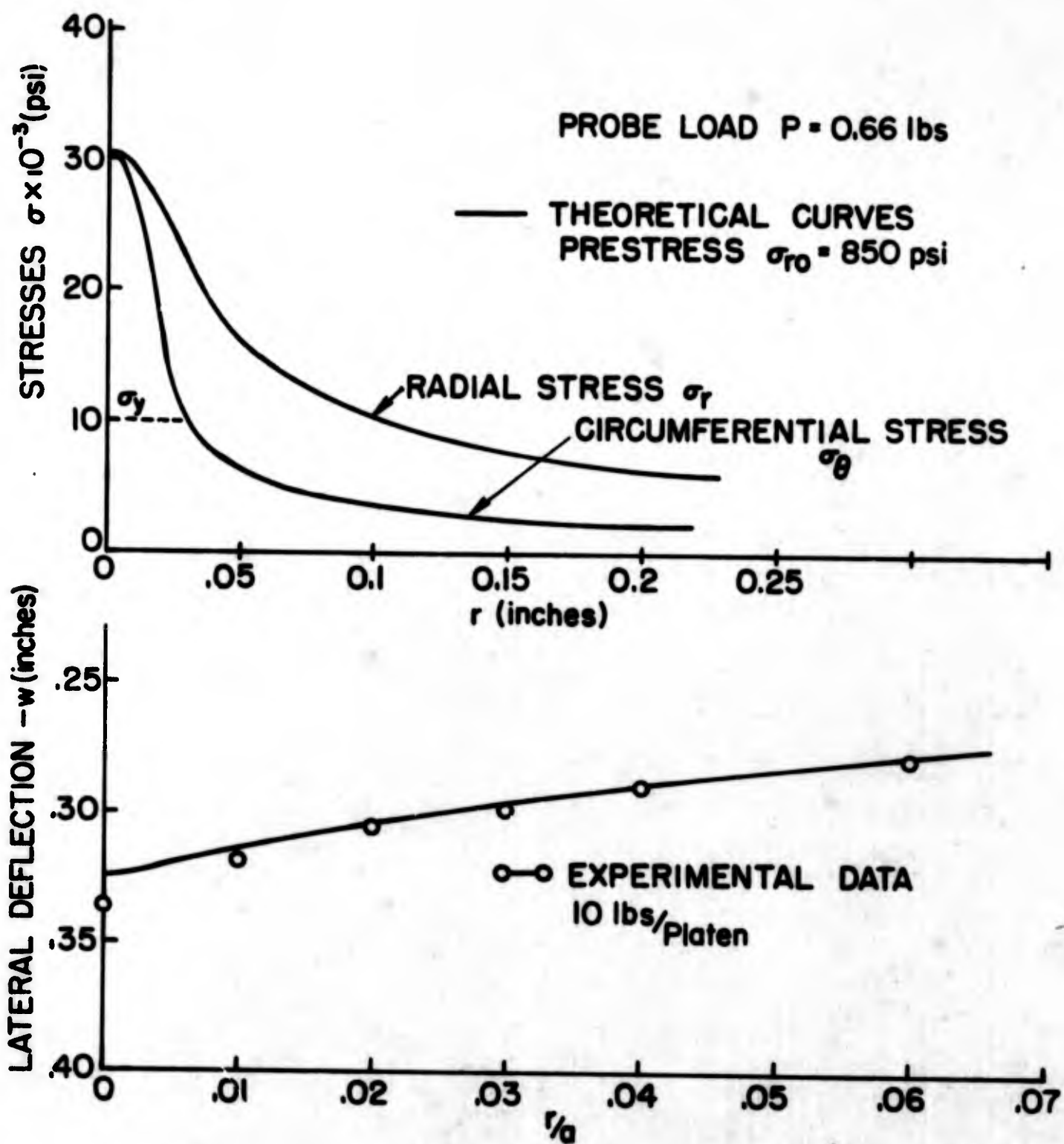


Fig. 4. Deflection w and Stresses σ_r and σ_θ vs. (r/a) for the Membrane in the Neighborhood of the Indenter.

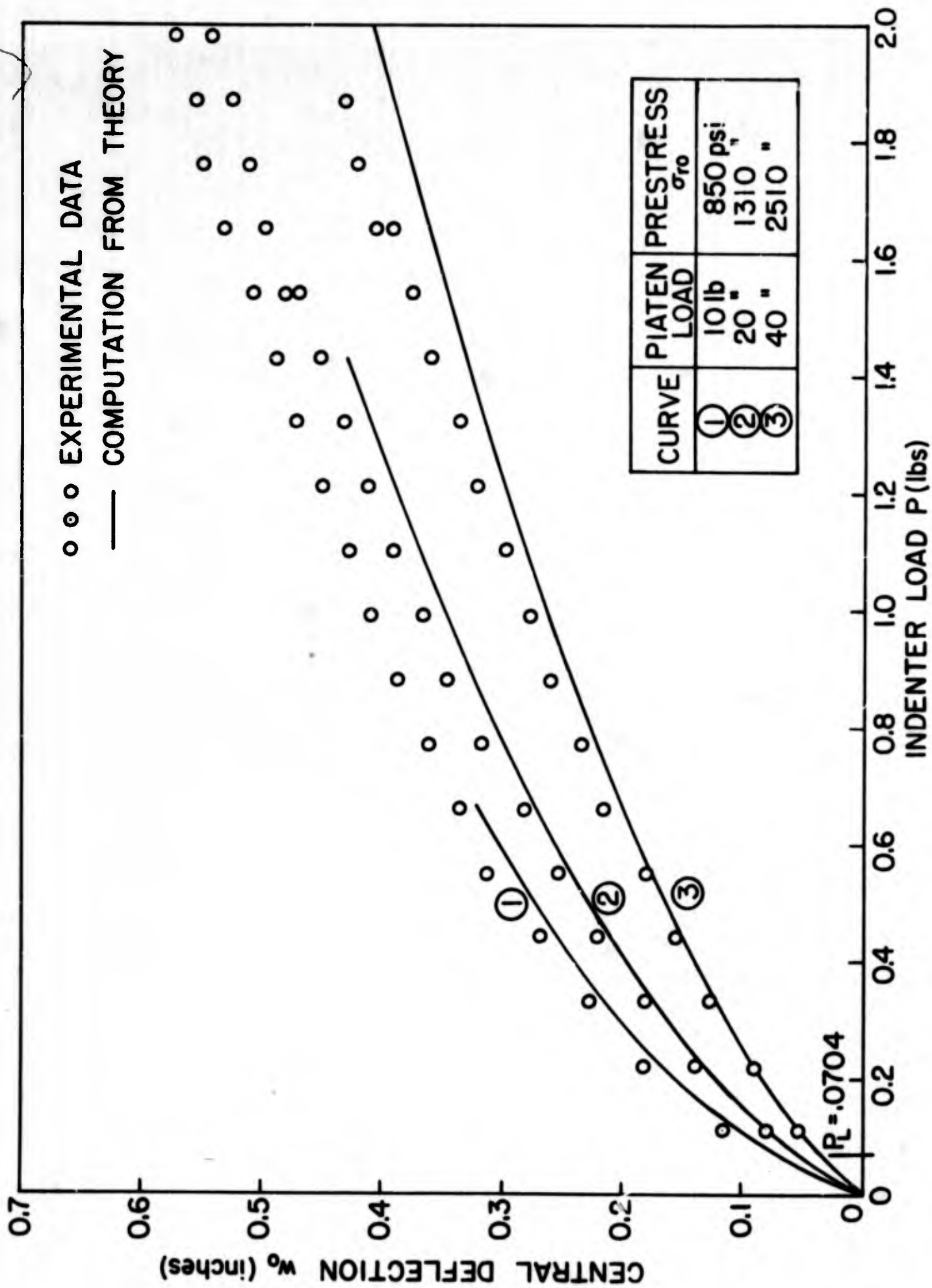


Fig. 5. Central Deflection vs. Indenter Load P for Fixed H_0 .

(50 grams). Even for this value, $P > P_L$ and $F_o < F_{oL}$, and the stresses in the neighborhood of the indenter as predicted by the theory, exceed the yield limit of the material (see Figs. 3 and 4). This indicates that plastic deformation of the membrane in the neighborhood of the indenter must have occurred in the experiments, causing larger transverse displacements w than those predicted by the elastic theory.

In Fig. 5, central load-deflection characteristics are shown in curves 1, 2, 3 — each for a fixed prestress. The values of σ_{ro} used are those determined as mentioned above for platen loads of 10, 20 and 40 lbs with the respective indenter loads of 0.66, 0.77, 0.88 lbs (300, 350 and 400 grams). Limiting value of load $P_L = 0.0704$ lb is also indicated. Although computations for negative C_o were made, they are not included on this graph for the reason given above, and the graphs shown are terminated at $C_o = 0$. Since experimental data were not available for loads below P_L , no direct comparison between theory and experiments was possible. However, discrepancy between theory and experiment decreases for smaller loads. In the neighborhood of limit load P_L , theory and experiments show good agreement.

Numerical results on the P vs. w_o relation obtainable from the theory in Ref. 2 are also obtained from the present theory by taking the limit as c/a goes to zero (see Eq.(4.32)). Better agreement is then obtained between theory and experiments (see Fig. o of Ref. 2), but this agreement is misleading. Since central displacement w_o is a decreasing function of indenter radius c for fixed P , then the error in neglecting the finite size of the indenter radius tends to balance the error in neglecting plastic flow.

APPENDIX A

It will now be shown that, if κ is sufficiently small, there exists a unique value of F_o^* which satisfies Eq.(3.16) and lies in the allowable domain (3.13a,b). Equation (3.16) is rearranged after substitution for F_ϵ^* from Eq.(3.10):

$$F_o^*{}^{3/2} - \frac{3}{2} + (3\sqrt{2}-4)\left(\frac{H_o}{Eh}\right)^{3/4} \left(\frac{2c}{a}\right)^{3/2} F_o^*{}^{-3/4} = 0 \quad (1A)$$

This can be expressed as a cubic equation in $F_o^*{}^{3/4}$ if both sides of this equation are multiplied by $F_o^*{}^{3/4}$. For convenience, the following quantities are defined:

$$x \equiv F_o^*{}^{3/4} \quad (2A)$$

$$x_L \equiv \kappa^{3/4} = \left(\frac{H_o}{Eh}\right)^{1/4} \left(\frac{2c}{a}\right)^{1/2} \quad (3A)$$

where, x_L is the lower bound on x in the allowable domain [Eq.(3.13b)], viz:

$$x > x_L > 0 \quad (4A)$$

Therefore, Eq.(1A) becomes

$$x^3 - \frac{3}{2}x + (3\sqrt{2}-4)x_L^3 = 0 \quad (5A)$$

To show under what conditions Eq.(5A) and inequality (4A) are both satisfied by a unique value of x , we look at the graph of the quantity $Q \equiv [(3\sqrt{2}-4)x_L^3]$ plotted first as a function of w , with the use of Eq.(5A), and then as a function of x_L . It is observed that if (5A) has a root $x = x_L > 0$, then

$$x_L = x_c \equiv \left(\frac{\sqrt{2}+1}{2}\right)^{1/2} \quad (6A)$$

Hence, x_c is the point of intersection of the two curves on the graph as is shown in Fig. 6. It then follows from the graph that for a given value of x_L there exists a unique value of x which satisfies (4A) and (5A), if and only if

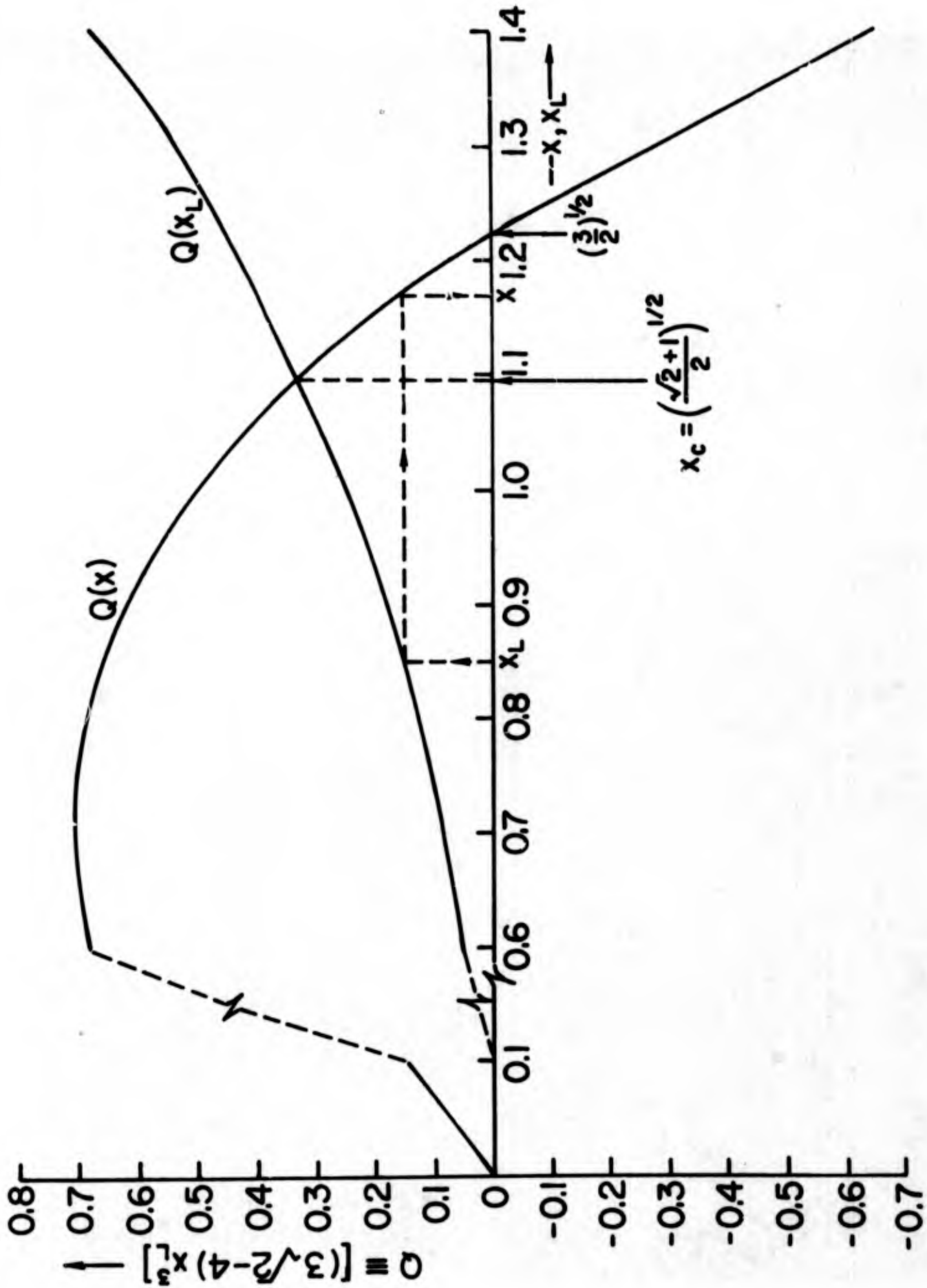


Fig. 6. Graph of Q as a function of x [from Eq. (5A)] and of x_L .

$$0 < x_L < x_c \quad (7A)$$

Furthermore, x lies in the corresponding interval

$$\left(\frac{3}{2}\right)^{1/2} > x > x_c \quad (8A)$$

Therefore, Eqs.(2A), (3A) and (6A), and inequalities (7A) and (8A) show that Eq.(3.16) has a unique root F_o^* , bounded as

$$\left(\frac{3}{2}\right)^{2/3} > F_o^* > \left(\frac{\sqrt{2+1}}{2}\right)^{2/3}, \quad (9A)$$

if and only if

$$0 < \kappa < \left(\frac{\sqrt{2+1}}{2}\right)^{2/3} \quad (10A)$$

If $F_o^* = \kappa = \left(\frac{\sqrt{2+1}}{2}\right)^{2/3}$, then with the use of Eqs.(3.9) and (3.10) there is obtained

$$F_\epsilon^* = F_o^* = \kappa = \left(\frac{\sqrt{2+1}}{2}\right)^{2/3} \quad (11A)$$

and

$$\epsilon \Big|_{F_\epsilon = F_\epsilon^*} = 1 \quad (12A)$$

In this case, therefore, the indenter is resting on the outer edge of the membrane when $F_o = F_o^*$.

If κ exceeds $[(\sqrt{2+1})/2]^{2/3}$, then the curve $C_o(F_o)$ cannot contain the point $C_o = 0$. The existence and continuity of $C_o(F_o)$ has not been shown for this case.

REFERENCES

1. W. Nachbar, "Finite Deformation of a Prestressed Elastic Membrane", SUDAER No. 141, November 1962.
2. W. E. Jahsman, F. A. Field and A. M. C. Holmes, "Finite Deformations in a Prestressed, Centrally Loaded, Circular Elastic Membrane", Proc. 4th U.S. Natl. Cong. Appl. Mech., A.S.M.E., 1962, pp. 585-594.
3. E. Reissner, "Rotationally Symmetric Problems of Thin Shells of Revolution", Proc. 3rd U.S. Natl. Cong. Appl. Mech., A.S.M.E., 1958, pp. 51-69.
4. L. M. Graves, The Theory of Functions of Real Variables, second edition, McGraw-Hill, N. Y., 1956, Chapter VIII, Theorem 7, p. 150.
5. L. M. Graves, *ibid.*, Chapter IV, Theorem 2, p. 57.
6. L. M. Graves, *ibid.*, Chapter VII, Theorem 2, p. 100.

PART II

FINITE INDENTATION OF AN ELASTIC-PLASTIC
MEMBRANE BY A SPHERICAL INDENTER

NOTATION

a	Outer radius of membrane.
b	Radius at point of tangency.
c	Radius of hemispherical head of indenter.
d	Radius of elastic-plastic boundary.
C_0	Integration constant, see Ref. 1.
E	Young's modulus.
F	$\equiv 2^{2/3} (\epsilon\rho)^{1/3} y^{1/2} \text{ctn } \beta$.
F_0	$\equiv \left(\frac{H_0}{Eh}\right) \left(\frac{4\pi Eha}{P}\right)^{2/3}$, combined loading parameter.
F_ϵ	$= F(\epsilon^2) = \left(\frac{2P}{\pi Eha}\right)^{1/3} \frac{c}{a}$.
F_d	$= F(\bar{\epsilon}^2)$.
h	Thickness of elastic-plastic sheet.
H_0	$\equiv h\sigma_{r0}$, Horizontal component of stress resultant at $r = a$.
P	Central indenter load.
P_L	$\equiv 4\pi Ehc s_L^2$, upper bound on P at elastic limit.
p	Transverse pressure on the elastic-plastic sheet under the indenter.
r	Radial co-ordinate.
s_r, s_θ, s_y	$\equiv (\sigma_r/E), (\sigma_\theta/E), (\sigma_y/E)$.
u	Horizontal displacement.
w	Transverse (vertical) displacement component.
w_0	$= -w(0)$; Central deflection.
y	$\equiv \left(\frac{r}{a}\right)^2$.
β	Angle of tangent rotation.
β_b	Angle of tangent rotation at $r = b$.

Notation (Continued)

β_d	Angle of tangent rotation at $r = d$.
ϵ	$\equiv \left(\frac{b}{a} \right)$
$\bar{\epsilon}$	$\equiv \left(\frac{d}{a} \right)$
$\epsilon_r, \epsilon_\theta$	Radial and circumferential midsurface strain components.
$\epsilon_r^e, \epsilon_r^p$	Elastic and plastic components of radial midsurface strain.
$\epsilon_\theta^e, \epsilon_\theta^p$	Elastic and plastic components of circumferential mid-surface strain.
ν	Poisson's ratio.
ρ	$\equiv \left(\frac{P}{2\pi Ehb} \right)$.
$\bar{\rho}$	$\equiv \left(\frac{P}{2\pi Ehd} \right)$.
σ_r, σ_θ	Radial and circumferential stress components.
σ_{r0}	Applied prestress.
σ_y	Yield stress.

SECTION 1. INTRODUCTION

The problem of finite, rotationally symmetric deformations of a prestressed circular elastic membrane, or sheet, subjected to transverse loading by an indenter has been considered in Ref. 1. It was shown that for indenter loads greater than the limit load P_L , stresses in the neighborhood of the indenter, as predicted by theory, exceed the yield limit of the material. For indenter loads greater than P_L , a comparison of deflections from theory and from experimental data of Jahsman, Field and Holmes [Ref. 2] showed good agreement except in the immediate neighborhood of the indenter.

In the present paper, which is a continuation of Ref. 1, elastic-plastic analysis of the indenter problem is considered. Figures 1 and 2 show the indenter problem geometry and nomenclature. The constrained region of the membrane is assumed to be in frictionless contact with the indenter. Since, in the elastic analysis, maximum stress in the membrane occurs under the indenter, it is reasonable to assume that yielding and plastic deformation of the membrane is incipient under the indenter and propagates outward as load increases. It is assumed that the plastic region is separated from the elastic region by a distinct circular elastic-plastic boundary of radius d . This elastic-plastic boundary may either lie in the constrained region of the membrane [Fig. 1] or, when the indenter load is sufficiently large, it may lie in the free region of the membrane [Fig. 2]. Both cases are considered.

The membrane is assumed to be of an ideal, elastic-perfectly plastic material obeying the Tresca yield condition and the associated flow rule [see Eqs.(2.17a,b) below] that is derived from the generalized plastic potential [Refs. 4,5]. Subject to subsequent verification from the solutions obtained, it will be assumed that positive increments in the indenter load P produce no unloading in the plastic portion of the membrane. Thus, the radius of the elastic-plastic boundary is assumed to be non-decreasing with P . Moreover, the components of the plastic strain rate $\dot{\epsilon}_r^P$ and $\dot{\epsilon}_\theta^P$ in the plastic region are assumed to be non-negative. The total strain components ϵ_r and ϵ_θ , and the elastic

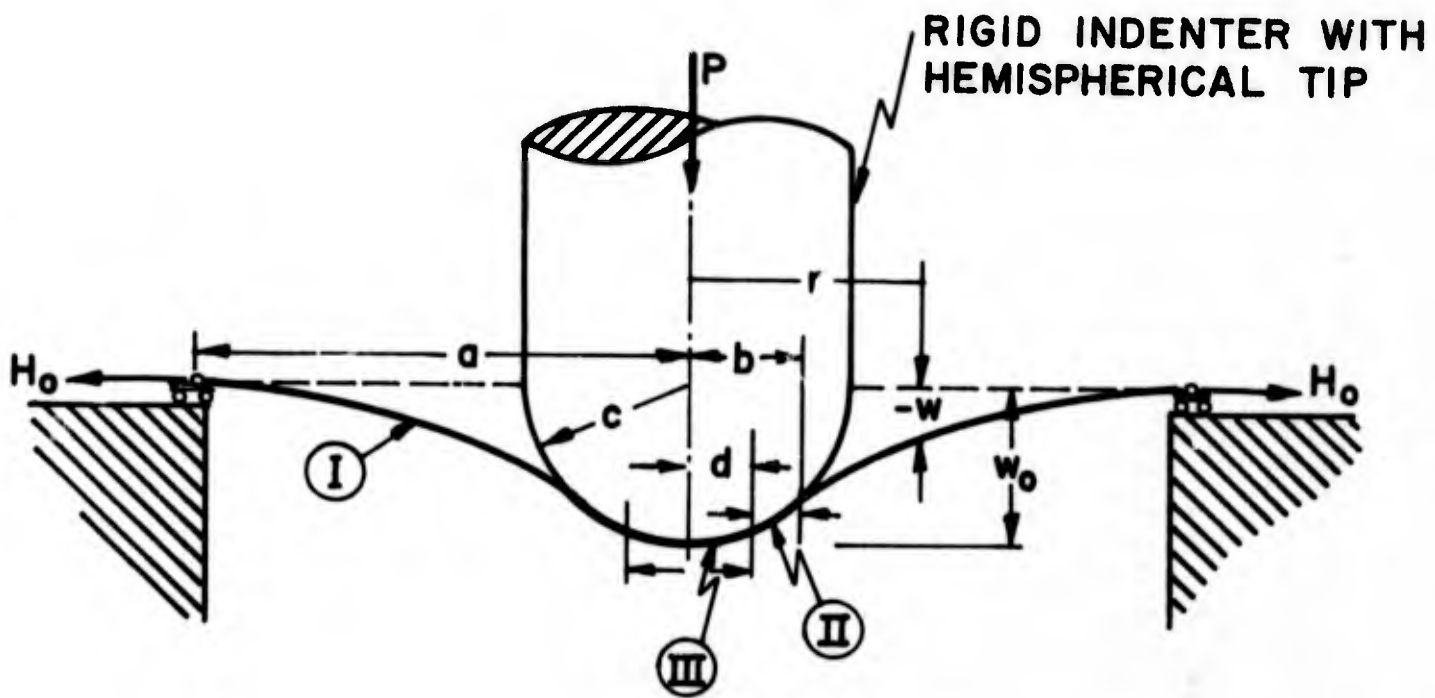
strain components ϵ_r^e and ϵ_θ^e , are thus, in general, continuous functions of the two independent variables r and P , except on the elastic-plastic boundary, and are related to the plastic strain components as:

$$\epsilon_r = \epsilon_r^e + \epsilon_r^p \quad (1.1a)$$

$$\epsilon_\theta = \epsilon_\theta^e + \epsilon_\theta^p \quad (1.1b)$$

The solution for the constrained plastic region is obtained in Section 2. The solution for the constrained elastic annular region was obtained in Ref. 1, and the solution for the free elastic annular region was obtained in Ref. 3. In Sections 3 and 4, respectively, complete solutions are obtained for the two cases of Figs. 1 and 2.

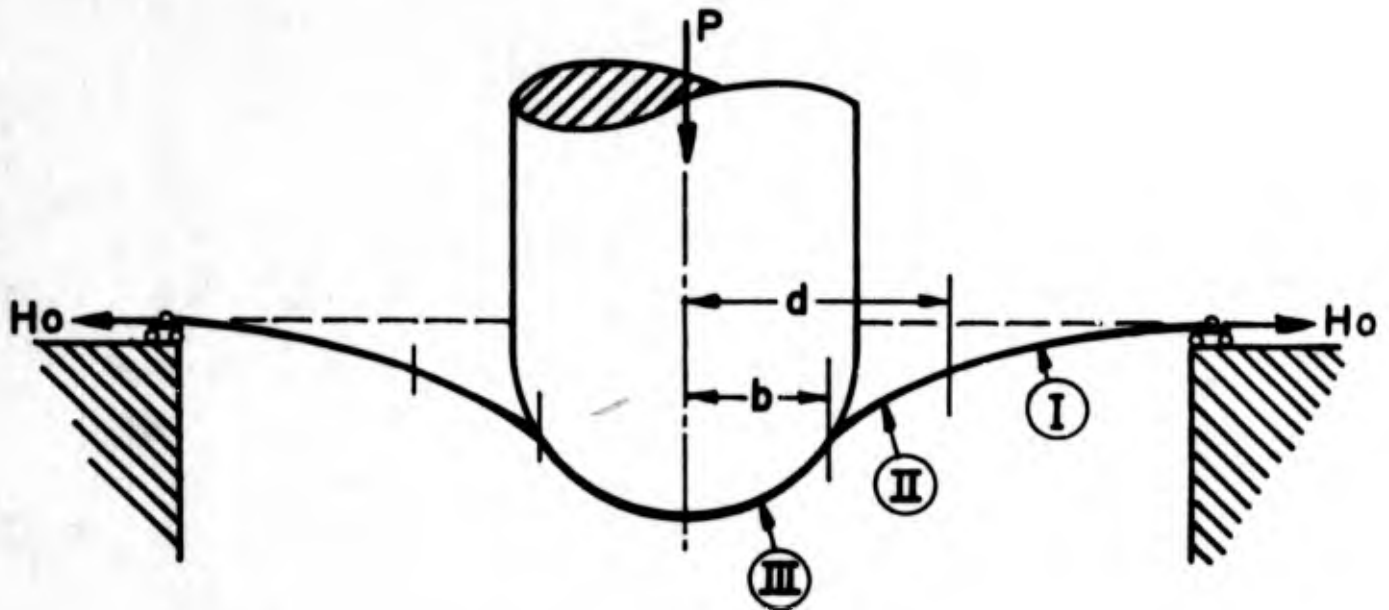
It is convenient in the development to use three representations for the independent variable. These also serve to identify regions of applicability of the analysis. The tangent rotation angle β is used in the constrained regions, the parameter y is used in the free annular elastic region, and the radial distance coordinate r is used in the free plastic region. Whenever the obtained results are to apply equally to all regions, the independent variable r is signified.



- Ⓘ FREE ELASTIC REGION ($b \leq r \leq a$)
- Ⓜ CONSTRAINED ELASTIC REGION ($d \leq r \leq b$)
- Ⓝ CONSTRAINED PLASTIC REGION ($0 < r \leq d$)

ELASTIC-PLASTIC BOUNDARY UNDER INDENTER.

Fig. 1. Deformed Elastic-Plastic Membrane: Elastic-Plastic Boundary under Indenter.



① FREE ELASTIC REGION ($d \leq r \leq a$).

② FREE PLASTIC REGION ($b \leq r \leq d$).

③ CONSTRAINED PLASTIC REGION ($0 < r < b$).

ELASTIC-PLASTIC BOUNDARY IN FREE REGION OF MEMBRANE.

Fig. 2. Deformed Elastic-Plastic Membrane: Elastic-Plastic Boundary in Free Region of Membrane.

SECTION 2. PLASTIC DEFORMATION OF MEMBRANE
IN FRICTIONLESS CONTACT WITH INDENTER

Finite deformation, small strain equations for an initially flat sheet are given in Ref. 1. The equations of equilibrium for contact without friction are:

$$\frac{d}{dr} (r s_r \cos \beta) - s_\theta + \frac{rp}{Eh} \sin \beta = 0 \quad (2.1a)$$

$$\frac{d}{dr} (r s_r \sin \beta) - \frac{rp}{Eh} \cos \beta = 0 \quad (2.1b)$$

When p is eliminated between Eqs. (2.1a,b), there is obtained

$$\frac{d}{dr} (r s_r) = s_\theta \cos \beta \quad (2.1c)$$

Elastic components of strain are given by

$$\epsilon_r^e = s_r - \nu s_\theta \quad (2.2a)$$

$$\epsilon_\theta^e = s_\theta - \nu s_r \quad (2.2b)$$

For a membrane undergoing elastic-plastic deformation, total strain components are given by Eqs. (1.1a,b).

Strain-displacement relations for total strain components are

$$(1+\epsilon_r) \sin \beta = \frac{dw}{dr} \quad (2.3a)$$

$$(1+\epsilon_r) \cos \beta = 1 + \frac{du}{dr} \quad (2.3b)$$

$$\epsilon_\theta = \frac{u}{r} \quad (2.3c)$$

and the compatibility relation for strains is

$$\frac{d}{dr} (r \epsilon_\theta) + 1 - (1+\epsilon_r) \cos \beta = 0 \quad (2.4)$$

The yield condition of Tresca is imposed. In the elastic analysis [Ref.1] it was shown that $s_r > s_\theta$ for $r > 0$. If this inequality is assumed to hold for plastic regions, Tresca's yield condition would become $s_r = s_y$. Then, by Eq. (2.1c) $s_\theta \cos \beta = s_y$, which indicates that $s_\theta > s_y$. This contradicts the initial assumption. It is therefore assumed that

$$s_\theta > s_r > s_z = 0 \quad (2.5)$$

in the entire plastic region, and therefore

$$s_\theta = s_y \quad (2.6)$$

at yield. It will be shown that Eq. (2.6) implies (2.5) both for the constrained plastic and the free plastic regions [see Eqs. (2.10) and (4.6b)].

For the constrained region,

$$\sin \beta = \frac{r + u(r)}{c} = \frac{r}{c} (1 + \epsilon_r) \quad (2.7)$$

follows from geometry and Eq. (2.3c). With the use of Eqs. (2.3b,c), the derivative of both sides of Eq. (2.7) is

$$\frac{d\beta}{dr} = c^{-1} (1 + \epsilon_r) \quad (2.8)$$

Since the differential operator transforms as [Eqs. (2.7) and (2.8)]

$$r \frac{d(\quad)}{dr} = \left(\frac{1 + \epsilon_r}{1 + \epsilon_\theta} \right) \sin \beta \frac{d(\quad)}{d\beta} ,$$

Eq. (2.1c) can be written with β as independent variable:

$$\frac{ds_r}{d\beta} + \left(\frac{1 + \epsilon_\theta}{1 + \epsilon_r} \right) \frac{s_r}{\sin \beta} = \left(\frac{1 + \epsilon_\theta}{1 + \epsilon_r} \right) s_y \frac{\cos \beta}{\sin \beta}$$

For small strains, this equation is approximated as

$$\frac{ds_r}{d\beta} + \frac{s_r}{\sin \beta} = s_y \operatorname{ctn} \beta \quad (2.9)$$

The solution of Eq. (2.9) which is finite at $\beta = 0$ is

$$s_r = s_y \left[\frac{\beta}{\tan(\beta/2)} - 1 \right] \quad (2.10)$$

Note that s_r is decreasing with increasing β . An expression for contact pressure p between the membrane and the indenter is obtained by using Eqs. (2.1b), (2.1c), (2.7) and (2.8):

$$p(\beta) = \frac{Eh}{c} s_y \frac{\beta}{\tan \beta/2} \quad (2.11)$$

The contact pressure p decreases with increase in β . It is observed from Eqs. (2.10) and (2.11) that s_r and p for the constrained plastic region are independent of the indenter load P .

The displacement component $w(\beta)$ is obtained from Eqs. (2.3a) and (2.8) by one integration; for the case of Fig. 1,

$$w(\beta) = w(\beta_d) - c(\cos \beta - \cos \beta_d), \quad r \leq d \leq b \quad (2.12a)$$

and for the case of Fig. 2,

$$w(\beta) = w(\beta_b) - c(\cos \beta - \cos \beta_b), \quad r \leq b \leq d \quad (2.12b)$$

The results to be obtained next are valid for all elastic-plastic boundaries whether in the constrained or free regions. At the elastic-plastic boundary $r = d$ (or equivalently $\beta = \beta_d$ and $y = \bar{c}^2$), continuity of stress component σ_r and displacement component u is required. These conditions are satisfied if

$$s_r(d-) = s_r(d+) \quad (2.13a)$$

and

$$\epsilon_\theta(d-) = \epsilon_\theta(d+) \quad (2.13b)$$

where the use of arguments $(d-)$ and $(d+)$ refers to limiting values for stresses and strains in the plastic region and elastic region, respectively, at the elastic-plastic boundary. With the use of Eqs. (2.2b), (2.6) and (2.13a), Eq. (2.13b) reduces to

$$s_y - s_\theta(d+) = -\epsilon_\theta^p(d-) \quad (2.14a)$$

Also, using Eqs. (2.2a) and (2.14a),

$$\epsilon_r(d-) - \epsilon_r(d+) = \epsilon_r^P(d-) + \nu \epsilon_\theta^P(d-) \quad (2.14b)$$

Since stresses in the elastic region must satisfy the condition

$$s_\theta(d+) \leq s_y \quad (2.15a)$$

then,

$$\epsilon_\theta^P(d-) \leq 0 \quad (2.15b)$$

Positive plastic work requires, however,

$$\epsilon_\theta^P(d-) \geq 0 \quad (2.15c)$$

Inequalities (2.15b,c) therefore imply that

$$\epsilon_\theta^P(d-) = 0 \quad (2.16a)$$

and hence

$$s_\theta(d+) = s_y \quad (2.16b)$$

Thus, at a general elastic-plastic boundary, s_r and s_θ are continuous, and ϵ_θ^P vanishes.

To determine the plastic strain components the flow rule for loading

$$\dot{\epsilon}_r^P = 0 \quad \left. \vphantom{\dot{\epsilon}_r^P} \right\} \quad 0 < r < d \quad (2.17a)$$

$$\dot{\epsilon}_\theta^P \geq 0 \quad \left. \vphantom{\dot{\epsilon}_\theta^P} \right\} \quad 0 < r < d \quad (2.17b)$$

is used, where, at a fixed r ,

$$(\dot{}) \equiv \frac{\partial()}{\partial P} \quad (2.17c)$$

The plastic strain components are now determined for the constrained plastic region. In this region, the stresses σ_r , σ_θ and contact pressure p are independent both of indenter load P and prestress σ_{r0} [Eqs. (2.6), (2.10) and (2.11)], and thus ϵ_r is independent of P .

It will be shown next that these conditions imply $\dot{\epsilon}_{\theta}^P = 0$, and indeed $\epsilon_{\theta}^P \equiv 0$, in the constrained plastic region. Therefore, the deformation in this region is statically determined.

Since the strain components ϵ_{θ}^e and ϵ_r^e are independent of P ,

$$\dot{\epsilon}_{\theta} = \dot{\epsilon}_{\theta}^P \quad \text{and} \quad \dot{\epsilon}_r = 0, \quad (2.18)$$

the partial derivative with respect to P of the compatibility condition (2.4) yields,

$$\frac{\partial}{\partial r} (r \dot{\epsilon}_{\theta}^P) + (1 + \epsilon_r) \dot{\beta} \sin \beta = 0 \quad (2.19a)$$

An equation for $\dot{\beta}$ is obtained from the derivative with respect to P of both sides of Eq. (2.7),

$$\dot{\beta} \cos \beta = \frac{r}{c} \dot{\epsilon}_{\theta}^P,$$

or

$$\dot{\beta} = \tan \beta \frac{\dot{\epsilon}_{\theta}^P}{(1 + \epsilon_{\theta})} \quad (2.19b)$$

Then Eq. (2.19a) becomes

$$r \frac{\partial \dot{\epsilon}_{\theta}^P}{\partial r} + \left[1 + \left(\frac{1 + \epsilon_r}{1 + \epsilon_{\theta}} \right) \frac{\sin^2 \beta}{\cos \beta} \right] \dot{\epsilon}_{\theta}^P = 0 \quad (2.19c)$$

The last two terms on the left-hand side above are nonnegative for $\beta < \pi/2$ (see inequality (2.22)), and therefore

$$\frac{\partial \dot{\epsilon}_{\theta}^P}{\partial r} \leq 0 \quad 0 < r < d \quad (2.19d)$$

By symmetry

$$\lim_{r \rightarrow 0} (\dot{\epsilon}_{\theta} - \dot{\epsilon}_r) = 0, \quad (2.20a)$$

and so, with the use of Eq. (2.18),

$$\lim_{r \rightarrow 0} \dot{\epsilon}_{\theta}^P = 0 \quad (2.20b)$$

Then, Eqs. (2.17b), (2.19d) and (2.20b) together imply that

$$\epsilon_{\theta}^P \equiv 0 \quad 0 < r < d \quad (2.20c)$$

and so

$$\epsilon_{\theta}^P = f(r) \quad 0 < r < d \quad (2.20d)$$

Now $f(r)$ must satisfy Eq. (2.16a), so that $f(d) = 0$. But, for loading, d is a continuous, nondecreasing function of P , while $f(r)$ is independent of P . Therefore, it is easily shown that $f \equiv 0$, and hence, from Eqs. (2.20d) and (2.16b)

$$\epsilon_{\theta}^P \equiv 0 \quad 0 < r \leq d \quad (2.21a)$$

Substitution of expressions for ϵ_r^e and ϵ_{θ}^e from Eqs. (2.2a,b) into the compatibility relation (2.4), and the use of Eqs. (2.6), (2.10), and (2.21a), determine ϵ_r^P as a function of β :

$$\epsilon_r^P(\beta) = \frac{1 - \cos \beta}{\cos \beta} + \frac{s_y}{\tan \beta/2} (\tan \beta - \beta) \quad (2.21b)$$

This equation shows that $\epsilon_r^P(\beta) > 0$ for $\beta > 0$. Therefore, Eq. (2.14b) implies

$$\epsilon_r(d^-) > \epsilon_r(d^+)$$

This inequality indicates that ϵ_r has a positive jump from the elastic into the plastic region.

Equation (2.21b) shows that the small strain assumption is violated as $\beta \rightarrow \pi/2$, and further, that $\epsilon_r^P \ll 1$ if and only if $\beta^2 \ll 1$. This latter conclusion is significant. It shows that even though no assumption of moderate rotation is made in obtaining the solution for the constrained plastic region, the solution is valid only when rotation remains moderate. It is shown in Section 4 below [see Eq. (4.6a)] that maximum rotation of the membrane occurs at $\beta = \beta_b$. Consequently,

$$\beta_b^2 \ll 1 \quad (2.22)$$

is necessary to satisfy the small strain assumption.

SECTION 3. ELASTIC-PLASTIC BOUNDARY UNDER THE INDENTER

In this section the growth of the plastic region under the indenter is considered for increasing indenter loads, and it is assumed that

$$0 \leq d \leq b \quad (3.1a)$$

The three regions of the membrane, viz. constrained elastic-plastic region, constrained annular elastic region, and free annular elastic region are shown in Fig. 1. In this case it is clear that

$$0 \leq \beta_d \leq \beta_b \quad (3.1b)$$

The proof given in Ref. 1 for the necessity of moderate rotations in the constrained elastic region [and, in consequence, for the entire membrane - see Ref. 3, Eq.(3.19)] does not hold for an annular elastic region of the present problem. However, inequality (2.22) does follow for $\beta_d = 0$, and it is shown in Appendix A that for positive values of C_0 , the solution obtained is consistent with inequality (2.22).

The solution obtained in Ref. 1 for the constrained elastic region is now modified for the present problem. With use of assumption (2.22), the integral of Eq.(2.8) of Ref. 1 can be written as

$$s(\beta) = s(\beta_d) + \frac{1}{4} (\beta_d^2 - \beta^2) \quad \beta_d \leq \beta \leq \beta_b$$

Upon comparison of this relation to Eq.(2.12b) of Ref. 1, it is observed that the integration constant $s(0)$ in the latter equation is replaced by

$$s(\beta_d) + \frac{1}{4} \beta_d^2$$

for the present analysis. With this replacement substituted into

Eq. (2.14a) of Ref. 1, the relation

$$\frac{1}{2} \left[s(\beta_d) + \frac{1}{4} \beta_d^2 \right] = s_r(\beta_b) - c_2 \beta_b^{-2} + \frac{1}{16} \beta_b^2$$

is formed. With this and Eqs. (2.14a,b), (2.15) and (2.16) of Ref. 1, the solution for $d \leq r \leq b$ is

$$s_r(\beta) = s_r(\beta_b) + c_2 \left(\frac{1}{\beta^2} - \frac{1}{\beta_b^2} \right) + \frac{1}{16} (\beta_b^2 - \beta^2) \quad (3.2a)$$

$$s_\theta(\beta) = s_r(\beta_b) - c_2 \left(\frac{1}{\beta^2} + \frac{1}{\beta_b^2} \right) + \frac{1}{16} (\beta_b^2 - 3\beta^2) \quad (3.2b)$$

$$\frac{u}{c} = (1-\nu) \left[s_r(\beta_b) + \frac{1}{16} (\beta_b^2 - \beta^2) \right] \beta - \frac{1}{8} \beta^3 - \frac{b^2}{\beta} \left[(1+\nu) + (1-\nu) \frac{\beta_b^2}{\beta_b^2} \right] \quad (3.2c)$$

and

$$p = \frac{2Eh}{c} \left[s_r(\beta_b) - \frac{c_2}{\beta_b^2} + \frac{\beta_b^2}{16} \left(1 - 2 \frac{\beta_b^2}{\beta_b^2} \right) \right] \quad (3.2d)$$

At the elastic-plastic boundary $\beta = \beta_d$, continuity of stress σ_r and displacement u is required. Continuity of u is satisfied by the continuity of stress components [Eqs. (2.13a) and (2.16b)] and by Eq. (2.16a). With the use of Eqs. (2.6) and (3.2b), continuity of s_θ is expressed as

$$s_y = s_r(\beta_b) - c_2 \left(\frac{1}{\beta_d^2} + \frac{1}{\beta_b^2} \right) + \frac{1}{16} (\beta_b^2 - 3\beta_d^2) \quad (3.3a)$$

Inequalities (2.22), (3.1b) imply $\beta_d^2 \ll 1$. Hence, with the use of Eqs. (2.10) and (3.2a), the condition for continuity of s_r is approximated as

$$s_y \left(1 - \frac{1}{6} \beta_d^2 \right) = s_r(\beta_b) + c_2 \left(\frac{1}{\beta_d^2} - \frac{1}{\beta_b^2} \right) + \frac{1}{16} (\beta_b^2 - \beta_d^2) \quad (3.3b)$$

Upon subtracting (3.3b) from (3.3a),

$$C_2 = -\frac{1}{16} \left(1 + \frac{4}{3} s_y\right) \beta_d^4 \quad (3.4)$$

Using Eqs. (3.3a) and (3.4), we then obtain an equation quadratic in β_d^2 , viz.

$$\frac{1 + \frac{4}{3} s_y}{2(1 - \frac{2}{3} s_y)} \beta_d^4 - \beta_b^2 \beta_d^2 + \frac{1}{2(1 - \frac{2}{3} s_y)} \beta_b^4 \left\{ 1 - \frac{16}{\beta_b^2} \left[s_y - s_r(\beta_b) \right] \right\} = 0 \quad (3.5a)$$

Since $\beta_d \leq \beta_b$, the only allowable root of Eq. (3.5a) is

$$\beta_d^2 = (1 - 2s_y) \beta_b^2 \left\{ 1 - \left[1 - \left(1 + \frac{8}{3} s_y\right) \left\{ 1 - \frac{16}{\beta_b^2} \left[s_y - s_r(\beta_b) \right] \right\} \right]^{1/2} \right\} \quad (3.5b)$$

Substitution of Eq. (3.4) into Eqs. (3.2a,b,c,d) then give expressions for the constrained elastic region $\beta_d \leq \beta \leq \beta_b$:

$$s_r(\beta) = s_r(\beta_b) - \left(1 + \frac{4}{3} s_y\right) \frac{\beta_d^4}{16} \left(\frac{1}{\beta^2} - \frac{1}{\beta_b^2} \right) + \frac{1}{16} (\beta_b^2 - \beta^2) \quad (3.6a)$$

$$s_\theta(\beta) = s_r(\beta_b) + \left(1 + \frac{4}{3} s_y\right) \frac{\beta_d^4}{16} \left(\frac{1}{\beta^2} + \frac{1}{\beta_b^2} \right) + \frac{1}{16} (\beta_b^2 - 3\beta^2) \quad (3.6b)$$

$$\frac{u}{c} = (1-\nu) \left[s_r(\beta_b) + \frac{1}{16} (\beta_b^2 - \beta^2) \right] \beta - \frac{1}{8} \beta^3 + \left(1 + \frac{4}{3} s_y\right) \frac{1}{16} \frac{\beta_d^4}{\beta} \left[(1+\nu) + (1-\nu) \frac{\beta^2}{\beta_b^2} \right] \quad (3.6c)$$

and

$$p = \frac{2Eh}{c} \left[s_r(\beta_b) + \left(1 + \frac{4}{3} s_y\right) \frac{1}{16} \frac{\beta_d^4}{\beta_b^2} + \frac{\beta_b^2}{16} \left(1 - 2 \frac{\beta^2}{\beta_b^2} \right) \right] \quad (3.6d)$$

In view of Eq. (3.5b), the unknown quantities remaining to be determined in Eqs. (3.6a,b,c,d) are β_b and $s_r(\beta_b)$. Conditions to determine these quantities will be developed next.

At the point of tangency $\beta = \beta_b$, Eqs. (2.20), (3.2) and (3.4) of Ref. 1 apply:

$$s_r(\beta_b) \beta_b^2 \frac{c}{a} = \frac{P}{2\pi Eha} \quad (3.7a)$$

$$\epsilon\rho = \frac{P}{2\pi Eha} \quad (3.7b)$$

$$F_\epsilon = \left(\frac{2P}{\pi Eha} \right)^{1/3} \frac{c}{a} = (4\epsilon\rho)^{1/3} \frac{c}{a} \quad (3.7c)$$

Equation (2.7) and inequality (2.22) are used to obtain

$$\beta_b \approx \frac{\epsilon}{(c/a)} \quad (3.7d)$$

and

$$\beta_d \approx \frac{\bar{\epsilon}}{(c/a)} \quad (3.7e)$$

where

$$\epsilon \equiv b/a \quad \text{and} \quad \bar{\epsilon} \equiv d/a .$$

Also, from Eqs. (1.3), (1.4) and (1.7) of Ref. 1 ,

$$s_r = \left(\frac{1}{2} \epsilon\rho \right)^{2/3} \frac{F}{y} \quad (3.7f)$$

$$s_\theta(y) = \left(\frac{1}{2} \epsilon\rho \right)^{2/3} \left(2 \frac{dF}{dy} - \frac{F}{y} \right) \quad (3.7g)$$

$$\frac{dF(y)}{dy} = (F^{-1} + C_0)^{1/2} \quad (3.7h)$$

for the free elastic region $\epsilon^2 < y < 1$.

At the point of tangency continuity of s_r and u are again imposed. Continuity of s_r is already implied by Eqs. (3.7a,b,c,f). Continuity of u is implied, therefore, by continuity of s_θ , and this condition can be expressed with use of Eqs. (3.6b) and (3.7g,h) as

$$s_r(\beta_b) + \left(1 + \frac{4}{3} s_y\right) \frac{1}{8} \frac{\beta_d^4}{\beta_b^2} - \frac{\beta_b^2}{8} = \left(\frac{1}{2} \epsilon \rho\right)^{2/3} \left[2 \left(\frac{1}{F_\epsilon} + C_o\right)^{1/2} - \frac{F_\epsilon}{\epsilon^2} \right]$$

With use of Eqs. (3.7a,b,c,d,e), the above equation simplifies to

$$\epsilon^4 + 4F_\epsilon^2 \left(\frac{1}{F_\epsilon} + C_o\right)^{1/2} \epsilon^2 - 4F_\epsilon^3 = \epsilon^4 \left(1 + \frac{4}{3} s_y\right) \quad (3.8a)$$

which has two roots for ϵ^2 . But since ϵ must be real, the only allowable root is

$$\epsilon^2 = 2F_\epsilon^2 \left\{ \left[\frac{2}{F_\epsilon} + C_o + \frac{1}{4} \left(1 + \frac{4}{3} s_y\right) \frac{\epsilon^4}{F_\epsilon^4} \right]^{1/2} - \left(\frac{1}{F_\epsilon} + C_o\right)^{1/2} \right\} \quad (3.8b)$$

All the relations necessary to determine a solution for both constrained and free regions have now been obtained. If P and H_o are regarded as the independent variables, then both F_ϵ and F_o are known functions of these independent variables only. The remaining unknown quantities β_b , β_d , $s_r(\beta_b)$ and C_o are determined by the following four equations: Eqs. (3.5b); (3.7a); (3.8b); and Eq. (1.9) of Ref. 1. The latter equation appears below as Eq. (3.16). Determination of these four quantities enables the solution to be specified for the constrained regions by means of equations given here, and for the free elastic region by the equations given in Sec. 1 of Ref. 1.

The uniqueness and the continuity with respect to P of solutions to the above mentioned set of equations are now considered. To facilitate this development, some useful inequalities and bounds are now considered. Equation (3.5b) and inequality (3.1b) together imply that

$$0 \leq (1 - 2s_y) \left\{ 1 - \sqrt{1 - \left(1 + \frac{8}{3} s_y\right) \left[1 - \frac{16}{\beta_b^2} \{s_y - s_r(\beta_b)\} \right]} \right\} \leq 1$$

Upon neglect of terms of order s_y^2 , this simplifies to

$$\frac{\beta_b^4}{16s_y} \geq \beta_b^2 - \frac{\epsilon \rho}{(c/a)s_y} \geq \frac{\beta_b^4}{6} \quad (3.9a)$$

or equivalently, with the use of Eq. (3.7d),

$$\frac{\epsilon^4}{16s_y \left(\frac{c}{a}\right)^2} \geq \epsilon^2 - \frac{\epsilon \rho (c/a)}{s_y} \geq \frac{\epsilon^4}{6\left(\frac{c}{a}\right)^2} \quad (3.9b)$$

Equation (3.8a), together with inequality (3.1a), implies that

$$0 \leq \epsilon^4 + 4F_\epsilon^{3/2} (1+F_\epsilon C_o)^{1/2} \epsilon^2 - 4F_\epsilon^3 \leq \epsilon^4 \left(1 + \frac{4}{3} s_y\right)$$

With the use of Eq. (3.7c), this is rearranged to obtain

$$\frac{\epsilon^4}{16s_y \left(\frac{c}{a}\right)^2} \geq - \left(\frac{\epsilon \rho}{4\left(\frac{c}{a}\right)s_y^2} \right)^{1/2} (1+F_\epsilon C_o)^{1/2} \epsilon^2 + \frac{\epsilon \rho (c/a)}{s_y} \geq \frac{\epsilon^4}{12\left(\frac{c}{a}\right)^2} \quad (3.10)$$

Then, by adding the corresponding sides of the two inequalities (3.9b) and (3.10), there is obtained

$$\frac{\epsilon^2}{8s_y \left(\frac{c}{a}\right)^2} \geq \left[1 - \left(\frac{\epsilon \rho}{4\left(\frac{c}{a}\right)s_y^2} \right)^{1/2} (1+F_\epsilon C_o)^{1/2} \right] \geq \frac{\epsilon^2}{12\left(\frac{c}{a}\right)^2} \quad (3.11a)$$

Finally, this is rearranged and written as

$$\left[1 - \frac{\epsilon^2}{8s_y \left(\frac{c}{a}\right)^2} \right] \leq \left(\frac{\epsilon \rho}{4\left(\frac{c}{a}\right)s_y^2} \right)^{1/2} (1+F_\epsilon C_o)^{1/2} \leq \left[1 - \frac{\epsilon^2}{12\left(\frac{c}{a}\right)^2} \right] \quad (3.11b)$$

Since $s_y \ll 1$, Eqs. (3.5b) and (3.8a) are approximated and expressed as

$$\bar{\epsilon}^2 = \epsilon^2 \left\{ 1 - \frac{4(c/a)}{\epsilon} [s_y - s_r(\epsilon^2)]^{1/2} \right\} \quad (3.12a)$$

and

$$\epsilon^4 + 4F_\epsilon^{3/2} (1+F_\epsilon C_o)^{1/2} \epsilon^2 - 4F_\epsilon^3 = \bar{\epsilon}^4 \quad (3.12b)$$

Upon substitution of $\bar{\epsilon}^2$ from Eq. (3.12a) into Eq. (3.12b), there is obtained

$$\epsilon^2 = \frac{\epsilon \rho (c/a)}{s_y} + 4s_y \left(\frac{c}{a}\right)^2 \left\{ 1 - \left[\frac{\epsilon \rho}{4s_y^2 \left(\frac{c}{a}\right)} \right]^{1/2} (1+F_\epsilon C_o)^{1/2} \right\}^2 \quad (3.13a)$$

With use of Eq. (3.7c), this is also expressed as

$$\epsilon^2 = \frac{F_\epsilon^3}{4s_y \left(\frac{c}{a}\right)^2} + 4s_y \left(\frac{c}{a}\right)^2 \left[1 - \frac{F_\epsilon^{3/2}}{4s_y \left(\frac{c}{a}\right)^2} (1+F_\epsilon C_o)^{1/2} \right]^2 \quad (3.13b)$$

Since F_ϵ is expressible as a function of F_o and H_o [Eqs. (1.8a) and (3.10) of Ref. 1],

$$F_\epsilon = 2 \left(\frac{H_o}{Eh} \right)^{1/2} \frac{c}{a} F_o^{-1/2} \quad (3.14)$$

Then, for fixed H_o , F_ϵ may be regarded as a function of F_o only, viz. $F_\epsilon(F_o)$. Hence, Eq. (3.13b) with substitution from Eq. (3.14) yields the function $\epsilon = \epsilon(F_o, C_o)$. Furthermore, when the right-hand side of Eq. (1.9) of Ref. 1 defines the function $I_1(F_o, C_o)$

$$I_1(F_o, C_o) = \int_{F_\epsilon(F_o)}^{F_o} \left(\frac{1}{v} + C_o \right)^{-1/2} dv \quad (3.15)$$

then Eq. (1.9) of Ref. 1 is written as

$$\epsilon^2(F_o, C_o) + I_1(F_o, C_o) - 1 = 0 \quad (3.16)$$

The left-hand side of Eq. (3.16) is considered in the F_o, C_o plane within the allowable domain which is determined by inequalities (3.13a, b) of Ref. 1, viz.

$$\frac{1}{F_o} + C_o > 0 \quad (3.17a)$$

$$0 < F_\epsilon < \left(\frac{H_0}{Eh}\right)^{1/3} \left(\frac{2c}{a}\right)^{2/3} < F_0 \quad (3.17b)$$

Equations (3.13b), (3.14) and (3.15) show that $\epsilon(F_0, C_0)$ and $I_1(F_0, C_0)$ are continuous functions of F_0 and C_0 in the allowable domain. The partial derivative with respect to C_0 of the left-hand side of Eq. (3.16) is

$$\begin{aligned} \frac{\partial}{\partial C_0} (\epsilon^2 + I_1 - 1) = & - \frac{F_\epsilon^{5/2}}{(1 + F_\epsilon C_0)^{1/2}} \left[1 - \frac{F_\epsilon^{3/2} (1 + F_\epsilon C_0)^{1/2}}{4s_y \left(\frac{c}{a}\right)^2} \right] - \\ & - \frac{1}{2} \int_{F_\epsilon}^{F_0} \left(\frac{1}{v} + C_0\right)^{-3/2} dv \end{aligned} \quad (3.18a)$$

The right-hand inequality of (3.11a), with Eq. (3.7c) used, implies

$$1 - \frac{F_\epsilon^{3/2} (1 + F_\epsilon C_0)^{1/2}}{4s_y \left(\frac{c}{a}\right)^2} > 0 .$$

Therefore, in the allowable domain, the right-hand side of Eq. (3.18a) is negative, and so

$$\frac{\partial}{\partial C_0} (\epsilon^2 + I_1 - 1) < 0 \quad (3.18b)$$

This partial derivative is a continuous function of F_0 and C_0 .

Inequality (3.18b) is sufficient to insure that if $C_0(F_0)$ exists, then it is the unique root of Eq. (3.16), and if it exists in a sub-domain of the allowable domain, then it is continuous there (cf. Ref. 1). However, as was the case in Ref. 1, we have had to restrict attention to positive values of C_0 only, in order to prove the existence of $C_0(F_0)$. Existence of $C_0(F_0)$ under this restriction is shown in Appendix A for the problem of the present section. With existence and uniqueness of C_0 , the existence and uniqueness of β_b , β_d and $s_r(\beta_d)$ follow from Eqs. (3.7a,d,e), (3.12b), and (3.16), and thus

existence and uniqueness of stress and displacement also follow.

Finally, the monotone dependence of C_o on F_o will be shown. The partial derivative with respect to F_o of the left-hand side of Eq. (3.16) is

$$\frac{\partial}{\partial F_o} (\epsilon^2 + I_1 - 1) = - \frac{\partial F_\epsilon}{\partial F_o} \frac{F_\epsilon^{1/2}}{(1 + F_o C_o)^{1/2}} \left\{ 6 \left[1 - \frac{F_\epsilon^{3/2}}{4s_y \left(\frac{c}{a}\right)^2} (1 + F_\epsilon C_o)^{1/2} \right] \cdot \left(1 + \frac{2}{3} F_\epsilon C_o\right) - 2 \right\} + \frac{F_o^{1/2}}{(1 + F_o C_o)^{1/2}} \quad (3.19a)$$

where, with the use of Eq. (3.14),

$$\frac{\partial F_\epsilon}{\partial F_o} = - \frac{1}{2} \frac{F_\epsilon}{F_o} \quad (3.19b)$$

Then Eq. (3.19a) becomes

$$\frac{\partial}{\partial F_o} (\epsilon^2 + I_1 - 1) = \frac{F_\epsilon^{3/2}}{F_o} \frac{1}{(1 + F_\epsilon C_o)^{1/2}} \left\{ 3 \left[1 - \frac{F_\epsilon^{3/2}}{4s_y \left(\frac{c}{a}\right)^2} (1 + F_\epsilon C_o)^{1/2} \right] \cdot \left(1 + \frac{2}{3} F_\epsilon C_o\right) - 1 + \frac{F_o^{3/2}}{F_\epsilon^{3/2}} \frac{(1 + F_\epsilon C_o)^{1/2}}{(1 + F_o C_o)^{1/2}} \right\} \quad (3.19c)$$

In the allowable domain, the last term in the curly brackets is seen to be greater than 1. Furthermore, the term in square brackets is shown above to be positive. Hence the right-hand side of Eq. (3.19c) is positive. Therefore,

$$\frac{\partial}{\partial F_o} (\epsilon^2 + I_1 - 1) > 0 \quad (3.19d)$$

in the allowable domain (3.17a,b).

The differential of Eq. (3.16) yields an expression for the derivative of C_o with respect to F_o :

$$\frac{dC_0}{dF_0} = - \frac{\frac{\partial}{\partial F_0} (\epsilon^2 + I_1 - 1)}{\frac{\partial}{\partial C_0} (\epsilon^2 + I_1 - 1)} \quad (3.20)$$

In view of inequalities (3.18b) and (3.19d), this derivative is positive in the allowable domain. This implies that $C_0(F_0)$ is a monotone increasing function. Therefore, for the case of small indenter radii, $C_0(F_0)$ is a continuous, monotone increasing function (see Appendix A).

Remark:

In the equations and inequalities obtained in the present section up to Eq.(3.11b), no terms of order s_y are neglected, although, $s_y \ll 1$. If we neglect such terms, the right-hand sides of inequalities (3.9a,b), (3.10) and (3.11a,b) become zero, and the inequalities are written as:

$$\frac{\beta_b^4}{16s_y} \geq \beta_b^2 - \frac{\epsilon\rho}{\left(\frac{c}{a}\right)s_y} \geq 0 \quad (3.21a)$$

$$\frac{\epsilon^4}{16s_y \left(\frac{c}{a}\right)^2} \geq \epsilon^2 - \frac{\epsilon\rho(c/a)}{s_y} \geq 0 \quad (3.21b)$$

$$\frac{\epsilon^4}{16s_y \left(\frac{c}{a}\right)^2} \geq - \left(\frac{\epsilon\rho}{4\left(\frac{c}{a}\right)s_y^2} \right)^{1/2} (1 + F_\epsilon C_0)^{1/2} \epsilon^2 + \frac{\epsilon\rho(c/a)}{s_y} \geq 0 \quad (3.22)$$

$$\frac{\epsilon^2}{8s_y \left(\frac{c}{a}\right)^2} \geq \left[1 - \left(\frac{\epsilon\rho}{4\left(\frac{c}{a}\right)s_y^2} \right)^{1/2} (1 + F_\epsilon C_0)^{1/2} \right] \geq 0 \quad (3.23a)$$

$$\left[1 - \frac{\epsilon^2}{8s_y \left(\frac{c}{a}\right)^2} \right] \leq \left(\frac{\epsilon\rho}{4\left(\frac{c}{a}\right)s_y^2} \right)^{1/2} (1 + F_\epsilon C_0)^{1/2} \leq 1 \quad (3.23b)$$

SECTION 4. ELASTIC-PLASTIC BOUNDARY IN FREE REGION OF MEMBRANE

It is now assumed that the elastic-plastic boundary lies in the free region of the membrane for sufficiently large indenter loads. This assumption is expressed by the inequality

$$b \leq d \leq a \quad (4.1a)$$

Hence, the increase of d under increasing indenter loads is considered in this section.

The membrane is separated into three regions which are shown in Fig. 2. The solution for the constrained plastic region ($0 < \beta \leq \beta_b$) was obtained in Section 2. The solution is obtained in this section for the free plastic region ($b \leq r \leq d$). No assumption of moderate rotation is made in obtaining this solution, but the solution obtained is valid only when rotations are moderate, as is discussed at the end of Section 2.

For the free annular elastic region, rotations are assumed to remain finite but moderate, that is

$$\beta^2 \ll 1 \quad \text{for} \quad d \leq r \leq a \quad (4.1b)$$

Thus, the elastic solution obtained in Ref. 2 can be used here. Since for an elastic region, it has been shown that $\beta(r)$ is monotone decreasing [Eq.(3.19) of Ref. 3], inequality (4.1b) is necessary and sufficient for

$$\beta^2|_{r=d} \equiv \beta_d^2 \ll 1 \quad (4.1c)$$

Numerical solutions (Fig. 7) show that (4.1c) is satisfied if c/a is small compared to unity.

For the solution of the elastic region, ϵ and ρ , as defined in Ref. 1 [Eq.(1.1c)], are replaced by $\bar{\epsilon}$ and $\bar{\rho}$ which are defined as $\bar{\epsilon} \equiv d/a$ and $\bar{\rho} \equiv P/2\pi Ehd$. Hence, $\bar{\epsilon}\bar{\rho} = \epsilon\rho \equiv P/2\pi Eha$.

Hence, in view of these relations, the quantity $(\bar{\epsilon} \bar{\rho})$ will be written as $(\epsilon \rho)$ for convenience.

The solution for $\beta_b(P)$ is obtained by using the conditions that s_r and ϵ_θ are continuous at the point of tangency. An expression for $s_r(r=b+)$ is first obtained by considering the equilibrium of the indenter with the free plastic region of the membrane. The equilibrium is expressed by

$$2\pi b h \sigma_r(b) \sin \beta_b = P \quad (4.2a)$$

At the point of tangency $r=b$, s_r and ϵ_θ are required to be continuous. Furthermore, $s_\theta = s_y$ in the plastic regions, and s_θ is continuous at $r=b$. Thus, ϵ_θ^e and ϵ_θ^p are required to be continuous independently. Therefore, in view of Eq. (2.21a)

$$\epsilon_\theta^p(r) = 0, \quad 0 < r \leq b \quad (4.2b)$$

and so, at $r=b$, Eq. (2.7) can be approximated as

$$\sin \beta_b = \frac{b}{c} [1 + \epsilon_\theta^e(b)] \cong \frac{b}{c} \quad (4.2c)$$

With the use of Eqs. (4.2a,b), $s_r(b)$ is then expressed in terms of P and β_b as

$$s_r(b) = \frac{P}{2\pi E h c \sin^2 \beta_b} \quad (4.2d)$$

At the point of tangency, continuity of s_r is given by $s_r(\beta_b) = s_r(b)$. This, with the use of Eqs. (2.10) and (4.2d), is written as

$$s_y \left[\frac{\beta_b}{\tan(\beta_b/2)} - 1 \right] = \frac{P}{2\pi E h c \sin^2 \beta_b}$$

This equation is rewritten as a transcendental equation for β_b :

$$\sin \beta_b (\beta_b \cos \beta_b + \beta_b - \sin \beta_b) - \bar{P} = 0 \quad (4.3a)$$

where the normalized load parameter \bar{P} is defined as

$$\bar{P} \equiv \frac{P}{2\pi h c \sigma_y} \quad (4.3b)$$

Equation (4.3a) indicates that $\bar{P}(\beta_b)$ is a continuous function of β_b in the interval $0 \leq \beta_b \leq \pi/2$, and that it has a maximum value of \bar{P}_u at $\beta_b = \beta_{bu}$. Furthermore, $\bar{P}(\beta_b)$ is strictly increasing for

$$0 < \beta_b < \beta_{bu}, \quad (4.4a)$$

and strictly decreasing for $\beta_{bu} < \beta_b < \pi/2$. For bounded strains, $\beta_b < \pi/2$, as is shown at end of Section 2. Thus, \bar{P}_u is the absolute maximum of $\bar{P}(\beta_b)$ in the interval $0 < \beta_b < \pi/2$. Therefore, it is concluded that a static solution to the indenter problem exists only for

$$0 < \bar{P} < \bar{P}_u \quad (4.4b)$$

Since the indenter problem is being considered for the case of positive loading only, β_b is therefore bounded by the inequality (4.4a). Then by the inverse function theorem, $\beta_b(\bar{P})$ is a continuous, monotone increasing function in the domain defined by inequalities (4.4a,b).

The graph of Eq.(4.3a) is shown in Fig. 7. It is seen that $\bar{P}_u \cong 0.6599$ and $\beta_{bu} \cong 1.257$ radians ($= 72^\circ$). Therefore, β_{bu} clearly violates the moderate β assumption, (2.22), and, in view of Eq.(4.8) below and of the remarks made at the end of Section 2, the small strain assumption is also violated at $\bar{P} = \bar{P}_u$. Consequently, it cannot be asserted with rigor that \bar{P}_u is an upper bound for \bar{P} ; however, see discussion below in Section 5.

The solution is now obtained for the free plastic region. In this case, $p = 0$ in equations of equilibrium (2.1a,b). Inequality (2.5) and yield condition (2.6) are assumed to hold. Thus, Eqs.(2.1a,b) are integrated, and appropriate integration constants determined with the use of boundary conditions at $r = b$, to obtain

$$s_r \cos \beta = s_y \left\{ 1 - \frac{b}{r} \left[1 - \frac{s_r(b)}{s_y} \cos \beta_b \right] \right\} \quad (4.5a)$$

and

$$s_r \sin \beta = \frac{(\epsilon \rho)}{\left(\frac{r}{a}\right)} \quad (4.5b)$$

With the use of Eqs.(4.5a,b), expressions for $\beta(r)$ and $s_r(r)$ are obtained:

$$\tan \beta = \left(\frac{\epsilon \rho}{s_y}\right) \left[\frac{r}{a} - \frac{b}{a} \left(1 - \frac{s_r(b)}{s_y} \cos \beta_b \right) \right]^{-1} \quad (4.6a)$$

and

$$s_r^2 = \left[\frac{(\epsilon \rho)}{\left(\frac{r}{a}\right)} \right]^2 + s_y^2 \left\{ 1 - \frac{b}{r} \left[1 - \frac{s_r(b)}{s_y} \cos \beta_b \right] \right\}^2 \quad (4.6b)$$

Therefore,

$$s_r = \frac{(\epsilon \rho)}{\left(\frac{r}{a}\right)} \frac{(1 + \tan^2 \beta)^{1/2}}{\tan \beta} \quad (4.6c)$$

Equation (4.6a) shows that β is a monotone decreasing function of r in the free plastic region. Hence $\beta \leq \beta_b$ for the complete membrane.

The expressions for the total strain components in the free plastic region are obtained next. It is shown in Appendix B [Eq.(B.5)] that

$$\epsilon_\theta^p \equiv 0 \quad b \leq r \leq d \quad (4.7a)$$

Hence, $\epsilon_\theta = \epsilon_\theta^e$; then with the use of Eqs.(2.2b) and (2.6)

$$\epsilon_\theta = s_y - \nu s_r \quad (4.7b)$$

where s_r is given by Eq.(4.6b).

Then ϵ_r can be determined by substituting ϵ_θ from Eq.(4.7b) into the compatibility condition (2.4) and using Eqs.(2.2b) and (2.1c):

$$\epsilon_r = \frac{1 + s_y(1 - \nu \cos \beta)}{\cos \beta} - 1 \quad (4.8)$$

With the use of Eq. (4.8) , Eq. (2.3a) becomes

$$\frac{dw}{dr} = [1 + s_y(1 - \nu \cos \beta)] \tan \beta \cong \tan \beta \quad (4.9a)$$

Substituting into this the expression for $\tan \beta$ from Eq. (4.6a) and integrating, we obtain

$$w(r) = w(d) - \frac{(\epsilon\rho)a}{s_y} \ln \left[\frac{\tan \beta(r)}{\tan \beta(d)} \right] \quad (4.9b)$$

Equations (4.8) and (4.9b) show that strain ϵ_r and displacement w become unbounded as $\beta \rightarrow \pi/2$.

Since we have previously assumed for Eq. (2.9) that ϵ_r is small compared to unity, and since it can be seen from Eq. (4.8) that ϵ_r is not small at β_b unless $\beta_b^2 \ll 1$, then the deflection profiles calculated from Eq. (4.9b) will become inaccurate for large β because of this inconsistency.

The solution to the indenter problem is now completed by considering the elastic portion of the membrane. At the elastic-plastic boundary $r = d$ (or $y = \bar{\epsilon}^2$) , continuity of displacement u and stress σ_r is required. This is equivalent to satisfying Eqs. (2.14a) and (2.17b). The continuity of s_r is equivalent to having β continuous. Then,

$$\tan \beta(d) = \tan \beta(\bar{\epsilon}^2) \quad (4.10a)$$

With the use of Eq. (4.6a), and Eq. (1.1d) of Ref. 1, this becomes

$$\frac{\epsilon\rho}{s_y \left\{ \frac{d}{a} - \frac{b}{a} \left[1 - \frac{s_r(b)}{s_y} \cos \beta_b \right] \right\}} = (4\epsilon\rho)^{1/3} \frac{\bar{\epsilon}}{F(\bar{\epsilon}^2)} \quad (4.10b)$$

Therefore,

$$F(\bar{\epsilon}^2) = \left(\frac{2}{\epsilon\rho} \right)^{2/3} s_y \bar{\epsilon}^2 \left\{ 1 - \frac{\epsilon}{\bar{\epsilon}} \left[1 - \frac{s_r(\epsilon)}{s_y} \cos \beta_b \right] \right\} \quad (4.10c)$$

Continuity of s_θ yields

$$s_y = \left(\frac{1}{2} \epsilon \rho\right)^{2/3} \left[2 \left(\frac{1}{F(\bar{\epsilon}^2)} + C_o \right)^{1/2} - \frac{F(\bar{\epsilon}^2)}{\bar{\epsilon}^2} \right] \quad (4.11a)$$

which is written conveniently as

$$C_o = \frac{1}{4} \left[s_y \left(\frac{2}{\epsilon \rho} \right)^{2/3} + \frac{F(\bar{\epsilon}^2)}{\bar{\epsilon}^2} \right]^2 - \frac{1}{F(\bar{\epsilon}^2)} \quad (4.11b)$$

With the use of Eq. (4.10c), Eq. (4.11b) becomes

$$C_o(\bar{\epsilon}^2) = s_y^2 \frac{2}{\epsilon \rho}^{4/3} \left\{ 1 - \frac{\epsilon}{2\bar{\epsilon}} \left[1 - \frac{s_r(\epsilon)}{s_y} \cos \beta_b \right] \right\}^2 - \frac{1}{F(\bar{\epsilon}^2)} \quad (4.11c)$$

Equations (1.8a) and (1.9) of Ref. 1, for the present case, become

$$F(1) = F_o \equiv \frac{H_o}{Eh} \left(\frac{2}{\epsilon \rho} \right)^{2/3} \quad (4.12a)$$

$$F(\bar{\epsilon}^2) = F_d \quad (4.12b)$$

and

$$1 - \bar{\epsilon}^2 = \int_{F_d}^{F_o} \left(\frac{1}{v} + C_o \right)^{-1/2} dv \quad (4.13)$$

With the use of Eqs. (4.12a,b), (4.10c) and (4.11c), F_d and C_o are expressible as functions of F_o , H_o and $\bar{\epsilon}$:

$$F_d = F_o \frac{s_y}{\left(\frac{H_o}{Eh} \right)} \bar{\epsilon}^2 \left\{ 1 - \frac{\epsilon}{\bar{\epsilon}} \left[1 - \frac{s_r(\epsilon)}{s_y} \cos \beta_b \right] \right\} \quad (4.14)$$

and

$$C_o = F_o^2 \frac{s_y^2}{\left(\frac{H_o}{Eh} \right)^2} \left\{ 1 - \frac{\epsilon}{2\bar{\epsilon}} \left[1 - \frac{s_r(\epsilon)}{s_y} \cos \beta_b \right] \right\}^2 - \frac{1}{F_d} \quad (4.15)$$

Equations (4.13), (4.14) and (4.15) are used to determine $\bar{\epsilon}$ and C_o with F_o and H_o considered as independent variables. Moreover, for fixed H_o , F_d and C_o may be regarded as functions of F_o and $\bar{\epsilon}$ only, viz. $F_d(\bar{\epsilon}, F_o)$ and $C_o(\bar{\epsilon}, F_o)$. Consequently, the right-hand side of Eq. (4.13) can be considered as a known function I_2 of $\bar{\epsilon}$ and F_o ,

$$I_2(\bar{\epsilon}, F_o) \equiv \int_{F_d(\bar{\epsilon}, F_o)}^{F_o} \left[\frac{1}{v} + C_o(\bar{\epsilon}, F_o) \right]^{-1/2} dv \quad (4.16)$$

and Eq. (4.13) is written as

$$\bar{\epsilon}^2 + I_2(\bar{\epsilon}, F_o) - 1 = 0 \quad (4.17)$$

Equation (4.17) will now be shown to determine implicitly a unique function $\bar{\epsilon}(F_o)$, by means of which solution to the indenter problem can be determined. Since $0 \leq \epsilon < (c/a)$ and $\epsilon < \bar{\epsilon} < 1$ are geometrical constraints, then, by Eq. (4.17), $0 < I_2(\bar{\epsilon}, F_o) < 1 - \epsilon^2$. It is necessary to consider the left-hand side of Eq. (4.17) in the F_o, C_o plane within the allowable domain which is determined by the two inequalities

$$\frac{1}{F_o} + C_o > 0 \quad (4.18a)$$

$$0 < F_d < F_o \quad (4.18b)$$

It is evident from Eqs. (4.14), (4.15) and (4.16) that $I_2(\bar{\epsilon}, F_o)$ is a continuous function of $\bar{\epsilon}$ and F_o in the allowable domain. The partial derivative with respect to $\bar{\epsilon}$ of both sides of Eq. (4.14) is

$$\frac{\partial F_d}{\partial \bar{\epsilon}} = F_o \frac{s_y}{\left(\frac{H_o}{Eh} \right)} 2\bar{\epsilon} \left\{ 1 - \frac{\epsilon}{2\bar{\epsilon}} \left[1 - \frac{s_r(\epsilon)}{s_y} \cos \beta_b \right] \right\} \quad (4.19a)$$

With the use of Eq. (4.15), this becomes

$$\frac{\partial F_d}{\partial \bar{\epsilon}} = 2\bar{\epsilon} \left(\frac{1}{F_d} + C_o \right)^{1/2} \quad (4.19b)$$

In the allowable domain, the right-hand side above is positive. Therefore

$$\frac{\partial F_d}{\partial \bar{\epsilon}} > 0 \quad (4.19c)$$

The partial derivative of Eq. (4.15) is

$$\frac{\partial C_o}{\partial \bar{\epsilon}} = \left(\frac{1}{F_d} + C_o \right)^{1/2} \left\{ F_o \frac{s_y}{H_o} \left[1 - \frac{s_r(\epsilon)}{s_y} \cos \beta_b \right] \frac{\epsilon}{\bar{\epsilon}^2} + \frac{2\bar{\epsilon}}{F_d^2} \right\} \quad (4.20a)$$

In this case again

$$\frac{\partial C_o}{\partial \bar{\epsilon}} > 0 \quad (4.20b)$$

Then the partial derivative of the left-hand side of Eq. (4.17) is

$$\frac{\partial}{\partial \bar{\epsilon}} (\bar{\epsilon}^2 + I_2 - 1) = 2\bar{\epsilon} - \left(\frac{1}{F_d} + C_o \right)^{-1/2} \frac{\partial F_d}{\partial \bar{\epsilon}} - \frac{1}{2} \frac{\partial C_o}{\partial \bar{\epsilon}} \int_{F_d}^F \left(\frac{1}{v} + C_o \right)^{-3/2} dv$$

With the use of Eq. (4.19b), this reduces to

$$\frac{\partial}{\partial \bar{\epsilon}} (\bar{\epsilon}^2 + I_2 - 1) = - \frac{1}{2} \frac{\partial C_o}{\partial \bar{\epsilon}} \int_{F_d}^F \left(\frac{1}{v} + C_o \right)^{-3/2} dv \quad (4.21a)$$

Therefore

$$\frac{\partial}{\partial \bar{\epsilon}} (\bar{\epsilon}^2 + I_2 - 1) < 0 \quad , \quad (4.21b)$$

and is a continuous function of $\bar{\epsilon}$ and F_o . Therefore for a given value of F_o , Eq. (4.17) can have only one root. The existence of $\bar{\epsilon}(F_o)$ as a function of F_o to satisfy Eq. (4.17) is not shown, but for a particular case for which numerical results were computed, $\bar{\epsilon}(F_o)$ is seen to exist for values of $P > P_m$, where P_m is defined in Appendix A.

SECTION 5. NUMERICAL RESULTS AND COMPARISON WITH EXPERIMENTS

A comparison is now made of the present theory with the experimental results of Ref. 2. The procedure used in the experiments was summarized in Ref. 1. Numerical results from the present theory are computed for the two cases discussed in Sections 3 and 4. However, for small indenter radii, the results of Section 4 are of prime interest, since this case covers a wide range of indenter loads and includes all indenter loads for which the experimental data of Ref. 2 was available. For brevity, only details of the procedure used to compute numerical results from the theory for the case of Section 4 will be described.

The value of yield stress σ_y for the mylar membrane is determined from the indentation data as follows. For various indenter load values used in the experiments, corresponding values of radius b at the point of tangency are obtained from the photographic data [Ref. 7]. The radial stress σ_r in the membrane at the point of tangency is then calculated by considering vertical equilibrium. For various indenter loads, this value is found to be almost constant and in the range 11,000 to 13,000 psi. Therefore, since σ_r is slightly less than yield in our analysis (Eq.(2.10) at $r = b$), we take $\sigma_y = 13,000$ psi. This value is in good agreement with the value $\sigma_y \cong 12,000$ psi obtained in uniaxial tension tests of strips of the mylar membrane material [Ref. 7]. However, since it was difficult to hold the strips tightly in the grips of the testing machine, this data was not relied upon exclusively. The solution obtained here is affected only slightly by this degree of uncertainty in σ_y .

For a given value of P , values of β_0 and ϵ are obtained with the use of Eqs.(4.3a,b) and (4.2c). Then for a given F_0 , or equivalently given P and σ_{r0} , the root $\bar{\epsilon}$ of Eq.(4.17) is determined with the use of Eqs.(4.14) and (4.15), and C_0 follows immediately. With the use of these values of ϵ , $\bar{\epsilon}$ and C_0 , and with application of Eqs.(1.7b), (1.4), (1.3), (1.2) and (1.5) of Ref. 1, stresses σ_r , σ_θ and displacements w , u are calculated for the free elastic region of the membrane. Stresses and displacements in the plastic

regions are then calculated with the use of Eqs.(4.6b,c) and (4.9b) for the free plastic region and Eqs.(2.10) and (2.12) for the constrained plastic region.

In order to make a valid comparison between theory and experimental data, values of P and σ_{ro} used in the experiments should be known with good accuracy. The values of P do satisfy this criterion, but the values of σ_{ro} could not be obtained to within less than 15% error (see Ref. 2, Table A1), whereas the membrane deflections were measured to within ± 0.002 inches. Therefore, to compare the predictions of the present theory with the experiments, the numerical value of σ_{ro} for a given value of P is determined by adjusting σ_{ro} in the theory so that the predicted deflections near the outer edge $r = a$ are in agreement with the experimental deflections. The values of σ_{ro} thus found agree to within $\pm 15\%$ of the experimental estimates (Ref. 2, loc. cit.).

The values of prestress σ_{ro} are then determined as described above for various platen loads and the corresponding indenter loads and these are shown in the following table:

Platen Load	Indenter Load P	Calculated Prestress σ_{ro}
10 lb./Platen	0.66 lbs.	850 psi
20 lb./Platen	0.77 lbs.	1310 psi
40 lb./Platen	0.88 lbs.	2510 psi

For each value of platen load, the experimental deflection profiles were available only for two values of indenter load. Hence, it is assumed in the present calculations that, for a given platen load, σ_{ro} remains constant for the complete range of indenter loading. The solutions for deflections and stresses are then obtained for all values of indenter loads with the use of the above values of σ_{ro} .

In Figs. 3a,b and 4a,b are shown curves for principal stresses σ_{θ} and σ_r and for transverse deflection w for prestress of 2510 psi

and 1310 psi, respectively, and for various values of the indenter load P . Theoretical deflections w are found to compare very well with the experimental data, except for the case $P = 1.54$ lb. and $\sigma_{ro} = 1310$ psi shown in Figs. 4a,b. This particular curve shows that theoretical deflections are considerably greater than the experimental deflections for the complete membrane and in particular along the outer edge of the membrane. This indicates that the prestress in the experiment must be greater than 1310 psi. It appears likely that the prestress has increased with load during indentation.

In Fig. 5, central load-deflection characteristics are shown in curves 1, 2, 3 - each for a fixed prestress. A comparison is made of the elastic theory (Ref. 1, Fig. 5) and the elastic-plastic theory with the experimental data. Both theories agree well with the experimental data for small indenter loads, but for large loads, the elastic-plastic theory shows a far better agreement with the experiments. For curve 1, wrinkling limit predicted by the theory is noted and wrinkles were observed in the experiments for loads larger than this wrinkling limit load. The theory and experimental data do not agree for loads larger than this wrinkling limit load, since the theory is valid only for the case of axisymmetric deformations. For curves 2 and 3, theory and experiments show very good agreement for loads lower than about 1.6 lbs., but for larger loads a significant difference is observed. Possible reasons for this discrepancy are summarized at the end of this section.

In Figs. 6 and 7, theoretical values of ϵ , $\bar{\epsilon}$ and β_b , β_d are shown as functions of indenter load P for the prestress $\sigma_{ro} = 2510$ psi. The values of ϵ , $\bar{\epsilon}$ and β_b , β_d are at the most only weak functions of σ_{ro} . The curves for $\sigma_{ro} = 850$ and 1310 psi differ from these by less than 2% and hence are not shown. The upper bound value for the indenter load, corresponding to $\bar{P}_u = 0.6599$ [Eq.(4.3b)], is $P_u = 2.021$ lbs. This value of indenter load is found to be in good agreement with the two values of experimental rupture load in Fig. 5.

The reasons for the remaining discrepancies between this theory and the experiments of Ref. 3 are now summarized. The first reason is that calculated values of σ_{ro} were assumed to remain constant during indenter

loading for a fixed platen load, whereas σ_{r0} is actually a weak function of $\beta(r=a)$ and consequently of P . Furthermore, σ_{r0} was probably affected by friction between the membrane and the outer supports when $\beta(r=a)$ is nonzero. The second reason is that the value of yield stress σ_y used in the theory is only approximately the yield stress of mylar. The third reason is the use of Tresca's yield criterion and the associated flow law of Tresca. Since directly under the indenter, $\sigma_r \approx \sigma_\theta = \sigma_y$, we are at a corner of the Tresca yield surface where there is the largest discrepancy between the Tresca flow law and the Mises flow law. It is possible that the Mises flow law would give better results, but it is much more complicated. Finally, for large loads, tangent rotation angle β_b becomes large (see Fig. 7) and thus the assumption of small strain is violated [see Eqs.(2.21b) and (4.8)].

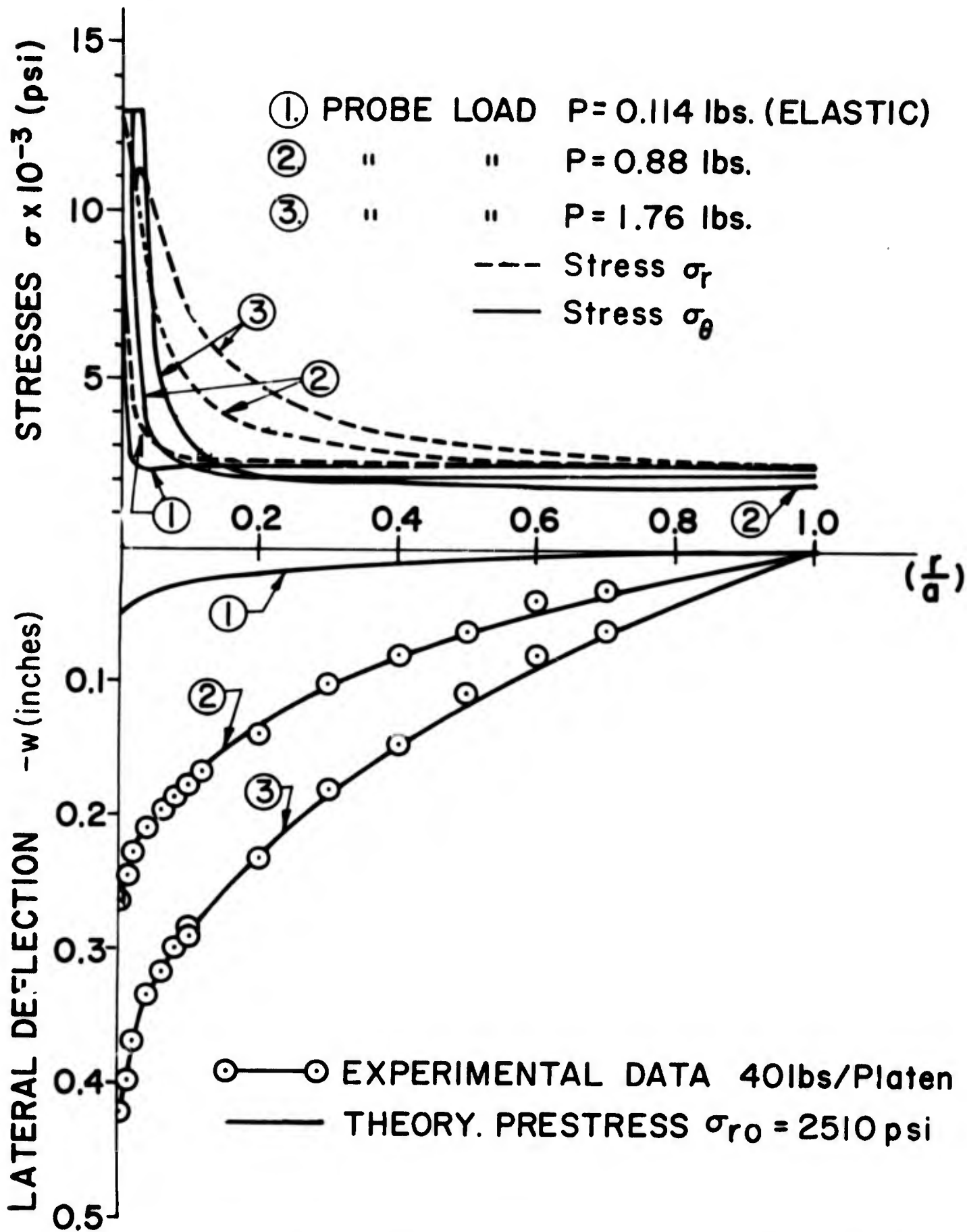


Fig. 3a. Deflection w and Stresses σ_r and σ_θ vs. (r/a) for Complete Membrane, with Prestress $\sigma_{r0} = 2510$ psi.

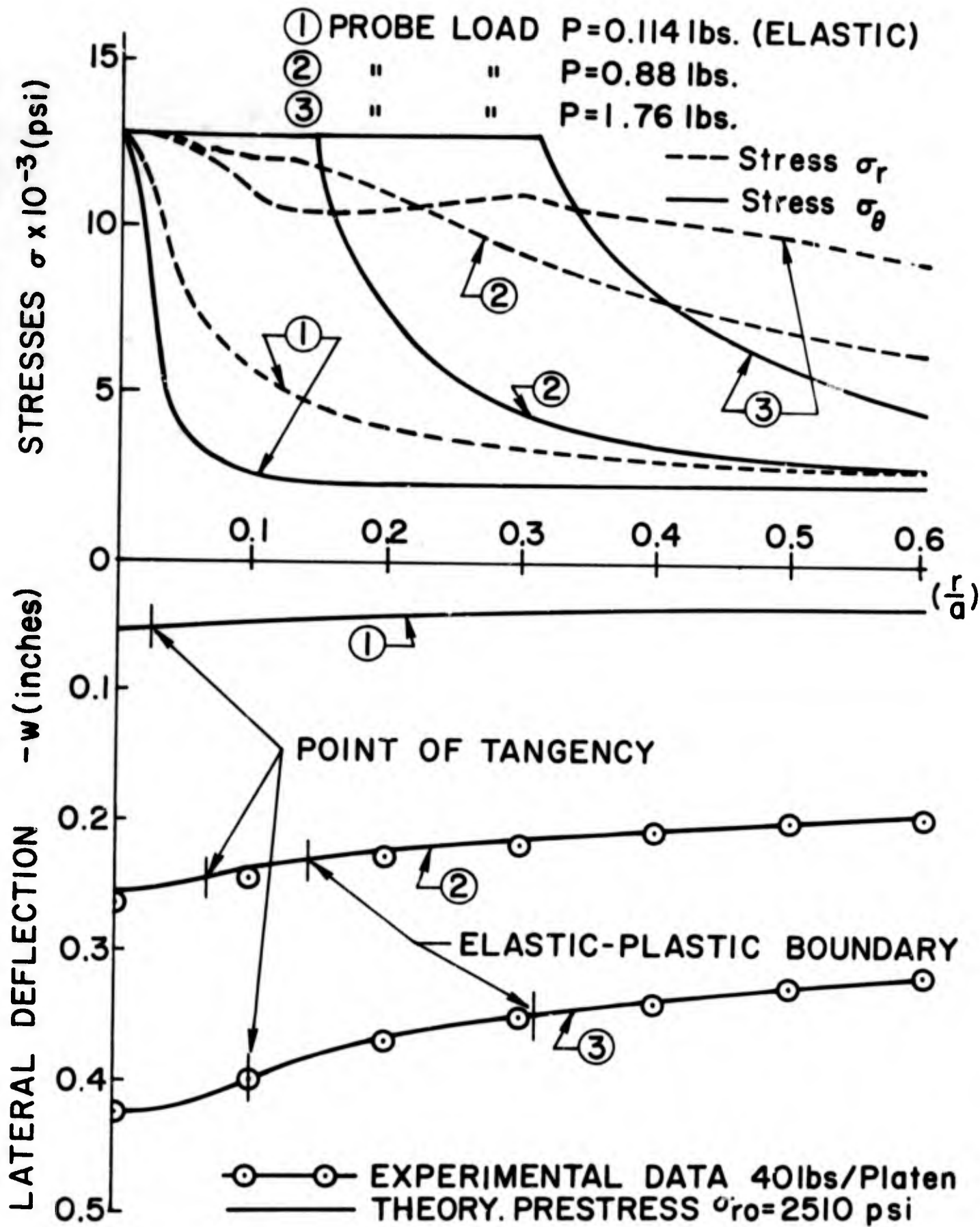


Fig. 3b. Deflection w and Stresses σ_r and σ_θ vs. (r/a) for Membrane in Neighborhood of Indenter, with Prestress $\sigma_{ro} = 2510$ psi.

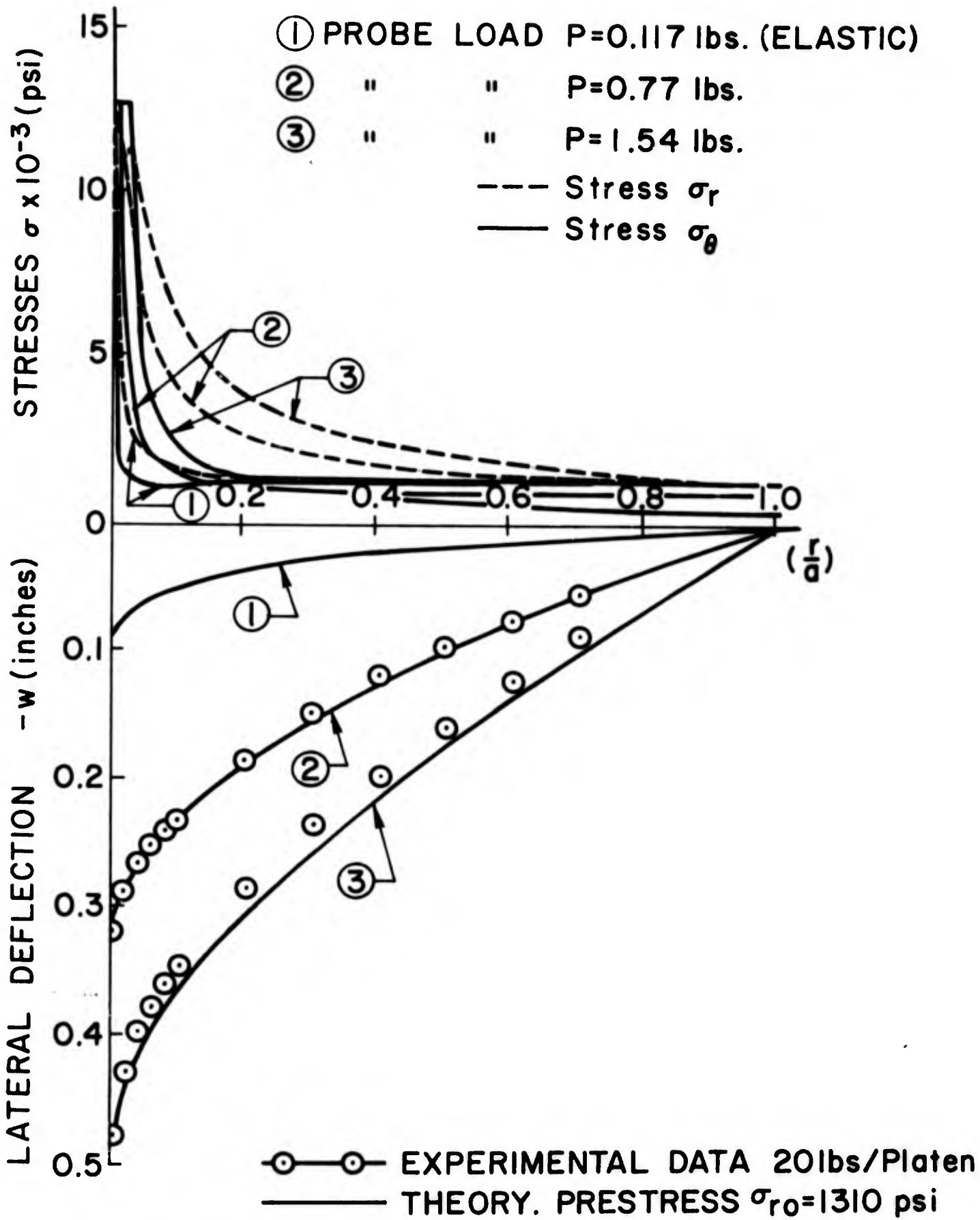


Fig. 4a. Deflection w and Stresses σ_r and σ_θ vs. (r/a) for Complete Membrane, with Prestress $\sigma_{r0} = 1310$ psi.

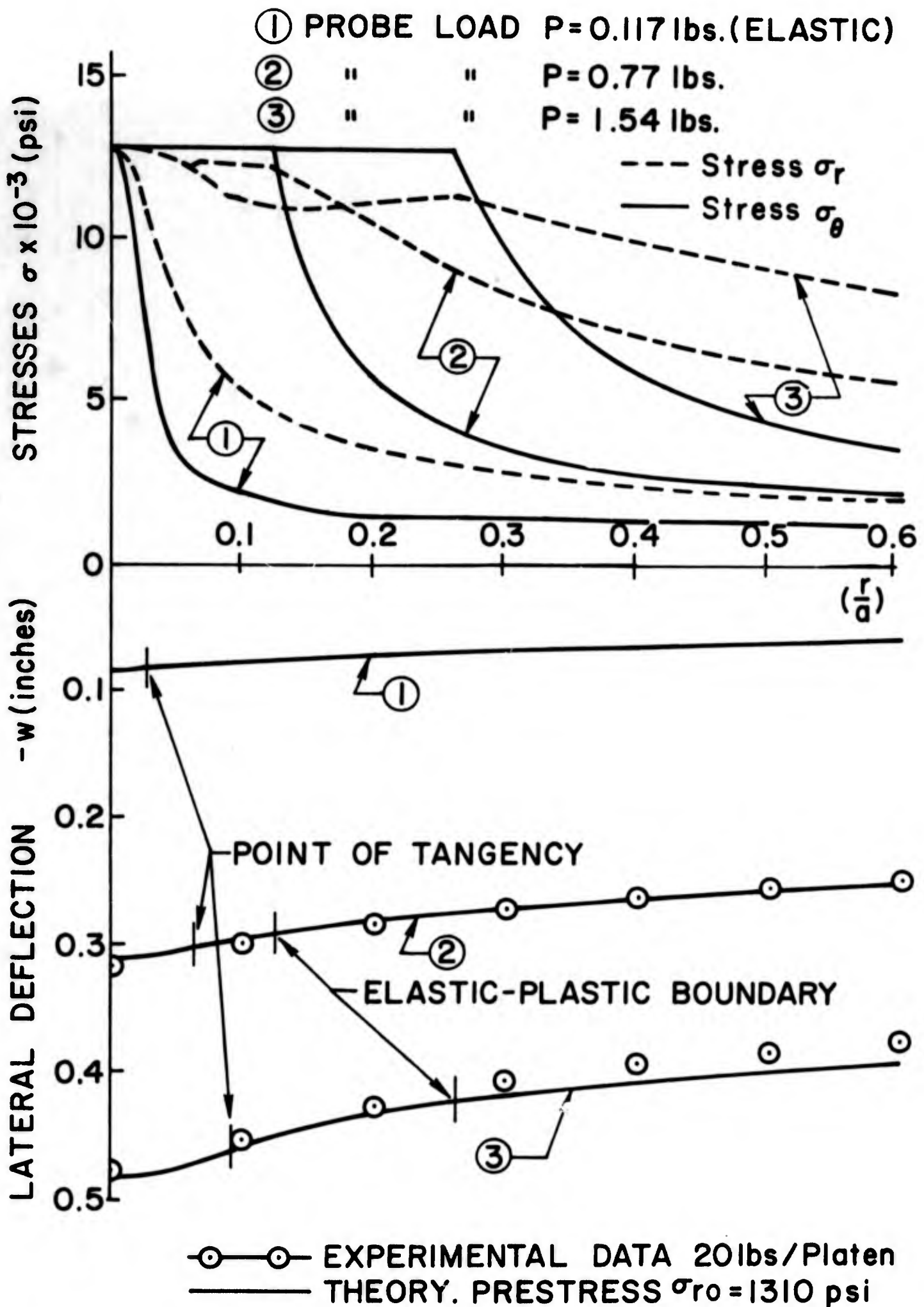


Fig. 4b. Deflection w and Stresses σ_r and σ_θ vs. (r/a)
 for Membrane in Neighborhood of Indenter, with Prestress $\sigma_{ro} = 1310$ psi.

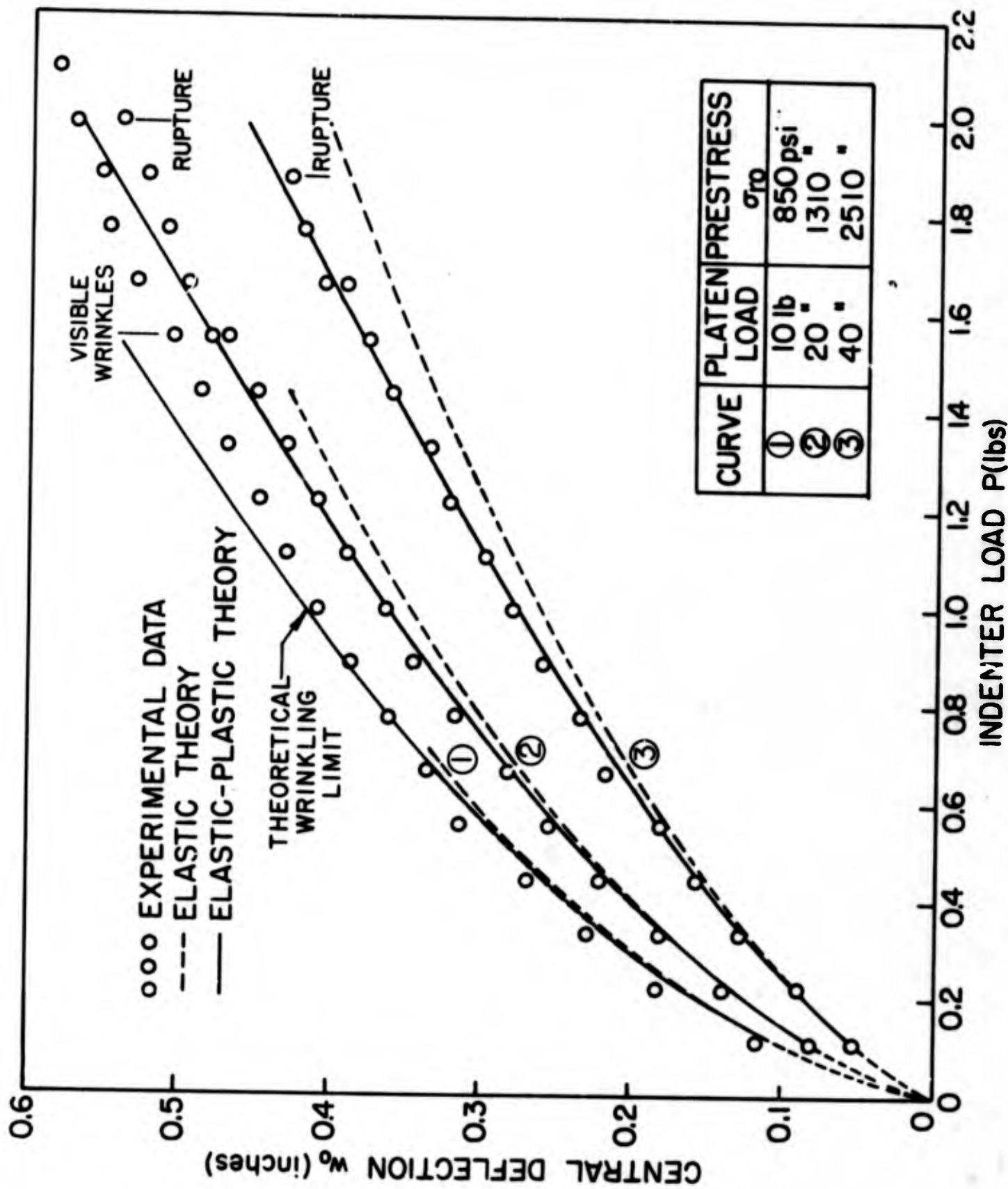


Fig. 5. Central Deflection vs. Indenter Load P for Fixed H_0 :
 Comparison of Theory and Experiments of Ref. 3.

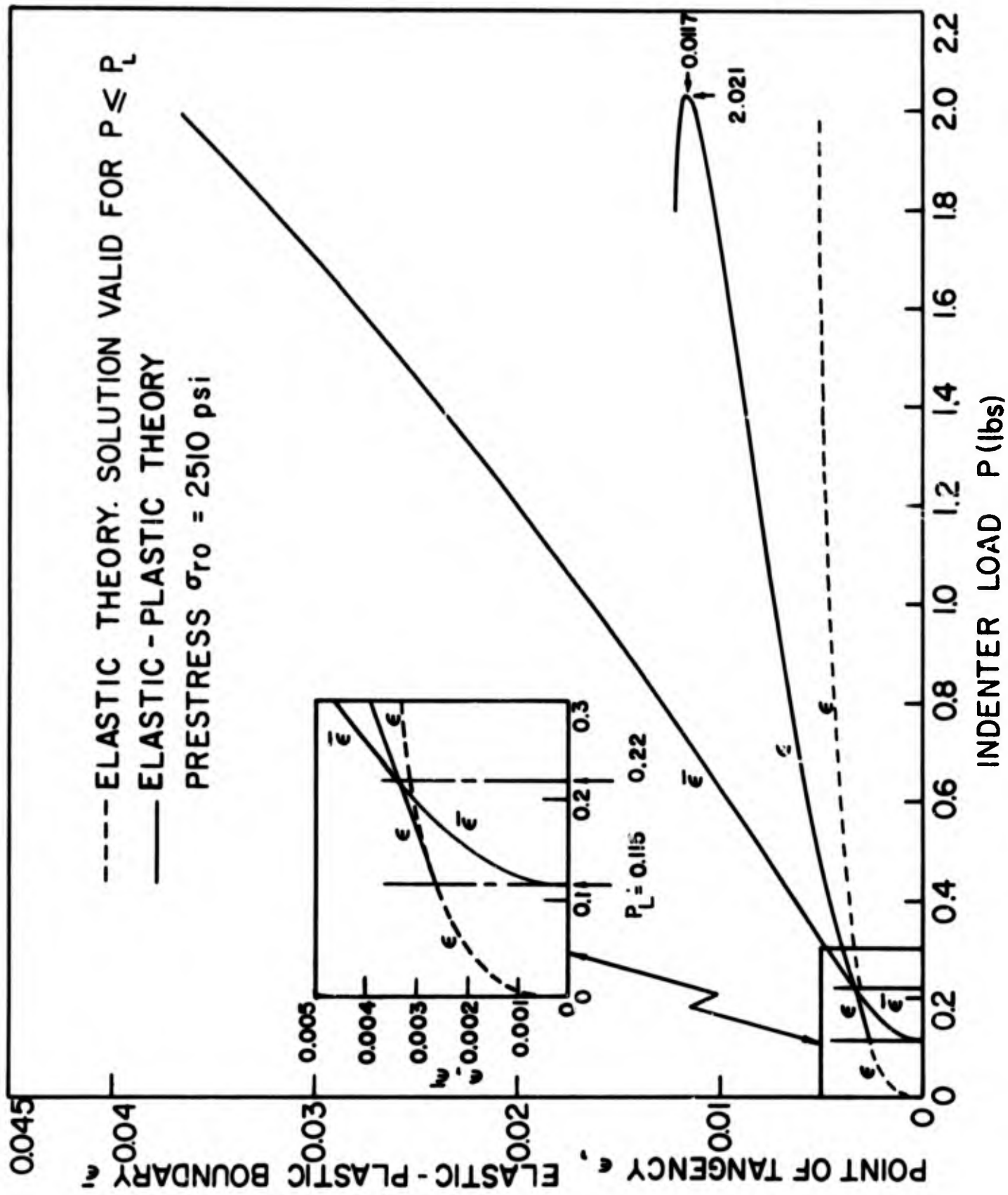


Fig. 6. $\epsilon \equiv (b/a)$ and $\bar{\epsilon} \equiv (d/a)$ vs. Indenter Load P for Fixed H_0 .

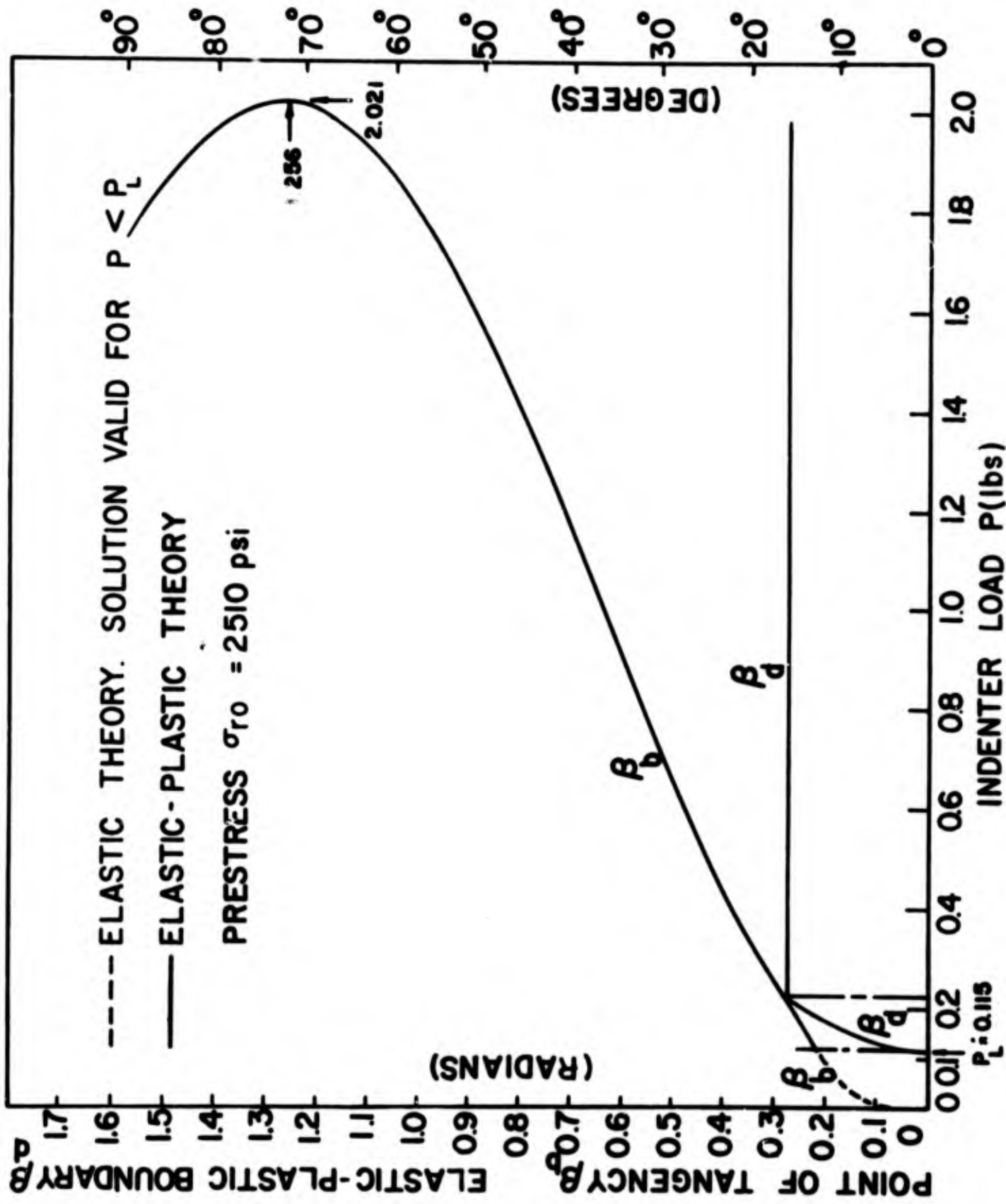


Fig. 7. β_b and β_d vs. Indenter Load P for Fixed H_0 .

APPENDIX A
 PROOF OF CONSISTENCY AND EXISTENCE OF SOLUTIONS
 FOR PROBLEM OF FIG. 1.

In Section 3, the order relation (2.22) is assumed in order to obtain a solution for the case when the elastic-plastic boundary is under the indenter. In the present appendix, order relation (2.22) is shown to be satisfied by the solution for C_0 positive and for arbitrary c/a . Also, the existence of $C_0(F_0)$ as a function of F_0 is shown for this problem.

In Section 1, certain assumptions are made regarding the solution for the plastic portion of the membrane. These assumptions are now stated explicitly for the problem of Fig. 1 for which solution is obtained in Section 3. The first assumption is that loads P_ℓ and P_m can be defined such that $\bar{\epsilon} = 0$ when $P = P_\ell$ and $\bar{\epsilon} = \epsilon \equiv \epsilon_m$ when $P = P_m$. The second assumption is that the radius $\bar{\epsilon}$ of the elastic-plastic boundary increases from zero to ϵ as indenter load P increases from P_ℓ to P_m and such that $\bar{\epsilon}$ and ϵ are in the interval

$$0 \leq \bar{\epsilon} \leq \epsilon \leq \epsilon_m \quad (\text{A.1})$$

when P is in the interval

$$P_\ell \leq P \leq P_m \quad (\text{A.2})$$

The proof of validity of the above assumptions is not given, but these assumptions are found to be valid for a particular case for which numerical results are given in Section 5, Figs. 6 and 7.

An expression for P_ℓ is now determined. With $\bar{\epsilon} = 0$ and $P = P_\ell$, left-hand equalities of (3.9b) and (3.10) are satisfied, and these are

$$\left[\frac{\epsilon^4}{16s_y \left(\frac{c}{a}\right)^2} \right]_{P=P_\ell} = \left[\epsilon^2 - \frac{(\epsilon\rho)c/a}{s_y} \right]_{P=P_\ell} \quad (\text{A.3})$$

$$\left[\frac{\epsilon^4}{16s_y \left(\frac{c}{a}\right)^2} \right]_{P=P_\ell} = \left[- \left(\frac{\epsilon\rho}{4s_y \frac{c}{a}} \right)^{1/2} (1 + F_\epsilon C_0)^{1/2} \epsilon^2 + \frac{(\epsilon\rho)c/a}{s_y} \right]_{P=P_\ell} \quad (\text{A.4})$$

Adding and subtracting (A.3) to (A.4), we obtain, respectively

$$\left[\frac{\epsilon^2}{8s_y \left(\frac{c}{a}\right)^2} \right]_{P=P_\ell} = \left[1 - \left(\frac{\epsilon\rho}{4s_y \frac{c}{a}} \right)^{1/2} (1 + F_\epsilon C_0)^{1/2} \right]_{P=P_\ell} \quad (\text{A.5})$$

and

$$\left\{ \epsilon^2 \left[1 + \left(\frac{\epsilon\rho}{4s_y \frac{c}{a}} \right)^{1/2} (1 + F_\epsilon C_0)^{1/2} \right] \right\}_{P=P_\ell} = \left[\frac{2(\epsilon\rho)c/a}{s_y} \right]_{P=P_\ell} \quad (\text{A.6})$$

Finally, ϵ^2 is substituted from (A.5) into (A.6), to obtain

$$\left[1 - \left(\frac{\epsilon\rho}{4s_y \frac{c}{a}} \right) (1 + F_\epsilon C_0) \right]_{P=P_\ell} = \left(\frac{\epsilon\rho}{4s_y \frac{c}{a}} \right)_{P=P_\ell},$$

which is rewritten as

$$\left[\frac{\epsilon\rho}{2s_y \frac{c}{a}} \left(1 + \frac{F_\epsilon C_0}{2} \right) \right]_{P=P_\ell} = 1$$

This equation, with the use of Eq. (3.7b), becomes

$$P_\ell = \frac{4\pi E h c s_y^2}{\left(1 + \frac{F_\epsilon C_0}{2} \right)_{P=P_\ell}} \quad (\text{A.7})$$

Note that the numerator of the right-hand side of Eq. (A.7) was defined as P_L in Ref. 1, Eq. (4.6), for C_0 positive only. Hence, for positive C_0 , Eq. (A.7) shows that $P_\ell < P_L$. Therefore, for

$P = P_L$ and C_0 positive, yielding and plastic deformation of the membrane has occurred. This conclusion is consistent with definition of P_L given in Ref. 1, Section 4.

The expressions for P_m and β_m are obtained next. With $\bar{\epsilon} = \epsilon = \epsilon_m$ and $P = P_m$, Eq. (3.12a) shows that $s_r(\epsilon_m^2) \cong s_y$, where a term of order s_y is neglected in comparison with unity. Then, Eqs. (3.7a,b) are used to obtain

$$\beta_b^2 \Big|_{P=P_m} \equiv \beta_{bm}^2 = \frac{P_m}{2\pi E h c s_y} = \left(\frac{\epsilon \rho}{s_y \frac{c}{a}} \right)_{P=P_m} \quad (A.8)$$

With use of Eqs. (A.8) and (3.7d), Eq.(3.12b) at $\bar{\epsilon} = \epsilon$ simplifies to

$$\left(\frac{\epsilon \rho}{s_y \frac{c}{a}} \right)_{P=P_m} = \frac{4s_y}{(1 + F \frac{C_0}{\epsilon})_{P=P_m}} \quad (A.9)$$

In this equation again a term of order s_y is neglected in comparison with unity.

Finally, with the use of Eqs. (A.8) and (A.9), there is obtained

$$\beta_{bm}^2 = \frac{4s_y}{(1 + F \frac{C_0}{\epsilon})_{P=P_m}} \quad (A.10)$$

and

$$P_m = \frac{8\pi E h c s_y^2}{(1 + F \frac{C_0}{\epsilon})_{P=P_m}} \quad (A.11)$$

In view of (A.1) and (A.2),

$$\beta_b \leq \beta_{bm} \quad \text{for} \quad P \leq P_m \quad (A.12)$$

where the equality holds only for $P = P_m$. Hence, for C_0 positive, Eq. (A.10) and (A.12) show that $\beta_b^2 \ll 1$ for $P \leq P_m$. Therefore, solution obtained in Section 3 is consistent with (2.22).

We now prove the existence of $C_o(F_o)$ as a function of F_o , which would satisfy Eq. (3.16). However, as was the case in Ref. 1, we restrict attention to positive C_o case only. Furthermore, since P is in the interval (A.2) for the solution of Section 3, F_o must satisfy the inequality

$$F_{o\ell} \geq F_o \geq F_{om} \quad (\text{A.13})$$

where

$$F_{o\ell} \equiv F_o \Big|_{P=P_\ell} \quad (\text{A.14})$$

and

$$F_{om} \equiv F_o \Big|_{P=P_m} \quad (\text{A.15})$$

At $P = P_\ell$ and $\bar{\epsilon} = 0$, the elastic solution obtained in Ref. 1 holds. For the elastic solution, existence of $C_o(F_o)$ was shown in Ref. 1. Hence, for the solution of Section 3, $C_o(F_o)$ exists for $F_o = F_{o\ell}$, and Eq. (3.16) is satisfied. Therefore, in view of (3.18b) and (3.19d), there exists a unique $C_o(F_o)$ in some neighborhood of $F_o = F_{o\ell}$, and in particular for $F_o < F_{o\ell}$ (see Ref. 6.). Furthermore, since (3.18b) and (3.19c) are satisfied for all $C_o > 0$, $C_o(F_o)$ exists for all F_o satisfying (A.13).

As a final topic in this Appendix, approximate expressions for P_ℓ , P_m , and β_{bm} are obtained for the case of small indenter radii. In this case, under the further restriction (4.10b) of Ref. 1, (4.11a) of Ref. 1 is satisfied. Therefore, with use of left inequality (A.13),

$$F_{\epsilon} C_o \Big|_{P \leq P_L} \leq F_{\epsilon L} C_{oL} \ll 1 \quad (\text{A.16})$$

Therefore, Eqs. (A.7), (A.11) and (A.16) are approximated as

$$P_l \cong P_L \equiv 4\pi E h c s_y^2 \quad (\text{A.17})$$

$$P_m \cong 2P_L \equiv 8\pi E h c s_y^2 \quad (\text{A.18})$$

and

$$\beta_{bm}^2 \cong 4s_y \quad (\text{A.19})$$

Equation (A.17) shows that yielding begins approximately when $P = P_L$,
as was shown in Ref. 1.

APPENDIX B

In this Appendix, it is shown that $\epsilon_{\theta}^P \equiv 0$ for the free plastic region ($b \leq r \leq d$) of the membrane (see Fig. 2). In the free plastic region, $\epsilon_{\theta}^P(r,P)$ is, in general, a function of the radial coordinate r and of the indenter load P .

It is shown in Section 2 that $\epsilon_{\theta}^P = 0$ at $r = d$ and for $0 < r \leq b$. Thus,

$$\epsilon_{\theta}^P(b,P) = 0 \quad (\text{B.1a})$$

and

$$\epsilon_{\theta}^P(d,P) = 0 \quad (\text{B.1b})$$

Moreover, Eq.(2.17b) shows that ϵ_{θ}^P must satisfy the condition

$$\frac{\partial}{\partial P} \epsilon_{\theta}^P(r,P) \geq 0, \quad b \leq r \leq d \quad (\text{B.2a})$$

This condition and the assumption that the elastic-plastic boundary radius d is an increasing function of P show that

$$\epsilon_{\theta}^P(r,P) \geq 0, \quad b \leq r \leq d \quad (\text{B.2b})$$

We also know, from Eq.(4.3a) with the use of Eq.(4.2c), that the radius b of the point of tangency is monotone increasing function of P (see Figs. 6 and 7).

With the use of these conditions on ϵ_{θ}^P , it is now shown that $\epsilon_{\theta}^P \equiv 0$ in some finite right-hand neighborhood of b . We consider any two values of indenter load P_1 and P_2 , such that $P_1 < P_2 < P_u$. Then the corresponding values of b satisfy $b_1 < b_2$. Hence, with the use of (B.1a) and (B.2b), respectively, there is obtained

$$\epsilon_{\theta}^P(b_1, P_1) = \epsilon_{\theta}^P(b_2, P_2) = 0 \quad (\text{B.3.a,b})$$

and

$$\epsilon_{\theta}^P(b_2, P_1) \cong 0 \quad (B.3c)$$

Therefore,

$$\frac{\epsilon_{\theta}^P(b_2, P_2) - \epsilon_{\theta}^P(b_2, P_1)}{(P_2 - P_1)} = - \frac{\epsilon_{\theta}^P(b_2, P_1)}{(P_2 - P_1)} \cong 0 \quad (B.3d)$$

If the strict inequality sign held, this implies $\partial \epsilon_{\theta}^P / \partial P < 0$ for some r is $b_1 < r < b_2$, which would contradict (B.2a). Therefore, the strict equality holds in both (B.3c) and (B.3d) and it is easily shown to follow from (B.3a) and (B.3d) that

$$\epsilon_{\theta}^P(r, P_1) \equiv 0 \quad \text{for } b_1 \leq r \leq b_2 \quad (B.4)$$

Thus ϵ_{θ}^P vanishes identically in an interval of finite length $(b_2 - b_1)$. However, $\epsilon_{\theta}^P(r, P_1)$ must be an analytic function of r for $b_1 < r < d$, since it is the solution to differential equations with analytic coefficients. Therefore, if ϵ_{θ}^P vanishes identically in a finite part of this range, it vanishes identically everywhere, viz. for any $P < P_u$ and its corresponding b :

$$\epsilon_{\theta}^P(r, P) \equiv 0 \quad , \quad b \leq r \leq d \quad (B.5)$$

REFERENCES

1. N. M. Bhatia and W. Nachbar, "Finite Indentation of an Elastic Membrane by a Spherical Indenter," SUDAER No. 182, February 1964. (This has been revised and is Part I of the present dissertation.)
2. W. E. Jahsman, F. A. Field, and A. M. C. Holmes, "Finite Deformations in a Prestressed, Centrally Loaded, Circular Elastic Membrane," Proc. 4th U.S. Natl. Cong. Appl. Mech., A.S.M.E., 1952, pp.585-594.
3. W. Nachbar, "Finite Deformation of a Prestressed Elastic Membrane," SUDAER No. 141, November 1962.
4. W. Prager, An Introduction to Plasticity, Addison-Wesley, Mass., 1959, Chapter 1.
5. W. T. Koiter, "Stress-Strain Relations, Uniqueness, and Variational Theorems for Elastic-Plastic Materials with a Singular Yield Surface," Quart. Appl. Math., Vol.11, 1953, pp. 350-354.
6. L. M. Graves, The Theory of Functions of Real Variables, second edition, McGraw-Hill, N. Y., 1956, Chapter VIII, Theorem 2, pp. 138.
7. W. E. Jahsman, Private Communication.

DOCUMENT CONTROL DATA - R&D

(Security classification of title, body of abstract and indexing annotation must be entered when the overall report is classified)

1. ORIGINATING ACTIVITY (Corporate author)		2a. REPORT SECURITY CLASSIFICATION	
Stanford University		Unclassified	
		2b. GROUP	
		NA	
3. REPORT TITLE			
FINITE INDENTATION OF ELASTIC AND ELASTIC-PLASTIC MEMBRANES BY A SPHERICAL INDENTER			
4. DESCRIPTIVE NOTES (Type of report and inclusive dates)			
Technical Report			
5. AUTHOR(S) (Last name, first name, initial)			
Bhatia, N. M. Nachbar, W.			
6. REPORT DATE		7a. TOTAL NO. OF PAGES	7b. NO. OF REFS
August 1964		107	7
8a. CONTRACT OR GRANT NO.		9a. ORIGINATOR'S REPORT NUMBER(S)	
DA-ARO(D)-31-124-G464			
b. PROJECT NO.			
20011501B704			
c.		9b. OTHER REPORT NO(S) (Any other numbers that may be assigned this report)	
d.		3106.6-M	
10. AVAILABILITY/LIMITATION NOTICES			
Distribution of this report is unlimited.			
11. SUPPLEMENTARY NOTES		12. SPONSORING MILITARY ACTIVITY	
None		U.S. Army Research Office-Durham Box CM, Duke Station Durham, North Carolina 27706	
13. ABSTRACT			
<p>PT1 Rotationally symmetric stresses and deformations are considered for a prestressed elastic sheet of circular outer boundary loaded transversely by a centered indenter with a hemispherical tip. A nonlinear membrane solution is obtained for the portion of the sheet that is in frictionless contact with the rigid tip of the indenter. This solution and the nonlinear membrane solution previously obtained by Nachbar for a prestressed annular membrane are used to obtain a complete solution for stresses and deflections of the indented membrane.</p> <p>PT2 The indenter problem defined above is reconsidered under the assumption that the membrane is composed of an elastic perfectly plastic material.</p>			
14. KEY WORDS		prestressed elastic sheet centered indenter hemispherical tip nonlinear membrane solution Indented membrane	